TABLE OF CONTENTS

Page

INTRODUCTION 1

CHAPTER 1 LITERATURE REVIEW 3
1.1 Biomaterials and tissue engineering 3
1.2 MSC for tissue engineering and cell therapy 5
1.3 Problematic of biomaterials and tissue engineering 7
1.4 Factors explaining lack of healing and survival of cells in biomaterials 8
1.5 Endovascular aneurysm repair (EVAR) example 13
1.6 Bioactive biomaterials 14
1.6.1 Physicochemical and biological modifications of biomaterials 14
1.6.2 Bioactive molecules for biomaterials 18
1.7 Literature review conclusions 24

CHAPTER 2 OBJECTIVES AND HYPOTHESES 25
2.1 General objective 25
2.2 Specific objectives 25
2.3 Hypotheses underlying the project 25

CHAPTER 3 MATERIALS AND METHODS 27
3.1 Preparation of bioactive surfaces with chondroitin sulfate 27
3.1.1 Amine rich plasma polymerization 28
3.1.2 EDC NHS covalent chemistry immobilization 29
3.2 Physicochemical characterization of bioactive surfaces 30
3.2.1 Contact angle measurement 30
3.2.2 AFM 32
3.2.3 CS grafting potential by Toluidine Blue 33
3.2.4 Amino group surface density by Orange II 35
3.2.5 Measure of protein adsorption 37
3.3 Preparation of a chitosan hydrogel with chondroitin sulfate 38
3.3.1 Materials for hydrogels preparation 38
3.3.2 Chitosan solution 39
3.3.3 Gelling agent solutions 39
3.3.4 Preparation of the hydrogels 40
3.3.5 Rheological testing of hydrogels 41
3.4 Effect of CS containing solution, surfaces and hydrogels on MSC 42
3.4.1 Cell types 42
3.4.2 Methods of characterization of the cellular response 43
3.4.2.1 Alamar blue 43
3.4.2.2 Crystal violet staining 44
3.4.3 Effect of growth factors and CS in solution 44
3.4.4 Cell behavior on bioactive surfaces 45

3.4.4.1 Cell culture on LP based bioactive coatings 45
3.4.4.2 Cell culture on amine plate based bioactive coatings 46
3.4.5 Cell culture in 3D chitosan hydrogels 46
3.5 Statistical Analysis 47

CHAPTER 4 RESULTS 49
4.1 Effect of biomolecules in solution 49
4.1.1 Effect of Growth factors 49
4.1.2 Effect of Chondroitin sulfate 52
4.1.2.1 CS effect on hMSC 52
4.1.2.2 CS effect on VSMC 56
4.2 Effect of bioactive surfaces 58
4.2.1 Physicochemical characterization of bioactive surfaces 58
4.2.1.1 Contact angle- wettability 58
4.2.1.2 AFM 59
4.2.1.3 CS grafting potential by Toluidine blue 61
4.2.1.4 Amino group density by Orange II 62
4.2.2 Adhesion and growth of hMSC on LP based bioactive coatings 64
4.2.2.1 Adhesion 64
4.2.2.2 Growth 67
4.2.3 Survival of hMSC on LP based bioactive coatings 70
4.2.4 Adhesion and growth of hMSC on amine plate based bioactive coatings 72
4.2.4.1 Adhesion and growth with different CS grafted densities 72
4.2.4.2 Antifouling effect of CS analyzed by protein adsorption 73
4.3 Effect of CS in chitosan hydrogels (3D scaffolds) 74

CHAPTER 5 GENERAL DISCUSSION, LIMITS AND PERSPECTIVES 81

CONCLUSION 93

APPENDIX I EGF AND CS EFFECT ON RAT MSC 95

LIST OF BIBLIOGRAPHIC REFERENCES 97

LIST OF FIGURES

Page

Figure 1.1 Tissue engineering key factors....3

Figure 1.2 MSC potential for tissue engineering through different mechanisms of action 6

Figure 1.3 Interaction between ECM and cells 9

Figure 1.4 Cell interactions with a substrate through protein ligands....10

Figure 1.5 Schematic representation of a stent graft implanted in an abdominal aortic aneurysm during EVAR procedure....14

Figure 1.6 Different structures of chondroitin sulfate....19

Figure 3.1 Experimental steps achieved during the project 27

Figure 3.2 Schematic view of low pressure plasma reactor used in the fabrication of LP 29

Figure 3.3 Illustration of contact angles formed by drops on solid surfaces....31

Figure 3.4 AFM principle....32

Figure 3.5 Toluidine Blue O structure....34

Figure 3.6 Orange II molecule 36

Figure 3.7 Hydrogels preparation methods 41

Figure 3.8 Cell-containing hydrogel inside a well 47

Figure 4.1 Effect of GF on hMSC viability after 4 and 7 days in low serum (LS; 2%) or serum free (SF) medium (cell source =Stem cell technologies). Results are expressed as percentage of alamar blue fluorescence signal compared to signal after 24h adhesion in complete medium (mean ± SD; N=1, n=4)....50

Figure 4.2 Effect of EGF on hMSC viability after 3 and 7 days in serum free (SF) medium (cells source = Texas A&M Institute for Regenerative Medicine). Results are expressed as percentage of alamar blue fluorescence signal compared to signal after 24h adhesion in complete medium (N=2, n=4)....51

Figure 4.3 Effect of VEGF on hMSC viability after 3 and 5 days in serum free (SF) medium (cells source = Lonza). Results are expressed as percentage of alamar blue fluorescence signal compared to signal after 24h adhesion in complete medium (N=1, n=4) 52

Figure 4.4 Effect of CS in solution on hMSC viability after 4 and 7 days in normal serum (NS), low serum (LS) or serum free (SF) medium (cell source =Stem cell technologies). Results are expressed as percentage of alamar blue fluorescence signal compared to signal after 24h adhesion in complete medium (mean ± SD; N=1, n=4 each) 53

Figure 4.5 Effect of CS in solution on hMSC viability after 3 and 7 days in normal serum (NS) and serum free (SF) medium (cells source = Texas A&M Institute for Regenerative Medicine). Results are expressed as percentage of alamar blue fluorescence signal compared to signal after 24h adhesion in complete medium (N=2, n=4) (*p<0.05)....54

Figure 4.6 hMSC after 5 days in SF and SF+CS. The round individual morphology may indicate that cells are about to detach from the surface 54

Figure 4.7 Dose response of CS on hMSC viability after 3, 5 and 7 days in serum free medium (SF). Results correspond to alamar blue fluorescence signal normalized to the signal after 24h adhesion in complete medium. Arrows indicate the conditions where cell detachment was observed (N=2, n=4) 56

Figure 4.8 Dose response of CS on VSMC viability after 3, 5 and 7 days in serum free medium (SF). Results correspond to alamar blue fluorescence signal normalized to the signal after 24h adhesion in complete medium. Arrows indicate the conditions where cell detachment was observed (N=2, n=4) 57

Figure 4.9 Contact angle measurement of bare PET, PET coated by LP and by LP+CS (mean ± SD; N=7, n=3) Significant difference was observed between each surface (*p<0.05) 59

Figure 4.10 AFM topographic (a.c) and phase (b,d) images of LP (a,b) and LP+CS (c,d) (10µm x 10µm)....60

Figure 4.11 AFM height measurements 3D image for LP+CS sample (2µm x 2µm) 60

Figure 4.12 TBO surface densities on PET, LP, LP+CS, AP and AP+CS (N=4, n=4) (*p<0.05).....61

Figure 4.13 TBO bounded on LP and LP+CS before desorption of the dye 61

Figure 4.14 Grafting of CS at different concentrations on AP (N=4, n=4).....62

Figure 4.15 Orange II surface densities on LP and AP (N=4, n=4) (*p<0.05).....63

Figure 4.16 Adhesion of hMSC on LP based bioactive surfaces (10,000 cells/surface) (cells source = Lonza). Results are expressed as percentage of alamar blue fluorescence signal compared to the signal of PET after 24h (N=2, n=4) (*p<0.05) 65

Figure 4.17 Adhesion of hMSC on LP based bioactive surfaces (15,000 cells/surface) (cells source = Lonza). Results are expressed as percentage of alamar blue fluorescence signal compared to the signal of PET after 24h (N=4, n=4) (* p<0.05 with all other surfaces; $^{\&}$ p<0.05 with PCP and PET).....65

Figure 4.18 Adhesion of hMSC on LP based bioactive surfaces (cells source = Texas A&M Institute for Regenerative Medicine). Results are expressed as percentage of alamar blue fluorescence signal compared to the signal of PET after 24h (N=8, n=4) (*p<0.05) 66

Figure 4.19 Representative images of hMSC adhesion (cells source = Texas A&M Institute for Regenerative Medicine) at 24h in PCP, PET, LP and LP+CS 67

Figure 4.20 Growth of hMSC on LP based bioactive surfaces (10,000 cells/ surface) (cells source = Lonza). Results are expressed as percentage of alamar blue fluorescence signal compared to the signal of PET after 24h (N=1, n=4, representative of 2 independent experiments) (* p<0.05 with all other surfaces at the same time point; $^{\&}$ p<0.05 with PCP and PET) 68

Figure 4.21 Growth ratio per surface type of hMSC on LP based bioactive surfaces (10,000 cells/surface) (cells source = Lonza). Results are expressed as percentage of alamar blue fluorescence signal compared to the initial signal (at 24h) on each surface (N=1, n=4, representative of 2 independent experiments) (* p<0.05; + confluency reached) 68

Figure 4.22 Growth of hMSC on LP based bioactive surfaces (cells source = Texas A&M Institute for Regenerative Medicine). Results are

expressed as percentage of alamar blue fluorescence signal compared to the signal of PET after 24h (N=8, n=4) (*p<0.05) 69

Figure 4.23 Representative images of hMSC growth (cells source = Texas A&M Institute for Regenerative Medicine) at 4d in PCP, PET, LP and LP+CS 70

Figure 4.24 Survival of hMSC (cell source = Lonza lot) after 3d or 7d in serum free medium. Results are expressed as percentage of alamar blue fluorescence signal compared to the signal of PET after 24h in complete medium (N=3,n=4) (*p<0.05).....71

Figure 4.25 Representative image of hMSC (cell source = Lonza) remaining on LP after 7 days in serum free medium 71

Figure 4.26 Morphology of hMSC (cell source = Stem cell technologies lot) when seeded on AP and AP+CS prepared using a concentration of 1% (w/v) of CS 72

Figure 4.27 Adhesion and growth of hMSC (cell source = Stem cell technologies lot) on amine plate (AP) based bioactive coatings prepared using different percentages of CS in the grafting solution. Bare AP and PCP are used as controls. Results are presented as alamar blue fluorescence signal (N=1, n=4, representative of 2 independent experiments).....73

Figure 4.28 Protein adsorption on amine plate based bioactive coatings prepared using different percentages of CS in the grafting solution. Results are presented as fluorescence intensity units (N=1, n=4, representative of 2 independent experiments) (*p<0.05) 74

Figure 4.29 Evolution of the storage modulus, G', at different time points at 37°C for chitosan-based hydrogels with 1% or 0% of CS (N=1, n=4) 75

Figure 4.30 Photograph of chitosan-based hydrogels with 1% or 0% CS after 1h of incubation at 37°C 75

Figure 4.31 Viability of hMSC entrapped in chitosan hydrogels with 1% or 0% CS after 24h, 4 and 7 days in alpha MEM medium (cells source = Texas A&M Institute for Regenerative Medicine). Results are expressed as percentage of alamar blue fluorescence signal compared to signal at 24h in hydrogels with 0% CS (N=1, n=4) 76

Figure 4.32 Viability of hMSC entrapped in chitosan hydrogels with 1% or 0% CS after 24h, 4 and 7 days in NutriStem XF medium (cells source = Texas A&M Institute for Regenerative Medicine). Results are expressed as percentage of alamar blue fluorescence signal compared to signal at 24h in hydrogels with 0% CS (N=3, n=3) 77

Figure 4.33 Evolution of the storage modulus, G', at different time points at 37°C for chitosan-based hydrogels with 0.05% or 0% of CS (N=1, n=3) 78

Figure 4.34 Photograph of chitosan-based hydrogel with 0.05% CS after 1h of incubation at 37°C 78

Figure 4.35 Viability of hMSC entrapped in chitosan hydrogels with 0.05% or 0% CS after 24h, 4 and 7 days in NutriStem XF medium (cells source = Texas A&M Institute for Regenerative Medicine). Results are expressed as percentage of alamar blue fluorescence signal compared to signal at 24h in hydrogels with 0% CS (N=2, n=3) 79

LIST OF ABREVIATIONS

AFM	Atomic force microscopy
AP	Commercial Amine Plates
BMP	Bone morphogenic protein
BMP-2	Bone morphogenic protein 2
CH	Chitosan
CM	Complete medium
CS	Chondroitin 4-sulfate
ECM	Extracellular matrix
EDC	N-(3-dimethylaminopropyl)-N'-ethylcarbodiimide hydrochloride
EGF	Epidermal growth factor
EVAR	Endovascular aneurysm repair
FBS	Fetal bovine serum
FGF	Fibroblast growth factor
GAG	Glycosaminoglycans
GF	Growth Factor
HCL	Hydrochloric acid
hMSC	Human mesenchymal stem cells
IGF-I	Insulin-like growth factor I
LBeV	Laboratory of Endovascular Biomaterials
LP	Low-pressure plasma polymerized nitride ethylene
LS	Low serum
MES	2-morpholinoethane sulfonic acid

NaOH	Sodium Hydroxide
NHS	N-hydroxysuccinimide
OPA	o-phthaldehyde
PAAm	Polyallylamine
PBS	Phosphate buffered saline
PCP	Polystyrene culture plate
PET	Polyethylene terephthalate
PLA	Poly(lactic acid)
PMDS	Poly(dimethylsiloxane)
rMSC	Rat mesenchymal stem cells
SD	Standard deviation
SDS	Sodium dodecyl sulfate
SF	Serum free medium
SHC	Sodium hydrogen carbonate
SPD	Sodium phosphate dibasic
SPM	Sodium phosphate monobasic
TBO	Toluidine Blue O
TRITC	Tetramethylrhodamine isothiocyanate
VEGF	Vascular endothelial growth factor
VSMC	Vascular Smooth muscle cell
VSMC	Vascular smooth muscle cells
XPS	X-ray photoelectron spectroscopy

LIST OF SYMBOLS AND UNITS OF MEASUREMENTS

Hz	Hertz
Pa	Pascals
Sccm	Standard cubic centimeters per minute
W	Watts

INTRODUCTION

Biomaterials are materials that intend to interact with biological systems for different purposes, such as replacing or enhancing a body part or function, and they are widely studied nowadays for a variety of particular applications. In the growing field of tissue engineering biomaterials are being used as scaffolds for cells to induce tissue repair and regeneration. Additionally, stem cell research has increased exponentially in the last years due to their potential in tissue engineering. Therefore, the combination of biomaterials with stem cells may provide an excellent template for tissue repair. However one of the main problems biomaterials face is the lack of biological interactions with cells. The lack of biological interactions may prevent cell survival adhesion and growth, thus impairing tissue regeneration.

Biomaterials functionalization by addition of biomolecules is an interesting approach for enhancing cell-biomaterial interactions. The addition of extracellular matrix (ECM) molecules which are normally present in the body and regulate cell behavior is promising for promoting biological interactions with biomaterials. Addition of specific ECM molecules to biomaterials may induce an adequate cell response by communicating with cells through specific ligands and inducing signaling pathways as they do in the body.

The general objective of this project is to study the potential of extracellular matrix components such as chondroitin sulfate and growth factors to enhance the bioactivity of biomaterials such as implantable devices and 3D scaffolds. More particularly we will investigate whether these molecules facilitate the adhesion, growth and survival of hMSC, which play a major role in tissue repair and tissue engineering applications.

Biomaterials' study will be divided in two settings: implantable devices in which biomolecules can be covalently immobilized by surface modification techniques and 3D scaffolds where biomolecules can be incorporated inside the biomaterial. Commercial plates functionalized with amino groups and Polyethylene terephthalate (PET) a commonly used

polymer in biomaterials were used to create bioactive surfaces for implantable devices and chitosan based hydrogels were used to create a bioactive 3D scaffold model. Prior to testing the biomolecules incorporated to the biomaterials, their effect in solution on hMSC was tested.

Chapter I will describe biomaterials and tissue engineering fields, the potential of mesenchymal stem cells (MSC) for tissue engineering and the problematic biomaterials field faces. A literature review on bioactive materials and the different techniques for enhancing bioactivity will also be included in this chapter. Chapter II and III will respectively present the objectives of the project and the methodology used for preparing the biomaterials and characterizing their physicochemical properties and biological response. Chapter IV will present the results, which were divided in three main sections: the effect of biomolecules in solution, the effect of bioactive surfaces and the effect of CS in 3D scaffolds (hydrogels) on hMSC. Results will be discussed in chapter IV, where the limits and perspectives of this project will also be addressed.

CHAPTER 1

LITERATURE REVIEW

1.1 Biomaterials and tissue engineering

A biomaterial is defined by the Consensus Conference of the European society for biomaterials as "material intended to interface with biological systems to evaluate, treat, augment or replace any tissue, organ or function of the body" (Merolli et Joyce, 2009). Tissue engineering evolved from the field of biomaterials development and refers to the practice of combining scaffolds, cells and biologically active molecules into functional tissues (NIH, 2015). In the growing field of tissue engineering, biomaterials are used as scaffolds for cells to induce tissue repair and regeneration (Figure 1.1). The economic activity within the tissue engineering sector has grown exponentially, with increasing numbers of products entering the market place and into clinical trials. The sales of regenerative biomaterials worldwide already exceed US$240 million per year (Lysaght, Jaklenec et Deweerd, 2008).

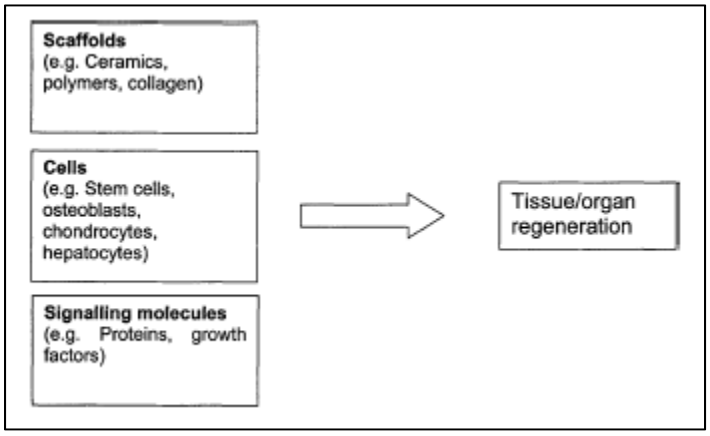

Figure 1.1 Tissue engineering key factors
Taken from (Vats et al., 2003)

As previously mentioned, in the case of this project, biomaterials will be separated in two kinds: implantable devices and scaffolds for tissue engineering. Implantable devices refers to biomaterials such as prosthesis that intend to replace a body part or function. Scaffolds refers to 3D matrix supports which can be made to attract cells from surrounding tissues (cell homing) or include cells (cell therapy). Such scaffolds are important since when transplanted alone, more than 90% of transplanted cells are lost in the first days after injection (Rodrigues, Griffith et Wells, 2010; Zhang et al., 2001). The cell death is related with the lack of interaction with a substrate and to the environment at the injured tissue where cells are injected. Multiples mechanisms are implied in this early cell death including hypoxia, ischemia (i.e. lack of blood flow), anoikis (i.e. cell death due to lack of ECM interactions), inflammation and oxidative stress (Azarnoush et al., 2005). Injecting cells within a biomaterial or scaffold which promotes adequate cell response may provide the matrix support needed to enhance cell survival after transplantation.

A promising example of a biomaterial for cell therapy are hydrogels, which are water-swollen polymeric materials that maintain a distinct three-dimensional structure. These scaffolds deliver the cells to the desired site in the patient's body and provide a space/support for new tissue formation. A variety of tissues are being engineered using this approach including arteries, bladder, skin, cartilage, bone, ligament and tendon (Lee et Mooney, 2001; O'Brien, 2011). Among the numerous synthetic and natural polymer-based hydrogels used as scaffolds for tissue engineering in the last decades, chitosan is an interesting natural biodegradable candidate. At the Laboratory of Endovascular Biomaterials (LBeV) injectable chitosan based thermosensitive hydrogels with enhanced mechanical properties for cell therapy have been developed (Assaad, Maire et Lerouge, 2015). These hydrogels represent a potential engineered construct for MSC delivery since they are injectable at room temperature and gel upon reaching body temperature (37°C). L929 mouse fibroblasts encapsulated within the hydrogels had shown increased viability and growth and hMSC viability has been sustained within these hydrogels (Ceccaldi et al., submitted 2015). Additionally the hydrogels supported CD8 T lymphocytes proliferation which makes them promising for their potential use in immunotherapy (Monette et al., 2016).

1.2 MSC for tissue engineering and cell therapy

A particularly interesting cell type for tissue engineering and cell therapy is mesenchymal stem cells (MSC). MSC are pluripotent stromal cells that have the potential to give rise to cells of diverse lineages. MSC can be found in all post-natal tissues and are characterized for their self-renewal capacity and differentiation into tissues of mesodermal origin (Abdi et al., 2008). MSC were identified in 1960s as bone cells capable of osteogenic differentiation (Friedenstein, Piatetzky et Petrakova, 1966). Nowadays, MSC are known for their capacity to differentiate into adipogenic, chondrogenic and osteogenic lineages. MSC are commonly extracted from bone marrow and adipose tissue but can be isolated from many other locations such as skin, liver and kidneys (Hoogduijn et Dor, 2011).

According to the international society for cellular therapy, in addition to the differentiation potential, MSC must also be plastic- adherent in standard culture conditions and possess a specific antigen expression analyzed by flow cytometry (positive CD105, CD73 and CD90, negative CD45, CD34, CD14, CD19 and HLA class II) (Dominici et al., 2006).

MSC are arising as a potential therapeutic tool due to their regenerative and immunomodulatory properties, low immunogenicity and because they are easily accessible and expandable in culture (Schuleri, Boyle et Hare, 2007). Figure 1.2 illustrates the potential of MSC for tissue engineering trough different mechanisms of action. They have the capacity to recruit at injured tissues and promote tissue repair (Pittenger et al., 2002). Their protection from tissue injury was thought to be due to tissue regeneration however recent approaches suggest that the beneficial effects also come from immunomodulation, since they secrete trophic factors that stimulate other cell lines (Abdi et al., 2008; Hoogduijn et Dor, 2011). It has been demonstrated that MSC strongly supress T-lymphocyte proliferation due to production of soluble growth factors, preventing inflammatory response and stimulating other cell lines for tissue regeneration (Di Nicola et al., 2002; Franquesa et al., 2012).

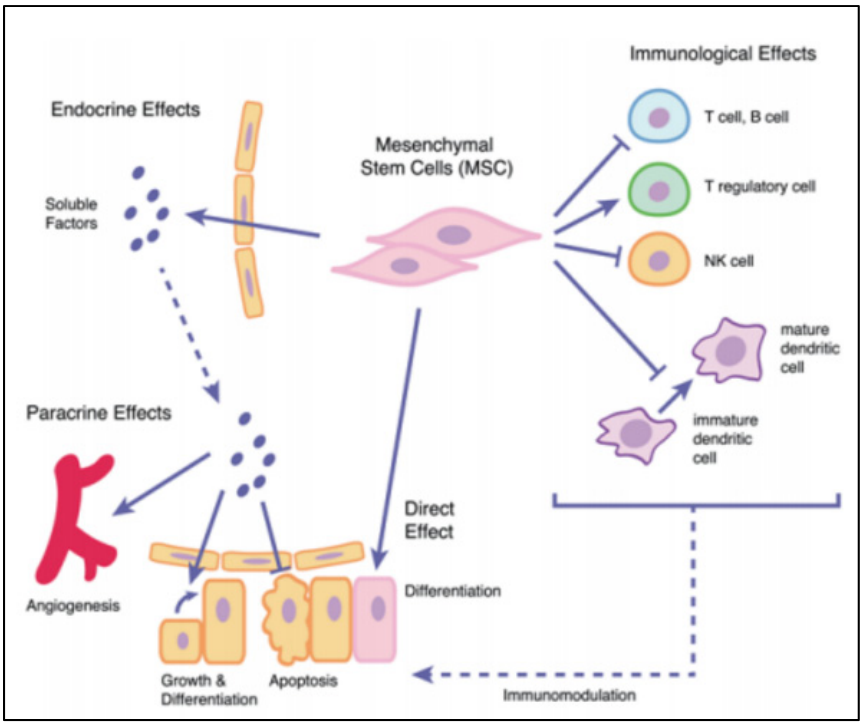

Figure 1.2 MSC potential for tissue engineering through different mechanisms of action
Taken from (Nguyen et al., 2015)

Tissue engineering with MSC is advantageous since as mentioned before, it is possible to induce innate regenerative capacity through signaling. A major challenge in biomaterials field is being able to engineer a scaffold with cells in such a way that it provides by itself regenerative signals to the surrounding cells. This will present an enormous advantage since prolonged *in vitro* culture prior to implantation is not required (O'Brien, 2011).

The paracrine effect (effect directed through secreted factors and signalling) of MSC has been studied through several cell transplantation assays and co-culture studies. MSC have been tested for tendon regeneration and meniscal regeneration with promising results (Pittenger et al., 2002) and cells transplanted into animal hearts have shown improved myocardial function (Robey et al., 2008). However MSC transplantation faces a huge problem since most of the cells are lost after a couple of weeks or even days of being transplanted (Discher, Mooney et Zandstra, 2009; Rodrigues, Griffith et Wells, 2010), either due to poor cell retention or cell death.

Combining biomaterials with MSC can help increase their retention at the desired site. However still into biomaterials there is an inability of MSC to resist cell death in engineered constructs after implantation (Deschepper et al., 2013). Cell death is mainly due to lack of biological interactions with the construct and nutrients deprivation in 3D scaffolds, as further detailed in section 1.4. Therefore biological interactions with the biomaterials need to be enhanced in order to promote cell survival as further explained in the next sections. Several examples of bioactive biomaterials with MSC are detailed in section 1.6.2.

Finally, it is important to consider that MSC cell culture present certain limitations such as a replicative senescence phenotype which end up in growth arrest and loss of cell multipotency after several passages, as well as an enormous donor variation in growth properties and differentiation potential (Siddappa et al., 2007). In order to avoid senescence and loss of multipotency cells are generally tested at early passages (<10) but donor variation still limits standardization of therapeutic tools.

The origin of the variability in growth and differentiation potential has been studied. Factors including methods of isolation, age and gender of the donor have been investigated for their implication (Phinney et al., 1999). Results indicate that variability may be due to several factors such as: bias in the sampling method, differences in MSC isolation methods, the tissue where MSC were extracted and the existence of distinct subpopulations within a tissue-derived primary culture (Hass et al., 2011; Phinney et al., 1999). As an example MSC from neonatal tissues possess increased proliferative capacity in comparison to MSC populations obtained from adult tissues (Hass et al., 2011).

1.3 Problematic of biomaterials and tissue engineering

One of the most important aspects in the biomaterials' field is the biocompatibility. Biomaterials should be harmless, nontoxic and they should not induce a pro-inflammatory response impairing healing. Also, the biomaterial mechanical properties should be consistent with the anatomical site into which it is going to be implanted and mimic the properties of

the body part that is replacing (O'Brien, 2011). In the case of tissue engineering and tissue repair, biocompatibility also mean that cells (either in situ or implanted with the materials) must adhere, function normally, migrate and proliferate in or on the biomaterial.

Unfortunately in many cases there is a lack of cell growth on implants: cells do not adhere to the surface of the implants due to a lack of biological interactions and this impairs the performance of the biomaterial, the healing around it and may cause further complications as further explained in section 1.4 and exemplified in section 1.5.

In the case of 3D scaffolds with cells, a big problem is the lack of cell survival inside the scaffold. Scaffolds for tissue engineering purposes present impaired cellular proliferation and cell death mainly due to insufficient nutrient and oxygen supply within the scaffolds (Bergemann et al., 2015). Additionally, in most constructs, the absence of a functional microenvironment, which interacts with cells to elicit a specific cellular response, has hampered the potential for clinical applications and the success of tissue engineering within the scaffolds (Vats et al., 2003). The factors explaining the lack of cell survival in biomaterials will be further detailed in the next section.

1.4 Factors explaining lack of healing and survival of cells in biomaterials

The main factor that may lead to inadequate cell survival and response around an implant or in a scaffold is the lack of biological interactions between the material and cells. Moreover, in many cases, the biological environment where biomaterials are implanted may also impair cell survival. Additionally, in the case of 3D scaffolds nutrients and oxygen deprivation at the interior of the scaffolds impairs cell survival. These factors will be further detailed in this section.

Lack of biological interactions

In the body, cells are normally in constant communication with the extracellular matrix (ECM) which is a constantly renewed complex network made of glycoproteins,

glycosaminoglycans, proteoglycans proteins and degradation enzymes produced by cells. It is extremely important for cells since components found in the ECM bind via integrin and other receptors in the cells to transduce survival signals (Figure 1.3). When cells lose their interaction with the ECM, adhesion-related survival signals are lost and cell death may be triggered. The ECM also serves for storing growth factors (proteins that enhance cell proliferation) and to maintain hydration and filtration of ions. One of the recent approaches used in cell transplant is the co-delivery of ECM molecules in order to improve the survival of transplanted cells (Jacob et al., 2001; Robey et al., 2008).

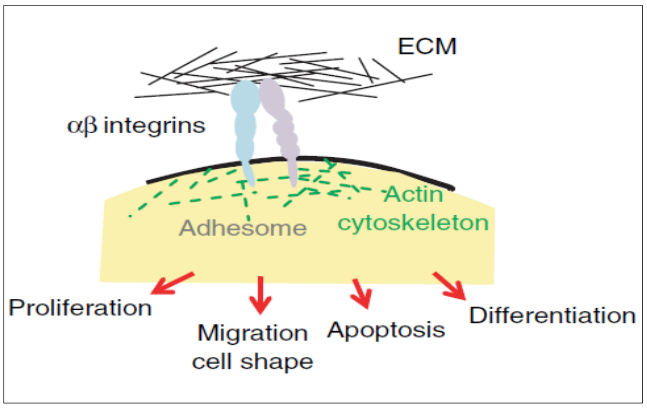

Figure 1.3 Interaction between ECM and cells
Taken from (Kim, Turnbull et Guimond, 2011)

In the case of biomaterials, the lack of interactions such as the ones present in the ECM can lead to inadequate cell survival and response, for the following reason:

Whenever a biomaterial is in contact with a biological environment, the first event that takes place is adsorption of proteins (albumin, fibronectin etc.) from surrounding fluids. At the beginning, usually the small proteins which are more abundant in the body (e.g. albumin) are the first ones to adsorb. Later on, however, these proteins are eventually replaced by other less abundant proteins but with a higher affinity to the biomaterial surface. This replacement is referred as Vroman effect (Schmidt, Waldeck et Kao, 2009; Vroman et al., 1977).

The affinity to the surface is determined by the surface properties of the biomaterial such as rugosity, chemical composition, porosity, hydrophobic or hydrophilic character and charge. For example surfaces with topographic features and bigger surface area provide additional sites for protein interactions and surfaces which present functional species (amino, carbonyl, carboxyl, and aromatic groups) that may interact by affinity with certain proteins. The protein adsorption is done through hydrophobic, ionic or electrostatic bonds. The type, concentration and conformation of the adsorbed proteins will further determine the cell response (Dee, Puleo et Bizios, 2003; Schmidt, Waldeck et Kao, 2009; Von Recum, 1998).

Cells will interact with the protein layer ligands (peptide units which are active sites of the proteins) through their different receptors (integrins, growth factor receptors, cadherines etc.) as illustrated in Figure 1.4. These interactions will trigger a signalling pathway in the cell determining its response (adhesion, proliferation etc.) (Schoen et Mitchell, 2013). Thus, adhesive proteins such as laminin, vitronectin or fibronectin will promote cell adhesion if they adsorb properly on a biomaterial surface (Schmidt, Waldeck et Kao, 2009). Unfortunately, in many cases surface properties of biomaterials are inadequate for promoting optimal biological interactions, due to their inability to promote appropriate protein adsorption and reproduce interactions that are normally present in the ECM (Dee, Puleo et Bizios, 2003).

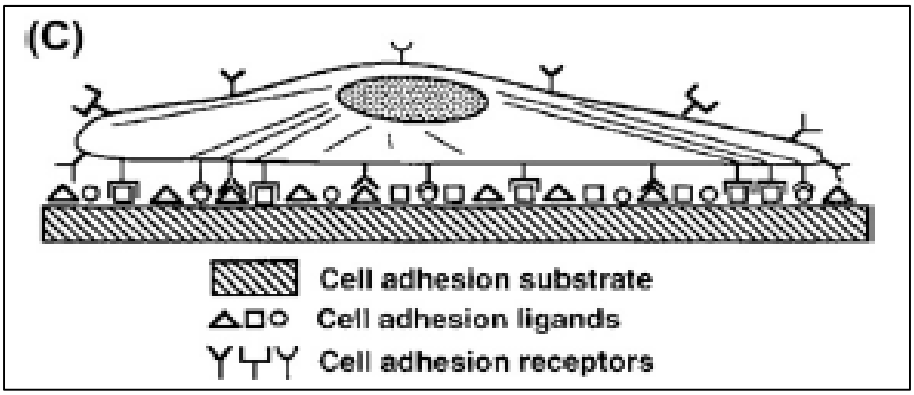

Figure 1.4 Cell interactions with a substrate through protein ligands
Taken from (Schoen et Mitchell, 2013)

Depending on the surface properties of the biomaterials the proteins will adsorb differently, in some cases the protein can unfold whenever adsorbed and therefore denaturation may take place. Denaturation is a rearrangement of the tridimensional structure of the proteins and may cause that the active site or ligand of the protein (which serves to communicate with cells) will no longer be available. As an example, hydrophobic or charged surfaces may induce unfolding of the protein packed structure due to interactions of hydrophobic groups within the protein structure and the biomaterial (Stefani, 2008). If the protein ligands are not available, communication between cells and the protein layer will be impaired leading to a lack of biological interactions.

In the case of MSC it has been reported that their adhesion to polymer surfaces and scaffolds is mediated through fibronectin and vitronectin adhesive proteins, as assessed by integrin expression and adhesion blocking studies (Chastain et al., 2006; Danmark et al., 2012). Additionally fibronectin has been identified as regulator of MSC migration, which induce MSC recruitment at sites of vascular remodeling (Veevers-Lowe et al., 2011). It has also been reported that MSC synthetize ECM proteins such as collagen type I, collagen type IV, laminin and fibronectin to mediate their adhesion, growth and multi-lineage differentiation inside scaffolds (Kollmer et al., 2012). Adhesive motif RGD is a fibronectin amino acid sequence (tripeptide L-arginyl-glycyl-L-aspartic acid; Arg-Gly-Asp) recognized by integrins, which is widely investigated for its effectiveness on prompting cell attachment, survival, migration and differentiation. On MSC it has shown to mediate cell-matrix interactions and prevent anoikis (Benoit et al., 2007). Biomaterials modifications which could enhance adsorption of the previous ECM adhesive proteins can potentially increase MSC interactions. Section 1.6 further details examples of biomaterials modifications for MSC.

Biological environment

The biological environment where biomaterials are implanted has an important role in the cell survival. In many cases biomaterials are implanted in injured tissue which presents an unfavorable environment for cell growth due to inflammation. At injured tissue site, immune response cells produce free radicals and cytokines which can directly damage cells, initiate

pro-apoptotic cascades (signalling pathways that trigger cell death) and prevent healing (Robey et al., 2008).

Nutrients and oxygen deprivation in 3D scaffolds

Studies on cell ingrowth into three-dimensional implants had showed difficulties such as impaired cellular proliferation and survival due to a restriction of medium diffusion in the scaffold, followed by insufficient nutrient and oxygen supply (hypoxic environment) (Bergemann et al., 2015). Hypoxia can create a potentially lethal environment for cells and limit cellular respiration and growth (Malda, Klein et Upton, 2007).

Scaffolds need high porosity, high surface area and structural strength in order to assure cell migration and nutrients diffusion. Pore channels need to provide space for cells retention, nutrients and oxygen diffusion as well as for cell interactions to take place (Vats et al., 2003). Currently the main limitation of cell encapsulation is to entrap cells within a scaffold with an appropriate diffusion coefficient (Loh et Choong, 2013). Super porous hydrogels (pores ranging from 100-600μm) have been developed in tissue engineering in order to improve diffusion properties, allowing cells to attach and proliferate following cell seeding (Keskar et al., 2009; Loh et Choong, 2013).

Homogeneous oxygen diffusion in 3D cell scaffolds is a main challenge for tissue engineering. Uneven oxygen supply impede uniform cellular growth on scaffolds, especially on central regions, where oxygen concentration might drop to negligible values after short periods of *in vitro* culture (Volkmer et al., 2008). Cell viability is correlated with local oxygen concentration inside 3D scaffolds, the lower oxygen, the more cell viability is affected (Bergemann et al., 2015). Perfusion cell culture modules developed *in vitro* have improved oxygen concentration at center regions of scaffolds, however shear stress caused by the perfusion flow impedes cell vitality (Bergemann et al., 2015).

In the particular case of MSC, they can withstand hypoxic conditions at *in vitro* culture but eventually hypoxic environment can lead to cell apoptosis *in vivo*. (Das et al., 2010; Yew et

al., 2013). It has been suggested that MSC are primarily affected by nutrient deprivation, however when long term hypoxia is combined with serum deprivation, massive MSC cell death is induced (Potier et al., 2007). Therefore a 3D scaffold which can allow nutrients and oxygen diffusion properly is primordial for MSC survival. Scaffold neovascularization has been the subject of tremendous work since it is generally recognized that cells aside from more than a few hundred microns from a blood vessel supply will show decreased viability (Gauvin et al., 2011). Additionally, hypoxic preconditioning of MSC and over expression of pro-survival genes can reduce hypoxia-induced cell death (Das et al., 2010).

1.5 Endovascular aneurysm repair (EVAR) example

A good example of the influence of both lack of biological interactions and biological environment on the lack of healing is the case of EVAR. This treatment aims at preventing the rupture of an abdominal aortic aneurysm (i.e. irreversible dilatation of the aorta due to atherosclerosis). It consists in implanting a stent graft via catheter to exclude blood flow (and pressure) from the aneurysmal sac (Parodi, Palmaz et Barone, 1991) (Figure 1.5). However aneurysmal wall presents inflammatory cells such as macrophages and lymphocytes T and B, which release cytokines that induce apoptosis of vascular cells, as well as a production of proteases which degrades the extracellular matrix (Ailawadi, Eliason et Upchurch, 2003; Henderson et al., 1999). In addition, the materials used in stent graft design, such as polyethylene terephthalate (PET) or polytetrafluoroethylene (PTFE), do not promote cell adhesion, migration or survival due to a lack of cell-surface interactions (Gigout et al., 2011; Lerouge et al., 2007). The alterations at the injured site and the lack of biological interactions with the material impair healing around the stent graft, characterized by poor tissue growth on the external surface of the implant, leading to clinical complications such as endoleaks (i.e. leakage of blood flow to the aneurism) and migration of the prosthesis (Ghouri et Krajcer, 2010).

Figure 1.5 Schematic representation of a stent graft implanted in an abdominal aortic aneurysm during EVAR procedure
Taken from (Cook Medical, 2016)

In order to enhance the healing around an implantable device such as a stent graft, the interactions between cell-biomaterial need to be improved. Good interactions between cells and biomaterials could lead to a better colonization *in vivo* and therefore improved healing.

1.6 Bioactive biomaterials

As mentioned before, it is primordial to develop a bioactive material which can improve the cell viability after implantation. This section describes the physicochemical and biological modifications that can be done to biomaterials in order to enhance their biological interactions and some examples of bioactive molecules that may enhance bioactivity.

1.6.1 Physicochemical and biological modifications of biomaterials

The recent approaches try to modify the current materials used in medicine (ceramics, synthetic polymers, natural polymers and composites) by using biological, mechanical and physicochemical methods to enhance their bioactivity. First the adequate material which

fulfill the physical and mechanical properties desired (resistance, porosity, durability, flexibility etc.) is selected and afterwards physicochemical modifications and/or functionalization by addition of biomolecules can be done to enhance its biological performance (Chu et al., 2002).

Physicochemical surface modifications

Biomaterials surface modifications are classified mainly in three categories: chemically or physically altering the atoms, compounds or molecules in the existing surface (chemical modification, etching, mechanical roughening etc.), overcoating the existing surface with a material having a different composition (coating, grafting, thin film deposition etc.) and creating surface textures or patterns. Usually surface modifications of biomaterials are thin, about 3-10nm, in order to avoid altering the mechanical properties of the material. Some examples of surface modifications are non-covalent coatings such as Langmuir-Blodgett film deposition and solvent coating, covalently attached coatings such as photografting, plasma deposition and chemical grafting or modifications of the original surface by ion beam etching and plasma etching (Ratner et Hoffman, 2013).

In the case of this project we are particularly interested by plasma polymerization technique. The LBeV laboratory, in collaboration with Professor Wertheimer at Ecole Polytechnique, has developed a plasma polymerized coating rich in primary amine groups (Ruiz et al., 2010; Truica-Marasescu et Wertheimer, 2008). Positively charged amino groups are well known to promote cell adhesion by attracting negatively charged proteins and possibly interacting directly with the negatively charged cell membrane. The plasma depositions can be created on a variety of materials and it has been proven that this coating enhance cell adhesion in different cell lines such as vascular smooth muscle cells (VSMC), human umbilical vein endothelial cells (HUVEC) and human fibroblasts from embryonic lung tissue (Gigout et al., 2011; Lerouge et al., 2007). Plasma polymerized coatings have also been used for modulating MSC behavior, as further detailed in the subsection on modifications of biomaterials for MSC.

Functionalization by addition of biomolecules

In order to enhance bioactivity, a variety of biomolecules such as enzymes, affinity proteins, cell receptor ligands and drugs have been immobilized on and within biomaterials (Hoffman et Hubbell, 2013). Some of the major methods for immobilizing biomolecules are: physical adsorption (through van der waals and electrostatic interactions or affinity recognition), physical entrapment (within microcapsules, hydrogels and mixtures), covalent attachment (through soluble polymer conjugates, conjugates on solid surfaces and conjugates within hydrogels) and attachment by the use of crosslinkers. Immobilization can be short term or long term depending on the affinity interactions, for example a covalent bond is more stable than an electrostatic interaction. In some cases such as in drug delivery, short term immobilizations of the biomolecules is needed, while in the case of adhesion peptides or adhesion proteins, the biomolecules are meant to remain attached or entrapped permanently (Hoffman et Hubbell, 2013).

In order to covalently bind a biomolecule to a biomaterial surface, reactive groups or spacer groups with end group chemistries are needed (e.g. –OH, -COOH $–NH_2$). Polymeric biomaterials are especially interesting for immobilizing since their surfaces may contain reactive groups or these can be created and used to covalently link biomolecules. Plasma methods are commonly used for the generation of chemically reactive surfaces for biomolecules immobilization (Hoffman et Hubbell, 2013; Sarra-Bournet et al., 2006; Siow et al., 2006). In the case of LBeV laboratory the previously mentioned amine-rich plasma coating has been used to covalently link chondroitin sulfate to enhance its bioactivity as detailed in section 1.6.2. Other examples of biomolecules incorporated to biomaterials for particularly enhancing interactions with MSC will be described next.

Modifications of biomaterials for MSC

Several physicochemical surface modifications and addition of biomolecules have been investigated for enhancing MSC interaction with biomaterials. According to literature, polymers surface modifications to create reactive groups or coatings as well as ECM

molecules incorporation are the main techniques used to modulate MSC behavior on biomaterials. Some examples are cited next.

Surface modifications by plasma polymerization techniques have been used for creating amine-rich coatings which have shown to improve MSC adhesion and prevent chondrocyte hypertrophy by preventing collagen type X expression (Mwale et al., 2006; Mwale et al., 2011; Rampersad et al., 2011). The previous amine-rich surfaces are promising for tissue engineering of cartilage and disc tissues with MSC.

Recent studies have described that chondrogenesis of MSC is promoted on glass slides by the presence of surface hydroxyl and carboxyl groups whereas amine and thiol surface groups stimulate osteogenesis (Curran, Chen et Hunt, 2005; 2006). Additionally, $–CH_3$ silane modified glass substrates have shown to improve MSC expansion (Curran et al., 2011). Small molecule chemical functional groups such as amino or phosphate groups have shown to control differentiation of MSC encapsulated in PEG hydrogels (Benoit et al., 2008).

Photoreactive polymer-modified surfaces with polyallylamine (PAAm) have shown to support MSC adhesion and proliferation while enhancing chondrogenic differentiation (Guo et al., 2008). Surfaces coated with positively charged Poly(L-lysine) prompted MSC adhesion, spread, proliferation as well as chondrogenic differentiation by inducing sox 9 aggregan and collagen expression (Lu et al., 2009). Also, poly(lactic acid) (PLA) modified by synthesizing a diblock copolymer with PEG has shown improved osteoblast differentiation (Lieb et al., 2003). Poly(dimethylsiloxane) (PMDS) surfaces coated with polydopamine have shown to contribute to the stability of MSC adhesion, proliferation and multipotency (Chuah et al., 2015).

In the case of stem cells, ECM molecules and adhesive protein motifs are widely used to induce cell adhesion, proliferation and differentiation (Roy, 2010). Fibronectin or collagen type I covalently immobilized on poly(dimethylsiloxane) (PMDS) surfaces have shown to improve adhesion, spreading and proliferation of MSC (Kuddannaya et al., 2013).

Photopolymerized PEG hydrogels modified with pendant phosphate groups and cell-adhesive RGD peptides rescued hMSC viability and survival when compared to umodified PEG hydrogels (Benoit et al., 2007; Nuttelman, Tripodi et Anseth, 2005). Other peptides sequences that allow cell adhesion and binding to collagen such as KELR have shown to induce chondrogenesis of hMSC when incorporated to PEG networks (Salinas et Anseth, 2009). Photo-cross-linked hydrogels with hyaluronic acid promoted chondrogenic differentiation by enhancing the expression of cartilage-specific markers (Chung et Burdick, 2009). Hydrogels with collagen have also been reported to induce chondrogenic differentiation of MSC (Noth et al., 2007). Heparin functionalized PEG gels have shown to modulate protein adsorption for hMSC promoting adhesion, proliferation and osteogenic differentiation (Benoit et Anseth, 2005).The potential of other ECM molecules such as chondroitin sulphate and growth factors in MSC will be further detailed in next section.

1.6.2 Bioactive molecules for biomaterials

The immobilization of molecules which can enhance convenient protein and cell interactions (such as ECM molecules) into biomaterials is promising for improving cell adhesion, viability and survival. If the biological interactions with the biomaterials are enhanced, healing around implantable devices and viability of cells injected within biomaterials can be improved. In this particular project, growth factors and chondroitin sulfate which are naturally found in the ECM will be studied for their potential in biomaterials.

Chondroitin Sulfate

Chondroitin sulfate (CS) is a glycosaminoglycan (GAG) which is naturally present in the extracellular matrix and it is one of the more abundant GAGs in the human body. GAGs are linear complex poly disperse natural polysaccharides, and CS in particular is composed of alternate sequences of D-glucuronic acid and differently sulfated residues of N-acetyl-D galactosamine linked by β(1→3) bonds. Depending on the disaccharide nature, CS with different carbohydrate backbones are known such as chondroitin-4-sulfate and chondroitin-6-

sulfate, Figure 1.6 illustrates the structures of disaccharides forming chondroitin sulfate (Volpi, 2007).

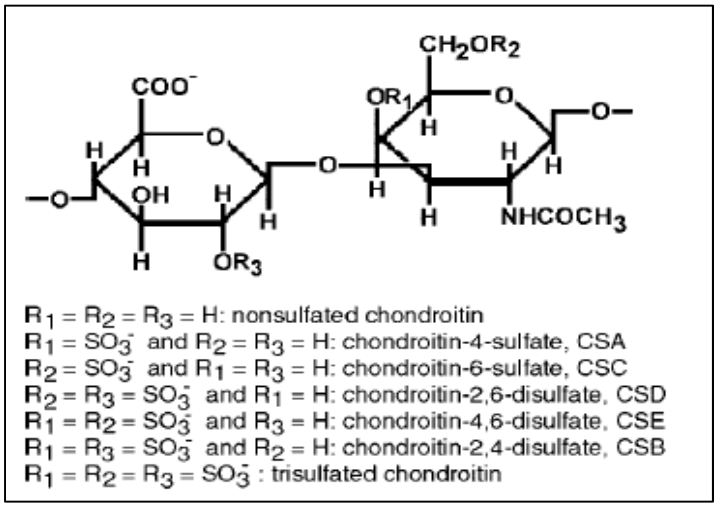

Figure 1.6 Different structures of chondroitin sulfate
Taken from (Volpi, 2007)

Naturally CS is anchored to proteoglycans which are glycoproteins built of several sulfated GAG chains and a variety of oligosaccharides covalently linked to a protein. The proteoglycans have different roles in the body such as function and organization of the ECM. The proteoglycans mediate the interactions between the ECM and the cells for the regulation of cell mechanisms such as migration, cell division and differentiation (Handley, Samiric et Ilic, 2006). CS mechanisms of action include stimulation of cell migration, proliferation and production of fibronectin, while improving tissue healing (Hinek, Boyle et Rabinovitch, 1992; Zou et al., 2009). CS has also been reported to increase the synthesis of proteoglycans by providing building blocks, reduce the effect of proteases which degrade ECM and reduce inflammation by stimulation of hyaluronate production (Monfort et al., 2008).

Recent studies have demonstrated that CS in solution helps to resist apoptosis in VSMC from rat and humans as well as in fibroblasts at a concentration of 125 µg/ml of CS after 24h in serum free media (Laplante et al., 2005; Raymond et al., 2004). The resistance to apoptosis is mediated through the augmentation of an anti-apoptotic protein (Bcl-xL) due to the presence of CS. At LBeV a CS dose response dependence effect on VSMC apoptosis has been

observed in cells seeded in amine-rich plasma coatings on PET (Lerouge et al., 2007). The higher the concentration of CS, the less percentage of apoptotic cells (concentrations ranging from 125µg/ml to 500 µg/ml) after 8h in serum free media.

In the literature, CS has been incorporated to biomaterials for a variety of applications. In the case of implantable devices the potential of CS and other ECM have been widely investigated; CS and collagen type I have been deposited into orthopedic implants for bone remodeling (Rammelt et al., 2006). CS with collagen has been used in layer by layer coatings for improving adhesion and growth of endothelial cells in vascular prosthesis (Liu et al., 2007). CS has also been previously immobilized for preventing fibrin adhesion and enhancing endothelial cell growth inside prosthesis (Kito et Matsuda, 1996). At LBeV, amine-rich plasma coating generated by plasma polymerization has been used to covalently immobilize CS in order to enhance the adhesion and prevent the apoptosis of VSMC (Charbonneau et al., 2007). CS was found as an ideal sublayer to immobilize growth factors and enhance cell survival due to low-fouling properties, since it prevents platelet adhesion (which allows to preserve visibility of immobilized growth factors) while presenting good cell adhesive properties (Charbonneau et al., 2011; Lequoy et al., 2014; Thalla et al., 2014). Low-fouling or antifouling is the capacity of a material to prevent attachment of biomolecules, cells or organisms (Hamming et Messersmith, 2008). Platelet adhesion prevention on CS coated surfaces is probably due to the electrostatic repulsion of the negative charges on sulfated CS and the additive effect of highly hydrophilic properties of CS on surfaces, since hydrophilicity is known to decrease platelet adhesion (Rodrigues et al., 2006; Thalla et al., 2014).

CS has also been investigated for its potential to optimize 3D scaffolds for tissue engineering. Type I collagen scaffolds with CS enhanced proliferation of chondrocytes and retention of proteoglycans (van Susante et al., 2001). Chitosan matrices with CS have also been developed in the aim of creating an artificial extracellular matrix and it has proven to promote binding efficiency of basic fibroblast growth factor (bFGF) and enhance human fibroblasts proliferation (Mi et al., 2006). Hydrogels with CS created by

photopolyzmerization of pre-functionalized CS with methacrylate groups have shown to support chondrocytes viability for cartilage tissue engineering applications (Li et al., 2004). Additionally, Hydrogels with CS and polyethylene glycol-dialdehyde have shown to speed the healing of injured tissue in maxillary sinus mucosa (Gilbert et al., 2004). All of the previous support the idea of CS as an interesting component of a cell-delivery scaffold for tissue engineering.

The effect of CS on MSC in biomaterials have also been explored. MSC proliferation has been studied on GAG-derivatized chitosan membranes and it was found that MSC growth increased as much as fivefold on GAG-immobilized membranes in comparison to normal tissue culture plastic or only chitosan. Results exhibit the highest cell density when membranes were prepared with chondroitin sulfate vs other GAGs (Uygun, Stojsih et Matthew, 2009). PEG/CS hydrogels created by photopolymerization of pre-functionalized CS with methacrylate groups have proven to provide a microenvironment that is conducive for MSC chondrogenesis, facilitating condensation of encapsulated MSC followed by early expression of cartilage specific markers and matrix component production (Varghese et al., 2008). PEG/CS hydrogels with incorporated bio-functional building blocks such as RGD peptides allow tridimensional culture and expansion on MSC. Additionally, the CS based hydrogel exhibited a binding to bone morphogenetic protein-2 (BMP-2), which mediated MSC osteogenic differentiation, indicating its potential in bone tissue regeneration (Anjum et al., 2006). Silk fibroin/gelatin–chondroitin sulfate–hyaluronic acid scaffolds have been previously fabricated providing a supportive structure and mimetic cartilage environment for MSC chondrogenesis, enabling cartilage regeneration (Sawatjui et al., 2015). The previous studies show the potential of CS in biomaterials with MSC for tissue engineering, as for example in regeneration of bone or cartilage.

Growth Factors

Growth factors are defined as extracellular signaling proteins that are involved in cell-to-cell communication. They bind to cells through specific high affinity plasma membrane receptors and induce signal transduction pathways leading to activation of mechanisms within the

responding cell. Growth factors are generally stored in the ECM and a whole range of cellular responses can be induced by them such as cell differentiation, transformation, proliferation, death and motility (Yorio, Clark et Wax, 2011).

The addition of growth factors to biomaterials surfaces can further optimize cell behavior such as cell survival, proliferation, migration, ECM production, or differentiation, to name just a few. The appropriate growth factor needs to be chosen according to the effect it has on the cell line of interest, for example in the case of VSMC it has been proven that epidermal growth factor (EGF) promotes cell growth, prevents cell apoptosis and enhances production of components of the ECM (Kaiura et al., 2000; Ying, Zhang et Sanders, 2007). In the case of human umbilical vein endothelial cells (HUVEC), vascular endothelial growth factor (VEGF) has been shown to promote survival, proliferation and migration (Bao et al., 2009; Olsson et al., 2006).

In the case of MSC a variety of GF have been tested in their ability to promote cell proliferation, migration and survival. Fibroblast growth factors (FGF) increase MSC proliferation when seeded at low densities and retain osteogenic, adipogenic and chondrogenic differentiation capacity at early mitogenic cycles while inducing chondrogenic differentiation after some passages (Rodrigues, Griffith et Wells, 2010). Transforming growth factor beta (TGF β) has shown increased cell proliferation and bias towards the chondrogenic lineage (Bonewald et Dallas, 1994; Longobardi et al., 2006). Platelet-derived growth factors (PDGF), VEGF and EGF have also reported positive effects on MSC proliferation (Rodrigues, Griffith et Wells, 2010). EGF is particularly interesting for MSC since it has been proven to protect the differentiation potential while enhancing MSC proliferation (Rodrigues et al., 2013; Tamama et al., 2006). EGF has also been identified as anti-apoptotic mediator of MSC when exposed to serum free conditions for short periods of time, by activating ERK1/2-dependent anti- apoptotic signaling pathways (Soulez et al., 2010).

The growth factors in biomaterials can be either immobilized in a biomaterial surface or retained within a 3D structure such as hydrogels, where the molecule may be gradually released. Hydrogels have proven to be particularly interesting for growth factor delivery, especially for promoting neovascularization where growth factors such as VEGF and FGF can be combined with the gels (Ishihara et al., 2003). This approach is one of the most common in the literature for the creation of vascularized scaffolds, which could avoid hypoxia induced cell death at ischemic environments after implantation (Silva et Mooney, 2007).

Moreover, immobilizing the growth factors on a biomaterial surface presents an interesting approach since their effect can be sustained during longer period of time at the site of interest (Masters, 2011). At LBeV, EGF has been covalently grafted to immobilized CS proving to decrease VSMC apoptosis and depletion in serum-free medium (Charbonneau et al., 2011; Charbonneau et al., 2012). In addition, growth factors such as EGF and VEGF have been grafted to CS in an oriented way in order to reach higher GF surface densities and enhance vascular cell survival more efficiently (Lequoy et al., 2014; Lequoy et al., 2016).

In the case of biomaterials with MSC, growth factors have been mainly incorporated to scaffolds in order to modulate differentiation of MSC for tissue engineering applications. Differentiation inducing growth factors such as TGFβ1 have been incorporated to scaffolds in order to enhance expression of cartilage-specific genes and provide an appropriate niche for chondrogenic differentiation of MSC (Park et al., 2009a; Park et al., 2009b). Insulin like growth factor I (IGF-I) releasing silk-fibroin scaffolds have also been developed proving to induce chondrogenic differentiation of hMSC (Uebersax, Merkle et Meinel, 2008). Additionally bone morphogenic protein (BMP) growth factors have been incorporated to biopolymers scaffolds via microsphere delivery to enhance MSC proliferation and osteogenic differentiation with a sustained GF delivery (Basmanav, Kose et Hasirci, 2008; Wang et al., 2009).

1.7 Literature review conclusions

As observed in the literature review, the main challenge that biomaterials face is the cell survival and growth, either around implantable devices or inside engineered scaffolds. A lack of appropriate biological interactions between the materials and the cells results in poor cell survival and growth. One interesting approach to enhance biological interactions is incorporating molecules from the ECM which normally regulate cell behavior and may enhance cell survival and proliferation. CS and growth factors such as EGF have proven to enhance bioactivity of the materials, promoting cell survival and growth. The combination of MSC with biomaterials is interesting for tissue engineering purposes due to their regenerative and immunomodulatory potential. Literature data suggest that CS can also help improve MSC behavior on biomaterials surfaces and in 3D scaffolds. However little data are available and their mechanism is unknown yet.

CHAPTER 2

OBJECTIVES AND HYPOTHESES

2.1 General objective

The general objective of this project is to study the potential of extracellular matrix components such as chondroitin sulfate and growth factors to enhance the bioactivity of biomaterials such as implantable devices and 3D scaffolds. More particularly we will investigate whether these molecules facilitate the adhesion, growth and survival of hMSC, which play a major role in tissue repair and tissue engineering applications.

2.2 Specific objectives

A. Study the effect of growth factors and CS in solution on hMSC growth and survival.
B. Demonstrate the capacity of bioactive surfaces with immobilized CS to enhance adhesion, growth and survival of hMSC.
C. Study the capacity of chitosan based hydrogels (3D scaffolds) with CS to enhance hMSC viability.

2.3 Hypotheses underlying the project

Several hypotheses based on the literature review will be verified in this project:

- The pro-adhesive, pro-proliferative and anti-apoptotic effects of CS coatings observed on VSMC apply to hMSC.
- There is a pro-survival effect of growth factors (EGF, VEGF or FGF) on hMSC when cultured in serum free conditions.

CHAPTER 3

MATERIALS AND METHODS

In this project, biomolecules such as growth factors and CS were first tested on MSC and based on the results, CS was chosen for its incorporation into biomaterials. Later on, the effect of the bioactive materials with CS on MSC was studied. In this chapter, the preparation and characterization of bioactive surfaces and hydrogels containing CS is first described. Then, the cell culture tests are detailed. Figure 3.1 summarizes the experimental steps achieved during this project.

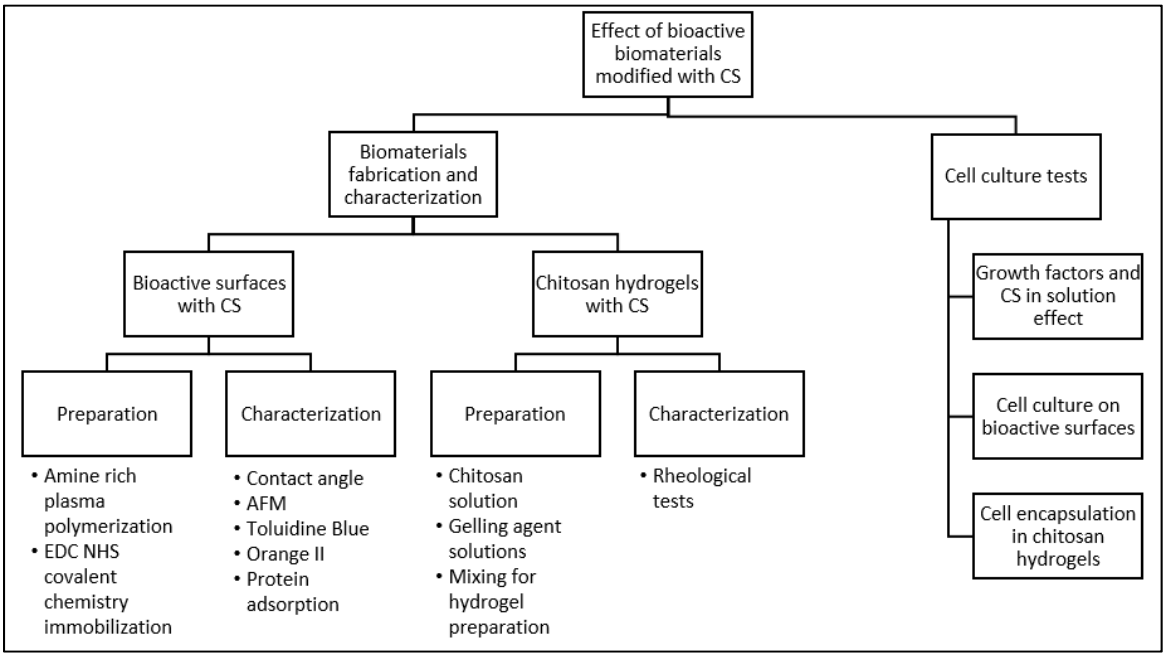

Figure 3.1 Experimental steps achieved during the project

3.1 Preparation of bioactive surfaces with chondroitin sulfate

Bioactive surfaces used in this project were created by grafting chondroitin sulfate on two kinds of substrates, either 96-well commercial amine plates (AP) obtained from BD biosciences (England, UK) or Polyethylene terephthalate (PET) films (50µM) obtained from GoodFellow (Huntingdon, England). In case of the PET films they were cleaned by 15

minutes sonication in ethanol 100% (Ethyl Alcohol Anhydrous, Brampton, Canada), dried with nitrogen air (Praxair, Missisauga, Canada) and a thin layer of primary amine-rich plasma polymerized coating was deposited in a low pressure plasma reactor as detailed below. In both cases, covalent grafting of CS on the amine-rich surfaces was achieved by NHS/EDC chemistry.

3.1.1 Amine rich plasma polymerization

Amine-rich plasma polymerization was performed with a low-pressure radiofrequency glow discharge using a mixture of ammonia (NH_3) and ethylene (C_2H_4) as published previously (Truica-Marasescu et Wertheimer, 2008). In this process, a cold plasma is created inside the reactor between the electrode and the walls of the cylindrical chamber due to the radiofrequency (Figure 3.2), allowing the polymerization of the gas and the creation of the thin layer. The PET samples (≈64cm^2) are deposited in the cylindrical chamber of the low pressure plasma reactor and pumps generate a vacuum higher than 10^{-4} Pa. After the vacuum level is reached, NH_3 and C_2H_4 (of 99.9 and 99.5% purity, respectively, Air Liquide Montreal, QC) are introduced at flow rates of 15 to 20 standard cubic centimeters per minute (sccm) respectively (ratio 3:4). The pressure during plasma operation is maintained constant at 80 Pa and the power at 10W. The time of the deposition is set at 8 min in order to obtain ≈100nm thick coatings (Ruiz et al., 2010; Truica-Marasescu et Wertheimer, 2008). The coated PET will be further referred as LP.

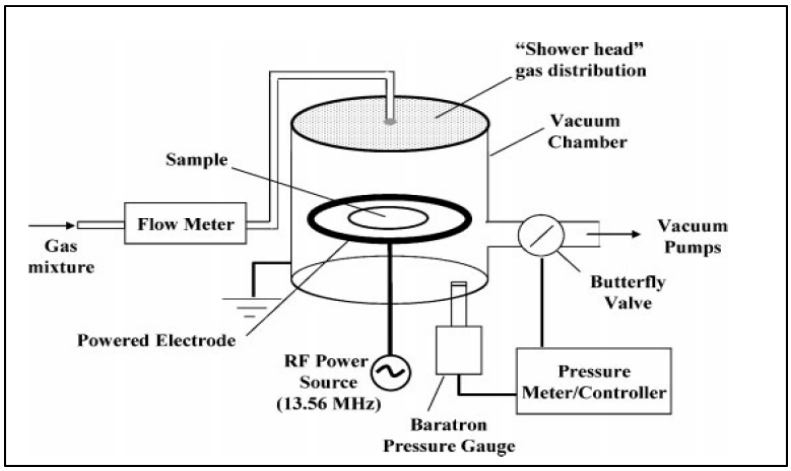

Figure 3.2 Schematic view of low pressure plasma reactor used in the fabrication of LP
Taken from (Truica-Marasescu et Wertheimer, 2008)

3.1.2 EDC NHS covalent chemistry immobilization

The covalent grafting of CS on the amine plates or LP was achieved by a wet chemistry reaction using N-(3-dimethylaminopropyl)-N'-ethylcarbodiimide (EDC), N-hydroxysuccinimide (NHS) and 2-morpholinoethane sulfonic acid (MES). EDC, NHS and MES were purchased from Sigma-Aldrich (Oakville, ON). The chondroitin sulfate is Chondroitin 4-sulfate or Chondroitin Sulfate A sodium salt from bovine trachea, suitable for cell culture (Sigma-Aldrich).

In this reaction EDC covalently attaches accessible carboxylic acids of CS to primary amines by amine bonding, while NHS boosts EDC-mediated reaction efficiency by stabilizing the o-acylisourea amine-reactive intermediate (Grabarek et Gergely, 1990). In this project an optimal concentration of 1% w/v CS solution, containing 40% v/v ethanol, $50 \cdot 10^{-2}$ M MES, $22.8 \cdot 10^{-3}$M EDC (EDC/COOH: 1), and $4.6 \cdot 10^{-3}$ M NHS (NHS/EDC: 0.2) was used, as proposed by (Charbonneau et al., 2012). Solutions were filtered through a 0.20µm filter (Corning, USA) prior to use. A filtered stock of CS dissolved in water at an intermediate concentration (10% w/v) was kept and used for the preparation of the grafting solution in order to avoid variation due to the filtration process (where some CS might be lost).

LP was exposed to the previously mentioned grafting solution (75ul/cm^2) for 1h at room temperature. After the reaction, surfaces were thoroughly rinsed with PBS 1X (2min) and Milli-Q water (2x2min) in ultrasonic bath in order to remove any unbound CS. Surfaces were transferred into a 24 well polystyrene well plate (Corning, USA) for the rinses. After the rinses, all surfaces were disinfected by immersion in 70% v/v ethanol for 5 min and a final rinse with Milli-Q water. Finally surfaces were dried overnight at room temperature.

CS grafting on commercial amine plates was performed by the previously described protocol but 100µl per well of reaction solution was used to immerge the surface. On the amine plates, gradient grafting of CS was also performed by diluting the previously mentioned grafting solution in 40% ethanol in water, for obtaining final concentrations of 1%, 0.5%, 0.1%, 0.01%, 0.001% and 0.0001% of CS (w/v) in the reaction solution and consequently graft less CS.

3.2 Physicochemical characterization of bioactive surfaces

The surfaces were characterized with different techniques in order to study their properties and possible impact on cell adhesion growth and morphology. In all cases, substrates of the coatings were analyzed too, such as PET or amine-rich surfaces, in order to compare them to the CS surfaces. Bioactive surfaces based on LP were analyzed by contact angle and atomic force microscopy (AFM). The CS grafted on the bioactive surfaces was quantified by using Toluidine blue O dye and the amino group content was determined by using Orange II dye. The antifouling properties of commercial amine plates with CS were studied by protein adsorption analysis using Texas Red. All these tests are described below.

3.2.1 Contact angle measurement

Contact angle measurement was used to study the surface wettability, i.e. capacity of a liquid to spread on a surface. If water is used, the contact angle describes the hydrophobic or hydrophilic character of the material. Figure 3.3. Illustrates the interfacial tensions present

when a droplet is placed on a surface: liquid-solid (γ_{sl}), liquid-vapor(γ_{lv}) and solid-vapor(γ_{sv}), they are related to the contact angle (i.e the tangent angle in the droplet profile) by the the Young Dupre equation (3.1). Usually small contact angles (lower than 90º) corresponds to high wettability while large contact angles (higher than 90º) corresponds to low wettability (Biophy Research, 2013; Bracco et Holst, 2013).

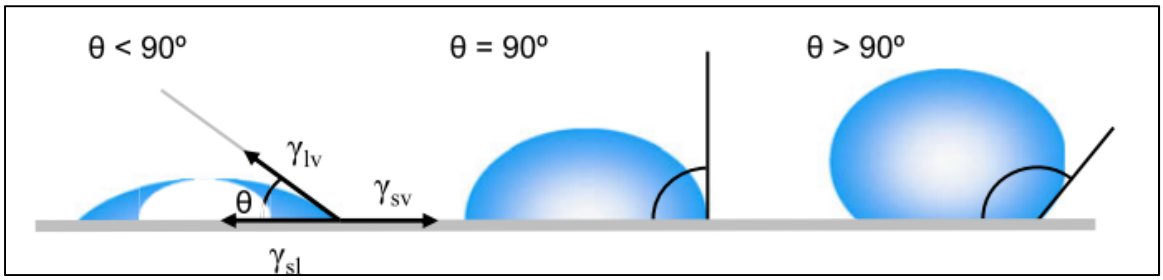

Figure 3.3 Illustration of contact angles formed by drops on solid surfaces
Taken from (Bracco et Holst, 2013)

$$\gamma_{sv} - \gamma_{sl} - \gamma_{lv}\cos(\theta) = 0 \qquad (3.1)$$

(Young Dupre equation)

Contact angle is largely used in the biomaterials domain since it is a low cost, simple technique that can give us information about the hydrophobicity and polar nature of materials. However contact angle does not give us information about the chemical composition of the material and the measurements can be affected by several factors such as contaminations and time between the measurement and the drop placing (Biophy Research, 2013; Temenoff et Mikos, 2008).

In this project the wettability of the surfaces was measured by static water contact angle, with a VCA Optima XE (AST products, Billerica, MA) and a syringe (100µl technical syringe, Hamilton, Reno, USA). After the preparation of surfaces as detailed in 3.1, the sample holder was cleaned with an aqueous solution of ethanol 70% v/v and the syringe was rinsed 5 times with Milli-Q water before use. Contact angle measurements were done using Milli-Q water drops of 2 µl size on samples of 1cm^2. The measurements were taken ≈3 seconds after the

droplet was placed on the surface. Three measurements were performed for each surface and three surfaces were prepared for each condition in each experiment.

3.2.2 AFM

Atomic force microscopy (AFM) is a technique that allows imaging the topography of a surface. This technique provides three dimensional images of the surface ultrastructure with molecular resolution. AFM is widely used for materials characterization since it obtains images in real time and requires minimal sample preparation. The AFM can be used to probe the physical properties of the sample such as molecular interactions, surface hydrophobicity, surface charges and mechanical properties. The AFM imaging is performed by sensing the force between a very sharp probe and the sample surface (Figure 3.4). The image is generated by recording the force changes as the sample is scanned by the probe in x and y directions (Dufrene, 2002).

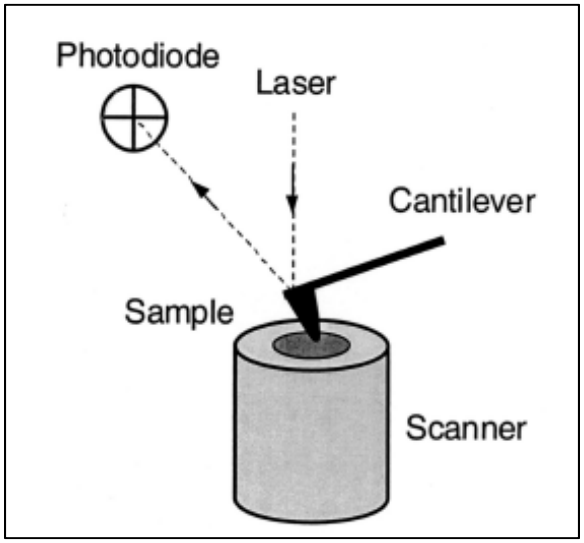

Figure 3.4 AFM principle
Taken from (Dufrene, 2002)

The sample is mounted on a piezoelectric scanner and the force is monitored by attaching the probe to a cantilever which acts as a spring. The force is then measured by the deflection of the cantilever. The deflection or bending of the cantilever is measured by a high resolution

optical method in which a laser beam is focused on the free end of the cantilever and the position of the reflected beam is detected by a photodiode as seen on Figure 3.4.

In an intermittent contact mode of AFM the cantilever moves rapidly with a large oscillation between the repulsive and attractive forces. In this mode, a piezoelectric element in the tip of the cantilever confers it an oscillation at determinate amplitude and when the tip is brought in close proximity of the sample surface, physical or chemical interactions (dipole-dipole forces, van der waals etc.) may occur between the sample and the tip causing a decrease in the oscillation amplitude. In order to maintain a constant oscillation amplitude, the height of the sample placed on the piezoelectric scanner is adjusted. The images are obtained by the measurements of the intermittent contact between the sample and the tip, captured by the optical system mentioned before. The shift on the phase signal (which corresponds to the difference between the initial frequency and the modified one) allows us to obtain a phase image. The phase image represents the properties of the material but is not possible to quantify them (Bowen et Hilal, 2009; Variola, 2015).

In this project LP based bioactive coatings were analyzed by AFM in order to determine if there is a change in the topography when grafting CS. The roughness value Rq obtained by the AFM analysis was compared between surfaces. Briefly LP surfaces where cut in $1cm^2$ squares, prepared as detailed in section 3.1.2, cleaned with nitrogen air (Praxair, Canada) and placed in the piezoelectric scanner for the AFM analysis. Samples were measured in duplicate and an area of 100 μm^2 was scanned from each sample. Representative images of 10x10 μm^2 and 2x2 μm^2 were captured.

3.2.3 CS grafting potential by Toluidine Blue

For the quantification of CS grafted in LP or commercial amine plates a colorimetric assay with Toluidine Blue O *(7-amino-8-methylphenothiazin-3-ylidene)-dimethylazanium;chloride* further referred just as TBO was used (Figure 3.5). TBO is a phenothiazine cationic dye which interacts with negatively charged groups via electrostatic attraction. It can be easily

detected by light absorption in the blue region. (Tiraferri et Elimelech, 2012; Wei et al., 2007).

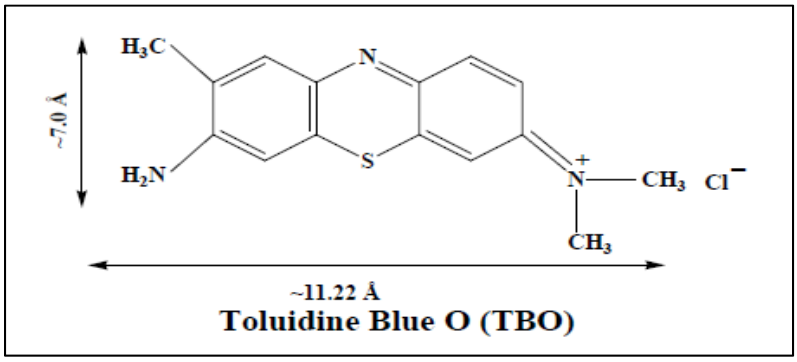

Figure 3.5 Toluidine Blue O structure
Taken from (Jebaramya, Ilanchelian et Prabahar, 2009)

TBO has affinity to sulfates, carboxylates and phosphate radicals. It can be detected by spectroscopy with a maximum peak of light absorption at a wavelength around 630 nm. Toluidine blue can be considered as a cation which interacts with the negative groups of chondroitin sulfate such as SO_3^- and COO^-. In alkaline conditions CS negative groups interact with TBO, while in acidic conditions the equilibrium tend to neutralize the negative charges of CS (for example COO^- becomes COOH) and the Toluidine blue can be released. (Sridharan et Shankar, 2012; Wei et al., 2007).

In this project, grafted CS was quantified through Toluidine blue adsorption based on a previously described method (Tiraferri et Elimelech, 2012). LP and PET were cut in circles of 10mm diameter with the help of a punch cutting set (General Tools, India). CS grafting was performed on LP and commercial amine plates as detailed in section 3.1.2. The surfaces were immerged in a 100µM solution of TBO (Sigma Aldrich, USA) in water adjusted at pH 10 with 1N NaOH. After 1h incubation at 40°C surfaces were rinsed three times with pH 10 buffer and let dry at room temperature. Pictures of the films before desorption of TBO were taken at 2X (Stereo microscope SZX10, Olympus, Canada). Desorption of TBO was induced by immerging the surfaces in 50% acetic acid (Sigma Aldrich, USA) solution in Milli-Q water. After the immediate desorption of TBO in the acetic acid solution, samples were

homogenized. The quantity of TBO was detected by reading 150µl samples of the desorption solution in 96 well plates at 630 nm and 531 nm. Samples were prepared in quadruplicate and read in triplicate.

For calculating the quantity of TBO released by each sample, the absorbance at 630nm was subtracted from the one at 531nm to cover only absorbance of TBO. From the previous values, back ground signal was subtracted and the absorbance values were converted to concentration values with use of a calibration curve. For the calibration curve, absorbance of TBO solutions (10µM to 0µM) in desorption liquid were read and a linear regression was performed. Concentration values of TBO were converted into moles by multiplying the concentration (molarity) by the volume of desorption liquid used on each sample. Finally the moles of each sample were divided by the area of the sample to present the quantity of TBO released per mm^2.

3.2.4 Amino group surface density by Orange II

Orange II is an anionic dye which has proven to be useful for amino group quantification in a reliable and specific way (Noel et al., 2011). It is a sensitive technique due to Orange II unique negative charge which interacts with the positive charge of amino groups (Figure 3.6). The quantification is done through a colorimetric assay. The principle of this technique is based on reversible electrostatic interactions between the negatively charged sulfonated dye and the positive charge of the protonated amino groups in acidic solution. After the interactions are performed in the acidic solution (pH 3), the release of Orange II into the solution is triggered under alkaline conditions (pH 12). The amount of Orange II can be quantified by reading the absorbance of the solution in which the Orange II was released and perform a calibration curve with known concentrations of Orange II. The absorbance for Orange II is read at 484 nm. (Noel et al., 2011).

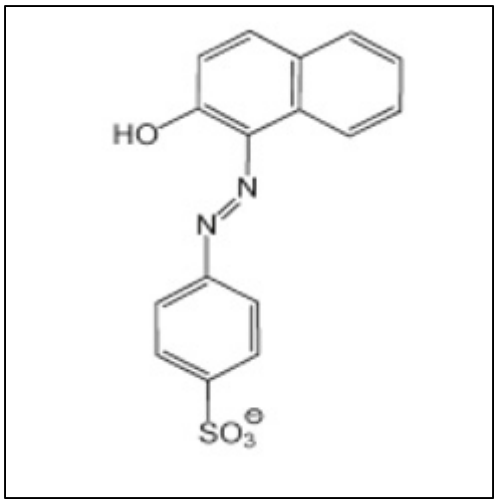

Figure 3.6 Orange II molecule
Taken from (Noel et al., 2011)

This colorimetric assay was chosen since it is economic, quantitative, fast, and much easier to perform on commercial amine culture plates than XPS or fluorescence spectroscopy with o-phthaldehyde (OPA). Orange II has been reported as one of the best anionic dyes for amino group quantification in contrast to other dyes such as Coomassie Brillant Blue due to its low steric hindrance (Noel et al., 2011).

For this project the amine groups of LP and commercial amine plates were quantified by Orange II based on a previously described method (Noel et al., 2011). LP and PET were cut in circles of 10mm diameter with the help of a punch cutting set (General Tools, India). Surfaces were immerged in a 14mg/ml solution of Orange II (Orange II sodium salt, Sigma Aldrich, USA) in pH3 Milli-Q water adjusted with HCl (Grade ACS, EMD Millipore, Germany). After 30 minutes of incubation in dark at 40°C, surfaces were rinsed 3 times with pH 3 Milli-Q water and let dry at room temperature. Desorption of the Orange II was induced by immerging the surfaces in pH 12 Milli-Q water adjusted with 1N NaOH (Fisher Scientific, USA) for 15 min at room temperature. After homogenization, samples of 150µl were taken and 1% of HCL was added. Samples were read at 484 nm in a 96 well plate. Samples were prepared in quadruplicate and read in triplicate.

For the quantification of Orange II, a standard curve was generated by measuring the absorbance of Orange II solutions at different concentrations ranging from 100μM to 0 μM. The concentration of Orange II on the samples was determined using the linear regression of the calibration curve which relates the absorption to the concentration. In order to obtain the moles of Orange II released, the concentration of Orange II (molarity) was multiplied by the volume of desorption liquid used on each sample. Finally the moles of each sample were divided by the area of the sample to present the quantity of Orange II released per mm^2.

3.2.5 Measure of protein adsorption

In order to evaluate the extent of protein adsorption on commercial amine plates grafted with CS, albumin from bovine serum conjugated with Texas Red fluorescent molecule was used. As explained in chapter I, protein adsorption is a phenomenon highly related with cell adhesion. Biomaterial properties may influence cell adhesion directly by cell-surface interactions or indirectly by modulating protein adsorption and subsequently, protein-mediated cell adhesion. The appropriate protein adsorption into a substrate may promote cell adhesion. Albumin is the most abundant protein in plasma thus it is very likely that albumin will be the first one to populate a biomaterial in the body. Later on, it may be replaced by other less abundant but more specific binding proteins that may enhance cell adhesion (Vroman effect) (Von Recum, 1998).

Therefore albumin adsorption on a biomaterial may indicate if the surface is appropriate for protein adsorption and may enhance cell adhesion or it can also indicate an antifouling potential of the material. As previously mentioned, antifouling is the capacity of a material to prevent attachment of biomolecules (such as proteins), cells or organisms (Hamming et Messersmith, 2008). Previous work at LBeV have shown that grafted CS can decrease protein adsorption and create low-fouling surfaces (Thalla et al., 2014).

In this project CS was grafted at different concentrations ranging from 1% to 0.0001% w/v of CS on commercial amine plates as described in section 3.1.2. In order to evaluate the

influence of CS concentration during grafting on protein adsorption, the surfaces were incubated with albumin from bovine serum conjugated with Texas red (Invitrogen, Molecular probes, USA), further referred to as Texas Red. Surfaces were incubated with 100µl per well of 0.2 mg/ml Texas red solution diluted in PBS 1X (modified PBS, without calcium chloride and magnesium chloride, Wisent bioproducts, Saint-Bruno, Canada). Surfaces were incubated for 2h in dark at room temperature. After incubation surfaces were rinsed three times with PBS 1X and five times with Milli-Q water to remove unbound protein. After the rinses, 50µl of Fluoromount (Sigma Aldrich, USA) was added per well.

Finally pictures were taken at 2X in the center of each well with the use of a fluorescence microscope (Olympus IX71 inverted system microscope, USA) and its TRITC filter. Fluorescence intensity of the images was analyzed with the software Image J (Fiji, Image J, USA).

3.3 Preparation of a chitosan hydrogel with chondroitin sulfate

Chitosan hydrogels with CS were prepared for evaluating the effect of CS on cell viability inside a 3D scaffold. For this part of the project, we used chitosan thermosensitive physical hydrogels previously developed by the team which have been shown to present good mechanical properties and cell viability (Assaad, Maire et Lerouge, 2015; Ceccaldi et al., submitted 2015; Monette et al., 2016). These gels were simply modified by adding low or high concentration of CS, without covalent binding. Mechanical properties of the hydrogels were studied prior to the cell encapsulation. Hydrogel preparation and mechanical characterization (rheology tests) are described next.

3.3.1 Materials for hydrogels preparation

The physical chitosan and chitosan-CS hydrogels were prepared by mixing an acidic chitosan solution with a basic gelling agent solution as described in the following text. Shrimp shell chitosan (Kitomer, PSN 326-501, Premium Quality, Mw 250 kDa, DDA 94%) was

purchased from Marinard Biotech (Rivière-au-Renard, QC, Canada). Sodium phosphate monobasic NaH_2PO_4 (SPM), sodium phosphate dibasic Na_2HPO4 (SPD), Sodium dodecyl sulfate (SDS) and Chondroitin sulfate A from bovine trachea (CS) were obtained from Sigma-Aldrich (Oakville, ON, Canada). Sodium hydrogen carbonate $NaHCO_3$ (SHC) was purchased from MP Biomedicals (Solon, OH, USA).

3.3.2 Chitosan solution

Chitosan (CH) was purified prior to use by a method published previously (Assaad, Maire et Lerouge, 2015). For the purification, 6 g of raw CH were dissolved in 600 mL of 0.1 M HCl by stirring overnight at 40°C. The acidic solution was filtered under vacuum to remove insoluble particles. The CH was then precipitated with 0.5 M NaOH under continuous stirring (pH 8–9). After the precipitation, 6 mL of SDS 10% (w/v) was added to the slurry and heated at 95°C for 5 min. After cooling down to room temperature, the pH was adjusted to 10 with 0.5 M NaOH. The slurry was filtered under vacuum and the hydrated CH was washed 5 times with 600 mL of Milli-Q water at 40°C. Finally, the CH was freeze-dried, ground and sieved to obtain the dried and purified CH powder.

After the purification, the chitosan solution for the hydrogels was prepared by solubilizing the chitosan powder in 0.1M HCl at 3.33% (w/v) overnight with a magnetic stirrer. Finally the solution was sterilized by autoclaving (20 min, 121°C) and stored at 4°C.

3.3.3 Gelling agent solutions

In this project hydrogels for characterization and for cell encapsulation were prepared. In both cases, the gelling agent (GA) used is a mixture of SHC and phosphate buffer (PB), at a final concentration in the hydrogel of 0.075M and 0.04M respectively. PB was prepared with a mixture of SPD and SPM at a molar ratio of 0.932/0.068 dissolved in Milli-Q water and adjusted at pH 8. SHC salt was further incorporated by dissolving it in PB. In case of the hydrogels containing CS, the CS was dissolved into the GA solution to obtain a final

concentration of 10000 µg/ml (1% w/v) or 500 µg/ml (0.05% w/v) in the hydrogel. All solutions were filtered through a 0.20µm filter (Corning, USA) prior to use. Table 3.1 shows the concentrations at which the gelling agent solutions were prepared and their final concentration in the hydrogel. The hydrogel preparation methods are described next.

Table 3.1 Concentrations of gelling agent

Hydrogels	Concentration in the GA solution			Concentration in the hydrogel		
	PB (M)	SHC (M)	CS (w/v)	PB (M)	SHC (M)	CS (w/v)
Characterization	0.10	0.1875	2.5%, 0.125% 0%	0.04	0.075	1%, 0.05% 0%
Cell encapsulation	0.20	0.375	5%, 0.25% 0%	0.04	0.075	1%, 0.05% 0%
In both cases chitosan initial and final concentrations (in the hydrogel) were 3.33 and 2% (w/v) respectively.						

3.3.4 Preparation of the hydrogels

The hydrogels for characterization were prepared by mixing CH solution with the previously described GA solution at a volume ratio 3:2 respectively. The mixing was done using 2 syringes (Terumo, USA) one containing the CH solution and other the GA, syringes were joined by a Luer lock (Qosina, USA) connector and the contents of the syringes were pushed from side to side (15 times) to mix both components. For cell encapsulation the hydrogel preparation was slightly different. Chitosan solution was first mixed with 2X concentrated GA solution at a volume ratio 3:1 using the same 2 syringe technique. Immediately after the mixing, the content was push into one syringe and another syringe containing a cell suspension (2.5M cells/mL in culture medium) at a ratio 4:1 was connected and the fillings

were mixed again. The cell culture conditions will be further detailed in section 3.4.5. Both hydrogel preparation methods are illustrated in Figure 3.7. Rheological properties of hydrogels prepared for cell encapsulation were also tested for comparison.

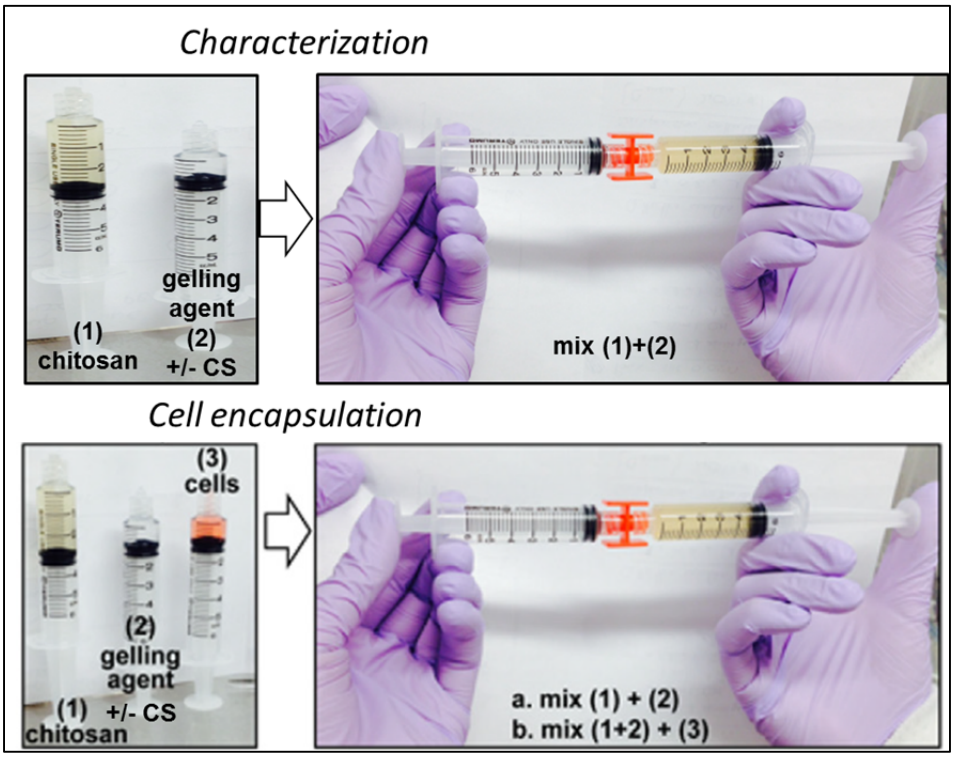

Figure 3.7 Hydrogels preparation methods
Adapted from (Monette et al., 2016)

3.3.5 Rheological testing of hydrogels

Since addition of CS could modify gel properties, hydrogels containing CS or not were characterized to study their gelation. If implantable, the hydrogel should remain liquid and stable at room temperature for its stocking and it should gel rapidly upon reaching body temperature. Rheology tests allow to verify the gelation kinetic at body temperature as well as the rigidity of the hydrogel by measuring the hydrogels storage modulus (G') and loss modulus (G") as a function of time. The storage modulus measures the stored energy (elastic portion) and the loss modulus measures the energy dissipated as heat (viscous portion) (Assaad, Maire et Lerouge, 2015).

Rheological properties were investigated using an Anton Paar instrument (Physica MCR 301, Germany) with coaxial cylinder geometry (CC10/T200). Immediately after preparing the hydrogel, the storage modulus (G') and loss modulus (G") were measured in the linear viscoelastic range, at a constant shear stress (1 Pa) and constant frequency (1 Hz). The measurements were carried out at 37°C for 1h for each 1.5mL sample. The measurements were repeated at least three times.

3.4 Effect of CS containing solution, surfaces and hydrogels on MSC

To evaluate the benefit of CS, biological tests were performed on MSC in contact with CS in solution or contained in bioactive surfaces or hydrogels. The cell culture tests are described next.

3.4.1 Cell types

In this project human mesenchymal stem cells (hMSC) from the bone marrow of three different donors were used from passages 4-8. The cells were obtained from Lonza products (Canada), Stem cell technologies (Canada) and Texas A&M Institute for Regenerative Medicine (USA). Lonza cells were expanded in Lonza's human Mesenchymal Stem Cell Growth BulletKit Medium (Lonza, Canada). Stem cell technologies and Texas A&M Institute for Regenerative Medicine cells were expanded in supplemented serum-free MSC NutriStem XF medium (Biological industry, Israel). All experiments were done in alpha MEM (1X) + Glutamax-I medium without ribonucleosides and desoxyribonucleosides (Gibco, USA). For experiments in complete medium, the medium was supplemented with 10% fetal bovine serum for MSCs (MSC FBS; Gibco, USA).

Primary rat mesenchymal stem cells (rMSC) extracted from rat bone marrow were a gift from Dr. Caroline Ceccaldi from LBeV laboratory (CRCHUM, QC, Canada). The rMSC experiments and expansion was done in alpha MEM (1X) + Glutamax-I medium without

ribonucleosides and desoxyribonucleosides supplemented with 10% fetal bovine serum (FBS; Gibco, USA). In case of serum free conditions, medium was used without FBS.

Vascular smooth muscle cells from rat embryonic thoracic aorta (a7r5 cell line, ATCC, Manassas, USA), further referred as VSMC were cultured from passages 2-4. VSMC experiments and expansion was done in Dulbecco's Modified Eagle's Medium/Nutrient Mixture F-12 Ham's Medium (DMEM/F12; Invitrogen, Burlington, Canada) supplemented with 10% FBS (Invitrogen, Burlington, Canada). In case of serum free conditions, the medium was used without FBS.

Trypsin 0.05% with EDTA4Na, modified PBS (without calcium chloride and magnesium chloride) and penicillin-streptomycin were purchased from Invitrogen (Canada). Experiments were done in the corresponding medium with 1% of penicillin-streptomycin to prevent contaminations.

3.4.2 Methods of characterization of the cellular response

For characterizing the cellular response in the different experiments, two main techniques were used: alamar blue and crystal violet. Alamar Blue was used to evaluate metabolic activity of the cells which can be related to its viability and crystal violet staining was used to fix and stain cells in order to observe their morphology.

3.4.2.1 Alamar blue

Alamar blue cell viability reagent dye is a redox indicator that yields a colorimetric change and fluorescent signal in response to metabolic activity of cells. It is a safe, non-toxic and fluorescent detection method. It is used for quantitative analysis of cell viability and cell proliferation. Damaged or non-viable cells have lower/no innate metabolic activity and generate a lower signal/or no signal, while viable cells generate a high fluorescent signal (Thermo Fisher Scientific, 2015).

Alamar blue also called resazurin is an oxidized, blue non fluorescent compound that in contact with cells is reduced to a pink fluorescent dye in the medium by cell activity. The reduction is likely caused by oxygen consumption through cells metabolism and mitochondrial enzymes. In this process a 10% (v/v) mix of resazurin in culture medium is added to the cells and incubated from 1-4h, during the incubation resazurin is reduced to resorufin and the change is measured by fluorimetry. There is a direct correlation between the reduction of resazurin in the growth medium and the quantity/proliferation of cells. This correlation has been demonstrated in several cell lines (O'Brien et al., 2000).

For the different experiments performed in this project the cell viability was studied by exposing the cells to alamar blue (Cedarlane Corp., Burlington, ON, Canada) added to the culture medium (10% v/v) for 4h at 37°C and 5% CO_2. After the incubation, the fluorescence signal was read using a microplate fluorescence reader (BioTek Instruments Inc., Synergy 4, USA) at 560 and 590 nm, for excitation and emission wavelengths, respectively.

3.4.2.2 Crystal violet staining

Cell density and morphology on surfaces was evaluated via crystal violet staining (Fisher Scientific, Ottawa, ON). Cells were incubated in a crystal violet solution (0.075% w/v in 3% v/v acetic acid solution) for 15 min, rinsed 3 times with Milli-Q water and air-dried. Finally pictures were captured at 5X using a microscope with a coupled camera (Leica Microsystems, Richmond Hill, ON, Canada).

3.4.3 Effect of growth factors and CS in solution

The growth and survival effect of CS in solution was tested in hMSC, rMSC, followed by VSMC for comparison. For this experiments CS was first dissolved in sterile water at an intermediate concentration of 0.05g/ml and sterilized using a 0.20µm sterile filter (Corning, USA). Then the CS was dissolved in the appropriate culture medium (in serum free or serum containing media) at different final concentrations to study the dose response.

Moreover various growth factors (Recombinant human epidermal growth factor (EGF), vascular endothelial growth factor (VEGF) and basic fibroblast growth factor (FGF) (Peprotech, USA)) were tested on hMSC and rMSC. To that effect, the GF were diluted at different concentration in serum free (0% FBS) or low serum (2% FBS) medium.

In all experiments, cells were seeded in tissue-culture polystyrene 96 well plates (Corning, USA) to reach an 80%- 90% confluency in complete medium after 24h of incubation (37°C, 5% CO_2). At 24h, cells were rinsed with PBS 1X and medium was changed with the different experimental conditions. The culture medium was changed every 2 days and new GF or CS were diluted in the medium prior to each media change. The cells metabolic activity was monitored at different time points (i.e. from 24h to 7days) by alamar blue method (100µl of 10% (v/v) alamar blue in complete medium (10% FBS) was used per well). Cell morphology and density was observed by staining cells with crystal violet (100ul/well).

3.4.4 Cell behavior on bioactive surfaces

In the following steps, the project was limited to CS only, since data with GF in solution was not convincing (see results section). hMSC adhesion and growth were tested on the CS-containing bioactive coatings in complete medium. Survival of cells in serum free medium was also tested on LP-based bioactive coatings. The methods used for cell culture on the coatings are described below.

3.4.4.1 Cell culture on LP based bioactive coatings

Cell adhesion and growth on CS-grafted surfaces: LP+CS coated PET was cut in 1cm^2 squares in sterile way, with the use of a scalpel and a sterile glass with a grid. The LP squares were placed over Parafilm (Bemis, USA) and CS grafting was performed as described in section 3.1.2. Cells were seeded using cloning cylinders placed on the surfaces (10 mm diameter glass cloning cylinder, 200 µl complete growth medium with cells) in 24 well plates (Corning, USA). Cell densities used were either 10,000 or 15,000 cells per surface for Lonza

lot or either 5,000 or 10,000 per surface for Texas lot. After 4h of seeding, the cloning cylinders were removed and the surfaces were rinsed with PBS 1X to detach non-adherent cells. Complete growth medium was added (500 µl/well) and cells were incubated at 37 °C and 5% CO_2 and the medium was changed every 2 days. After different time points (24h, 4d and 7d) cell metabolic activity was evaluated by alamar blue (500µl per well, 450µl being transferred to a new plate after the incubation for the reading). Finally cells were stained with crystal violet (500µl/well).

Cell survival on bioactive coatings: a similar protocol was used except that, after 24h of incubation in complete medium, cells (15 000 cells/cloning) were rinsed with PBS 1X and serum free medium was added (500 µl/well). Cells were incubated in serum free conditions for 3 days and 7 days. In each experiment, four samples per condition were used.

3.4.4.2 Cell culture on amine plate based bioactive coatings

In order to compare the effect on cells of different CS-grafted amine-rich surfaces, commercial amine plates were also used to create bioactive coatings. CS was grafted on 96 well commercial amine plates, and cell behavior was tested as described above, except the following small differences: i) A CS concentration gradient was used since the concentration used on LP prevented cell adhesion on amine plates (see results section), ii) Cells were seeded in complete medium at a density of 5000 cells/well, in 200 µl of complete growth medium, iii) In addition to alamar blue, cell morphology and density was observed and pictures were captured at 5X (Leica Microsystems, Richmond Hill, ON, Canada).

3.4.5 Cell culture in 3D chitosan hydrogels

The hydrogels for cell encapsulation were prepared as described in section 3.3. The hydrogels samples containing the cells (250000 cells in 0.5mL each) were deposited in 48 well culture plates (Corning, USA) and left to gel for 5 min in the incubator (37°C, 5% CO_2). After the gelation, 0.5 ml of cell culture medium (alpha MEM with 10%FBS or NutriStem

XF medium) was added on top of the gel and samples were put back in the incubator. Figure 3.8 illustrates a cell-containing hydrogel inside a well. Cell culture medium was changed twice per week. Cells were incubated in the hydrogels at different time points (24h, 4d, and 7d). Cell metabolic activity was evaluated by alamar blue using the following method: 500µl of 10% (v/v) alamar blue in complete medium was added per well. The samples were homogenized by mixing the hydrogel with the solution and after the incubation, 100µl were transferred to a 96 well plate for fluorescence reading. In each experiment three samples per condition were used.

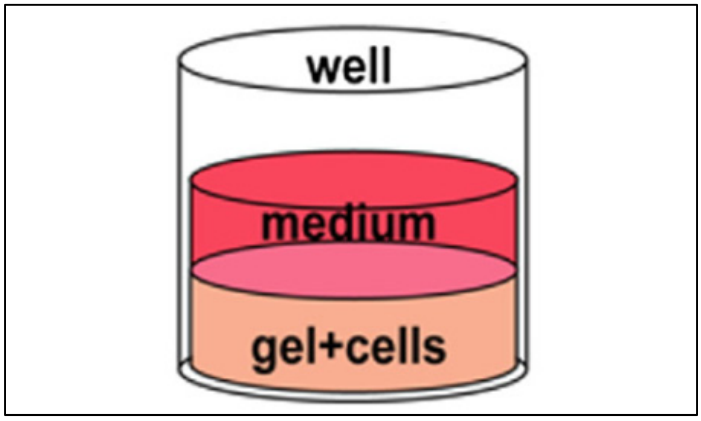

Figure 3.8 Cell-containing hydrogel inside a well
Adapted from (Monette et al., 2016)

3.5 Statistical Analysis

All the results are expressed as mean ± standard deviation (SD). Statistical analysis was done using Statgraphics software (Statgraphic centurion, statpoint technologies Inc., USA). To determine if a statistical difference between means existed, one way ANOVA was used. For comparing two conditions, independent two sample t-test with equal variances was used. A p-value lower than 0.05 was considered significant for all tests. When multiple means were compared, Tukey honestly significant difference test was used with a confidence level of 95%. Each experiment figure indicates on its label the number of independent experiments done (N), and the number of samples per condition used for each independent experiment (n).

CHAPTER 4

RESULTS

4.1 Effect of biomolecules in solution

Before any grafting on the surfaces, the effect of CS and various growth factors (GF) on cell survival and growth was first tested in solution, by adding them in the culture media, either in normal serum (NS, 10% FBS), low serum (LS, 2% FBS) or in serum free medium (SF, 0% FBS).

4.1.1 Effect of Growth factors

MSC were exposed to different GF in solution, in order to identify which would better enhance cell survival once grafted in bioactive surfaces. EGF, VEGF and FGF were tested on the different hMSC lots used in this project. EGF effect was also tested in rMSC. The growth factors tested and their concentrations were based on literature review as described in section 1.6.2.

In this project, cell metabolic activity (alamar blue) was used to evaluate the number of viable cells at each time point, and it is expressed as viability percentage, calculated as the ratio of fluorescence signal to the control signal (after 24h adhesion). Although it is called "viability", this result depends both on the survival and possible proliferation of cells, which are more or less promoted depending on the type of media used (normal media (NS, 10% FBS), low serum concentration (LS, 2% FBS) or without serum (SF)). Figure 4.1 presents the viability percentage of hMSC (Stem cell technologies lot) in presence of EGF at increasing concentrations and FGF at 1ng/ml after 4 and 7 days in LS and SF. EGF at a concentration of 10 ng/ml (concentration at which a pro-survival effect has been observed in other cell lines such as VSMC (Lequoy et al., 2014)) was also tested in combination with FGF. In SF, cell survival was about 40% after 4 and 7 days, while in LS cell number increased above initial

numbers raising 130-140% at 4 days and around 160% after 7 days. However, in both SF and LS, adding GF had no significant effect when compared to media without GF.

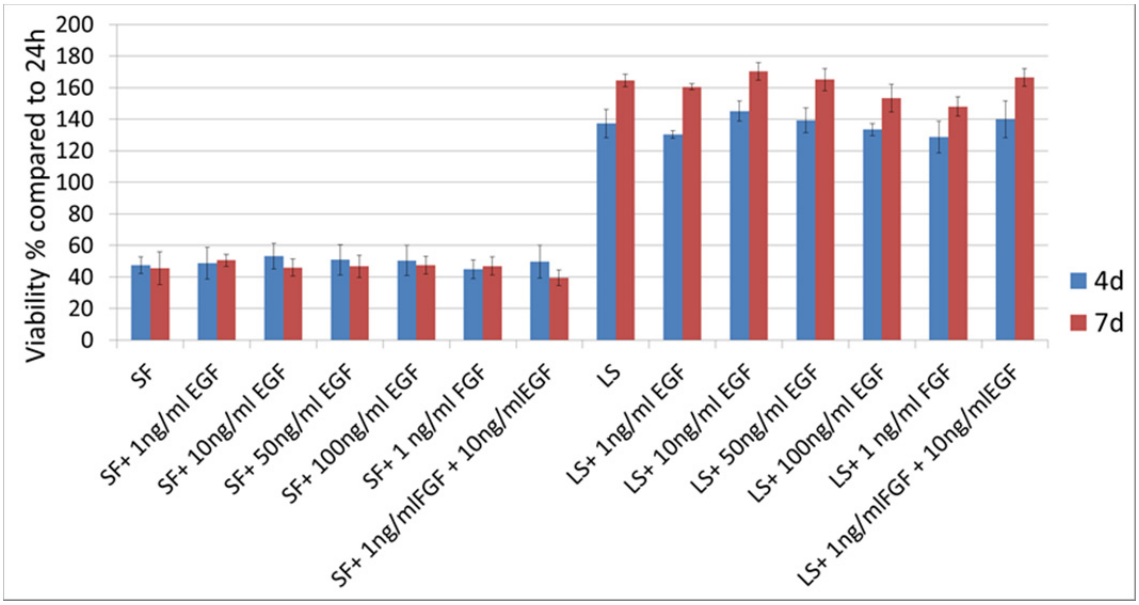

Figure 4.1 Effect of GF on hMSC viability after 4 and 7 days in low serum (LS; 2%) or serum free (SF) medium (cell source =Stem cell technologies). Results are expressed as percentage of alamar blue fluorescence signal compared to signal after 24h adhesion in complete medium (mean ± SD; N=1, n=4)

Since these negative results were unexpected, the tests were repeated with hMSC from Texas A&M Institute for Regenerative Medicine (as shown in Figure 4.2). In all cases, results were similar, i.e. no statistical difference was found between SF or SF+EGF. Results suggest that, under the conditions tested, these GF do not provide any pro-survival effect.

EGF does not provide a growth advantage in complete media either, the effect of EGF in NS (10% FBS) was also tested but results indicated no statistical difference between NS or NS+EGF (data not shown). The effect of EGF in SF was also tested on rat MSC (rMSC) to analyze if there is a difference between species. Results indicated no survival advantage either (Results shown in appendix; Figure-A I-1).

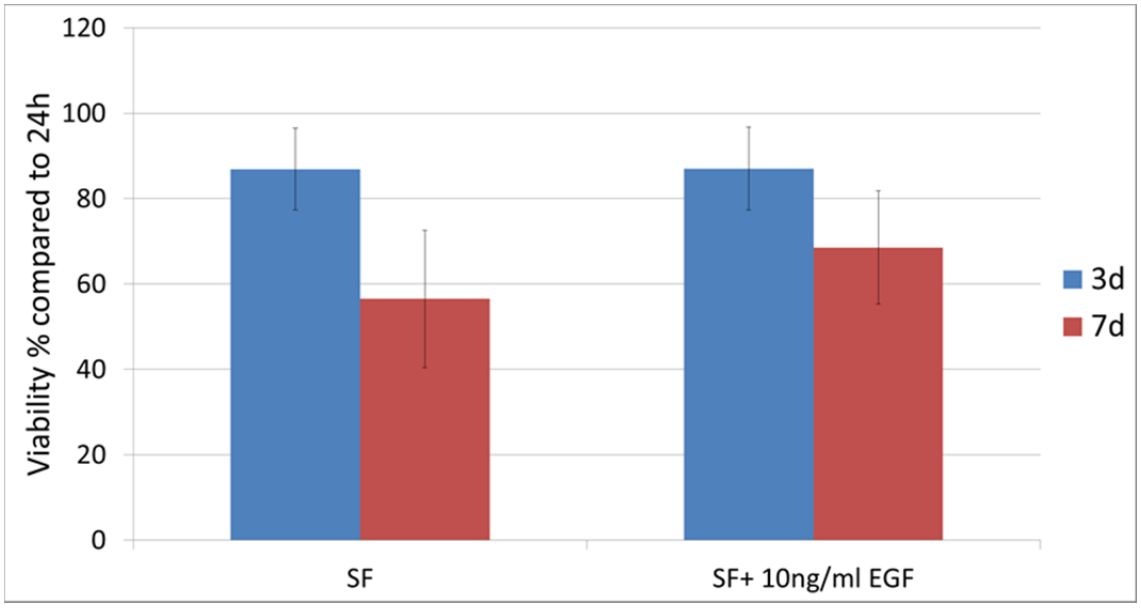

Figure 4.2 Effect of EGF on hMSC viability after 3 and 7 days in serum free (SF) medium (cells source = Texas A&M Institute for Regenerative Medicine). Results are expressed as percentage of alamar blue fluorescence signal compared to signal after 24h adhesion in complete medium (N=2, n=4)

Finally, VEGF effect in SF was tested but no pro-survival effect was observed either (Figure 4.3). Therefore since a GF that provides a pro-survival effect to MSC could not be found when tested in solution, no growth factors covalently grafted in bioactive surfaces were tested in this project (in contrast to the bioactive surfaces with GF tested previously by LBeV in other cell lines as described in the literature review (Charbonneau et al., 2012; Lequoy et al., 2014)). The rest of the project was exclusively focused on the effect of CS.

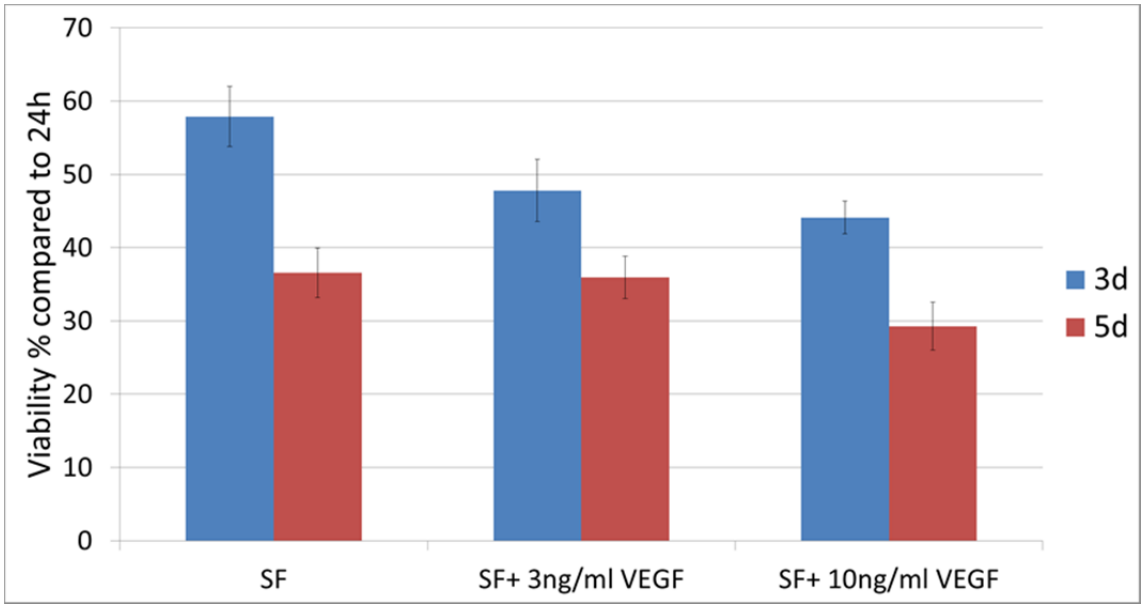

Figure 4.3 Effect of VEGF on hMSC viability after 3 and 5 days in serum free (SF) medium (cells source = Lonza). Results are expressed as percentage of alamar blue fluorescence signal compared to signal after 24h adhesion in complete medium (N=1, n=4)

4.1.2 Effect of Chondroitin sulfate

The effect of CS was first tested on hMSC. Then, tests were also performed on rat MSC and VSMC to compare cell behavior in response to CS among different cell lines.

4.1.2.1 CS effect on hMSC

Figure 4.4 presents the effect of CS (at 250µg/ml) on the survival of hMSC (Stem cell technologies lot) after 4 and 7 days in NS, LS and SF. As expected, cell viability decreases when decreasing the FBS concentration in culture media. In NS or LS, adding CS has no significant effect when compared to media without CS. However a very pronounced effect is observed when cells are immersed in SF, cells viability being lower in SF+CS than in SF for each time point.

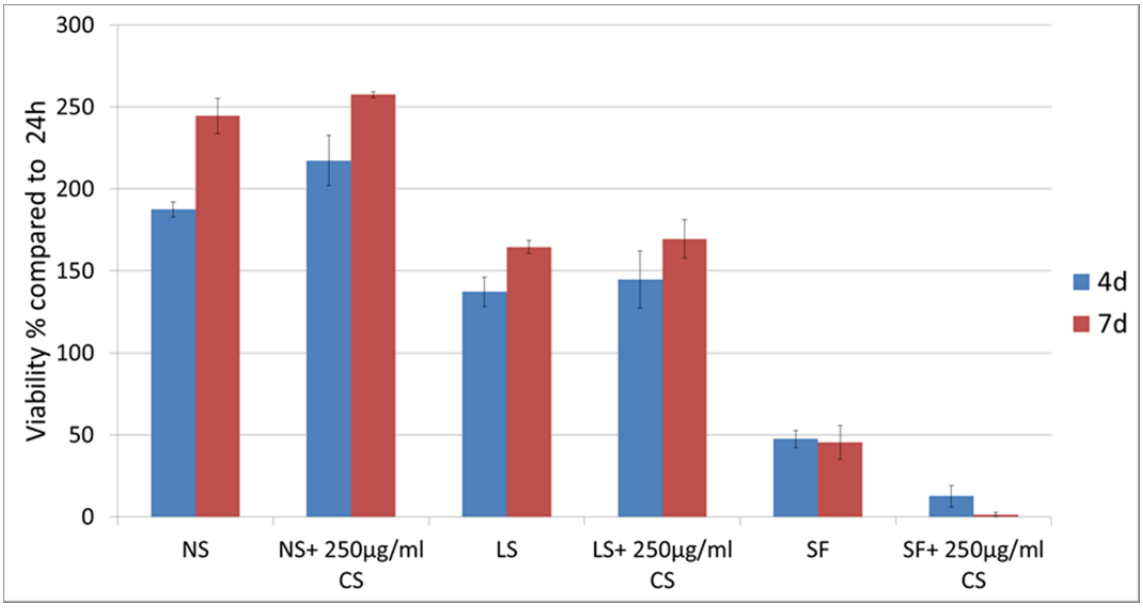

Figure 4.4 Effect of CS in solution on hMSC viability after 4 and 7 days in normal serum (NS), low serum (LS) or serum free (SF) medium (cell source =Stem cell technologies). Results are expressed as percentage of alamar blue fluorescence signal compared to signal after 24h adhesion in complete medium (mean ± SD; N=1 n=4 each)

The effect observed in SF+CS was similar with the other hMSC lots used in this project, as shown with hMSC from Texas A&M Institute for Regenerative Medicine ($p<0.05$, Figure 4.5). Cells were observed under the microscope after exposing them to SF+CS; round cell morphology suggests that cells are detaching from the surface as seen in Figure 4.6. The morphology induced by CS in SF was not observed in SF without CS.

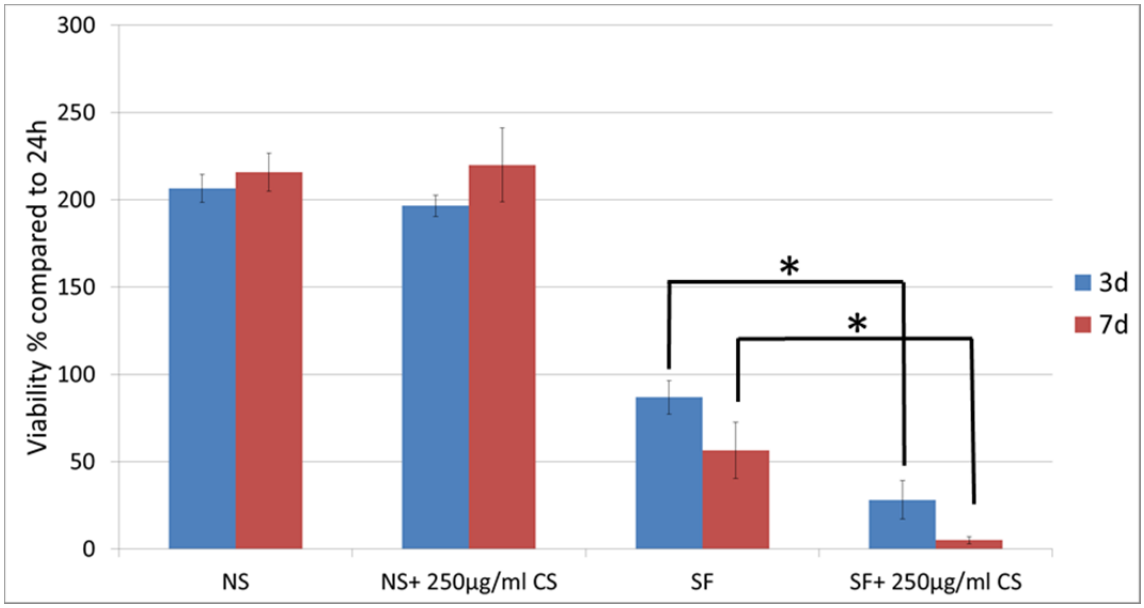

Figure 4.5 Effect of CS in solution on hMSC viability after 3 and 7 days in normal serum (NS) and serum free (SF) medium (cells source = Texas A&M Institute for Regenerative Medicine).Results are expressed as percentage of alamar blue fluorescence signal compared to signal after 24h adhesion in complete medium (N=2, n=4) (*$p<0.05$)

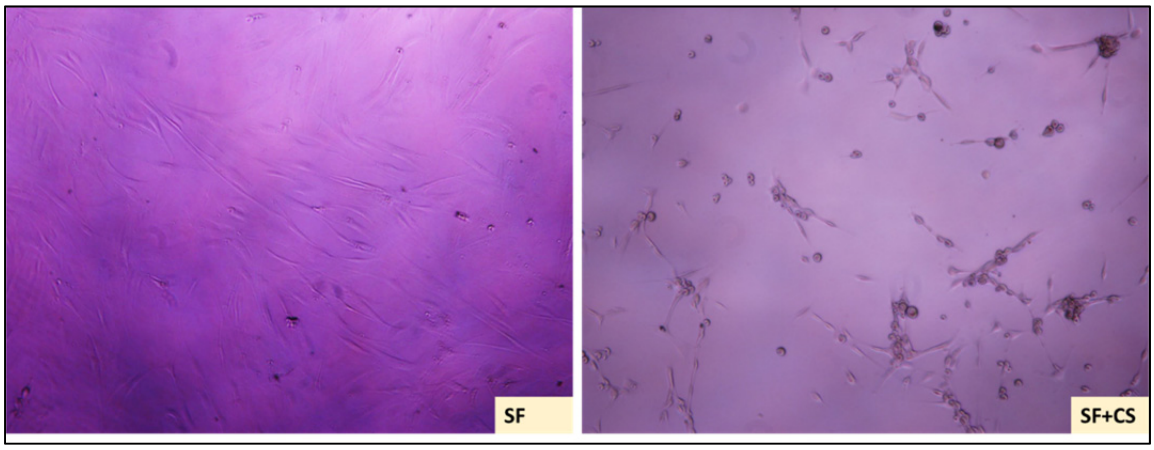

Figure 4.6 hMSC after 5 days in SF and SF+CS. The round individual morphology may indicate that cells are about to detach from the surface

The effect of SF+CS in hMSC was also compared to rMSC to analyze if there could exist a difference when the same cell type is analyzed between species. Results show that at 3 days of exposure to SF+CS rat cells are resistant to cell detachment but by 5 days cell detachment was induced ($p<0.05$, Results shown in appendix; Figure-A I-2).

In order to further confirm hMSC detachment caused by CS in SF conditions, a dose response experiment was done by exposing cells to a gradient of CS concentrations in serum free conditions (1, 10, 50, 100 or 250 µg/ml) for 3, 5, and 7d (Figure 4.7). At 3 days, cells exposed to 250 µg/ml of CS in SF were already detaching as demonstrated by the low viability percentage and confirmed by a round morphology observed in the microscope (pictures not shown). However, at this time point, no significant difference was observed between SF condition and all the other inferior concentrations of CS in SF.

At 5 days, cells exposed to 250 µg/ml of CS in SF continued to detach and moreover cells exposed to 100 µg/ml started to detach and to exhibit a round morphology, while lower concentrations of CS in SF were not affected. At 7 days, while cells exposed to 250 µg/ml and 100 µg/ml continue to detach, cells exposed to 50 µg/ml started to detach too, while lower concentrations of CS in SF were not affected.

Results suggest that there is a clear dose-dependent effect to CS concentration in SF. The more CS in the media, the faster they start detaching and as time of exposure continues, cell detachment begins at lower CS concentrations.

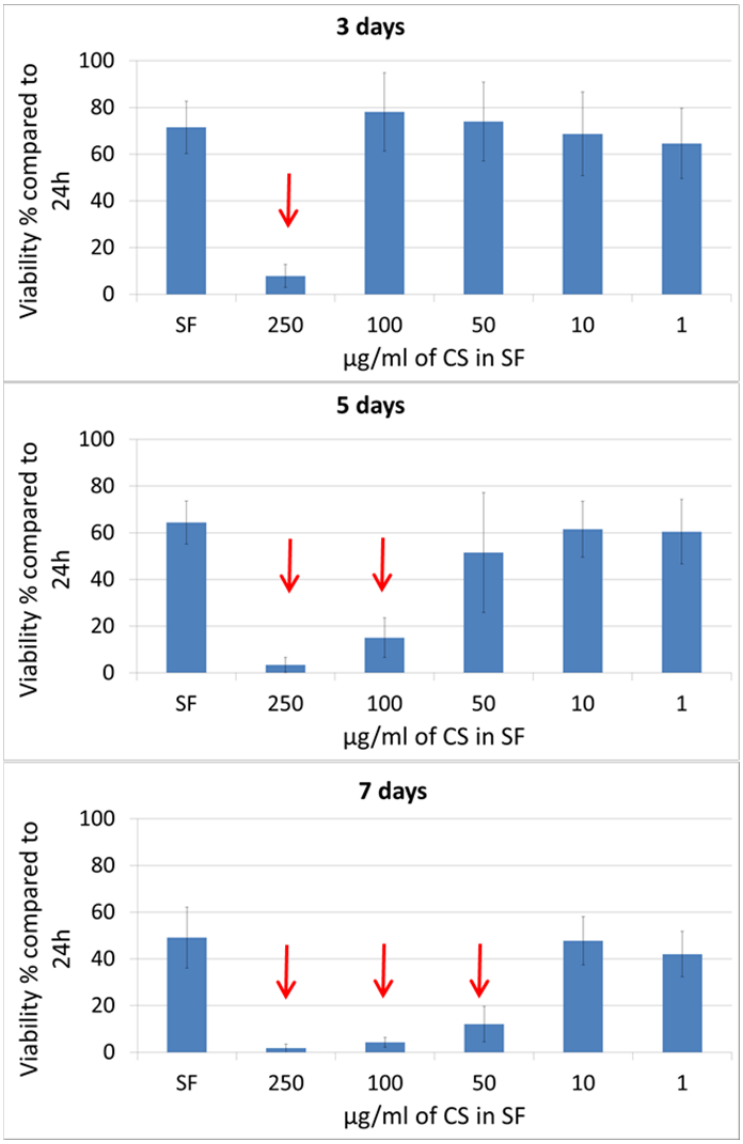

Figure 4.7 Dose response of CS on hMSC viability after 3, 5 and 7 days in serum free medium (SF). Results correspond to alamar blue fluorescence signal normalized to the signal after 24h adhesion in complete medium. Arrows indicate the conditions where cell detachment was observed (N=2, n=4)

4.1.2.2 CS effect on VSMC

In order to determine if the cell detachment effect of hMSC in SF+CS is exclusive to this cell line, the same dose response experiment described in section 4.1.2.1 was performed on

VSMC (Figure 4.8). The same effect was observed at exactly the same time points, suggesting that the effect is not exclusive to a particular cell line.

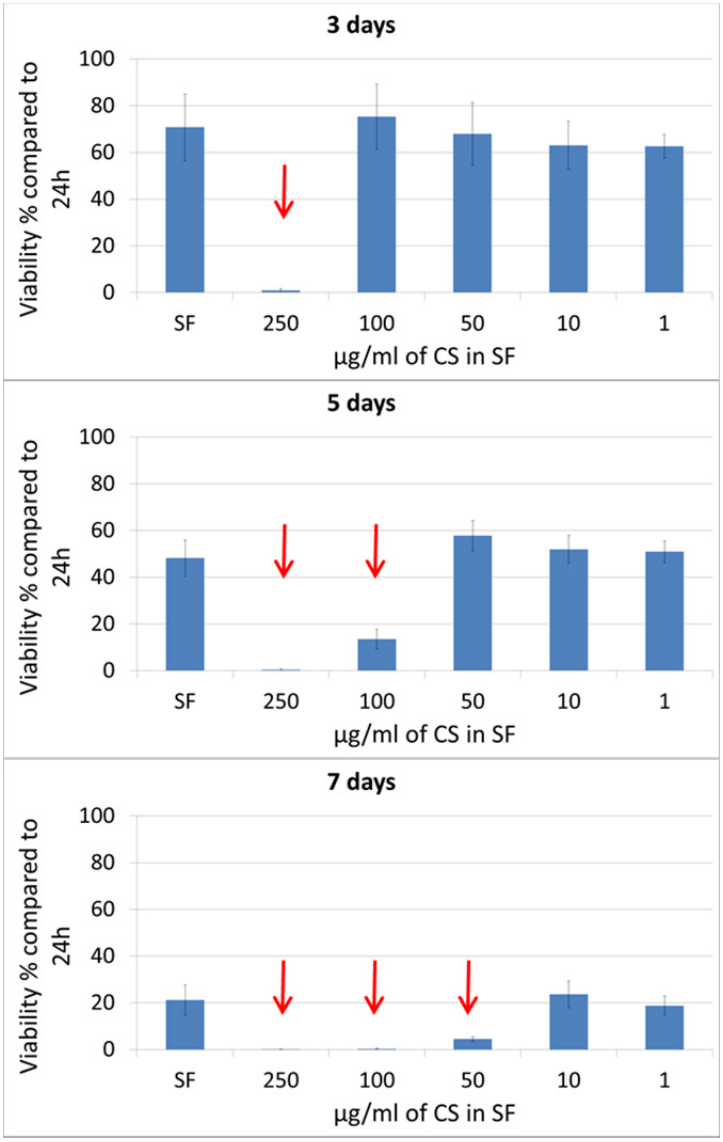

Figure 4.8 Dose response of CS on VSMC viability after 3, 5 and 7 days in serum free medium (SF). Results correspond to alamar blue fluorescence signal normalized to the signal after 24h adhesion in complete medium. Arrows indicate the conditions where cell detachment was observed (N=2, n=4)

4.2 Effect of bioactive surfaces

Despite the unexpected effect of soluble CS on MSC, bioactive CS containing surfaces and hydrogels may remain interesting to enhance MSC behavior, as it is the case with VSMC (Lequoy et al., 2014). Therefore, in the following section, CS grafted surfaces were created as described in section 3.1, characterized by physicochemical methods, and tested for their effect on hMSC cells as described in sections 3.2 and 3.4.4 respectively.

4.2.1 Physicochemical characterization of bioactive surfaces

Previous work had already confirmed CS grafting on amine-rich surfaces using this method (Charbonneau et al., 2011), therefore surface characterization was kept to a minimum. Bioactive surfaces with CS based on either LP or commercial amine plates were analyzed by contact angle measurement and AFM to explore their wettability and roughness, respectively. The CS grafted was quantified by using Toluidine blue O dye since changes in cell behavior were observed between amine plates and LP with CS as further detailed in sections 4.2.2 and 4.2.4. Since CS covalently grafts to available amino groups on the surfaces, the primary amine content of the bioactive surfaces was determined by Orange II dye. Results of this characterization methods are shown below.

4.2.1.1 Contact angle- wettability

The contact angle of PET, LP and LP+CS was measured. The aim of the experiment is to analyze if a difference in contact angle (wettability) exists between the surfaces. Through this experiment, the hydrophobic or hydrophilic character of the different surfaces can be investigated and further related to cell response.

As shown on Figure 4.9, PET has the highest value with a mean of 67 degree. After the plasma deposition the LP exhibits a contact angle of 60 and CS grafting led to a decrease of the contact angle to 56. The three means are statistically different from each other ($p<0.05$).

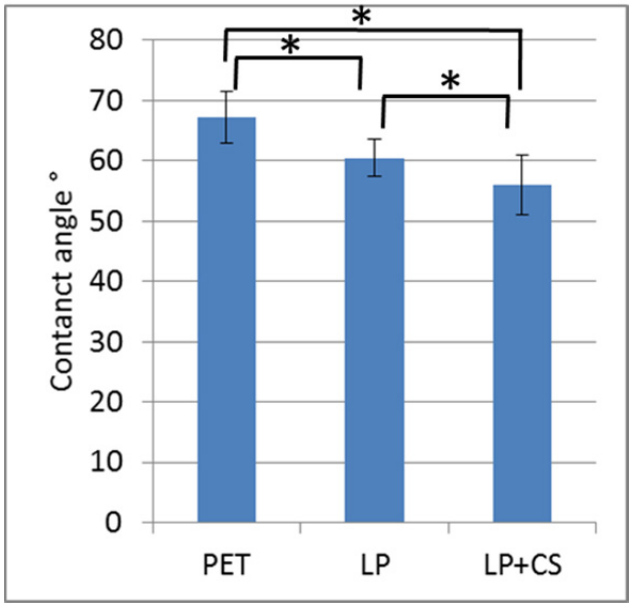

Figure 4.9 Contact angle measurement of bare PET, PET coated by LP and by LP+CS (mean ± SD; N=7, n=3) Significant difference was observed between each surface (*p<0.05)

4.2.1.2 AFM

Topographic and phase images of LP based bioactive surfaces were obtained using AFM to verify the homogeneity of the coating and compare the rugosity. Figure 4.10 shows the topographic and phase images of LP (a,b) and LP+CS (c,d). Except the lines observed in the LP+CS topographic image (Figure 4.10, c), which can be related to PET manufacturing process, the surfaces appear homogeneous. The roughness values (Rq) were 0.747 nm for LP and 1.838 nm for LP+CS. This indicates that CS grafting increases the roughness compared to LP, however both surfaces are relatively smooth. Figure 4.11 illustrates in 3D the height measurements of an LP+CS sample, as observed, the sample is homogeneous with around the same roughness through all the analyzed area.

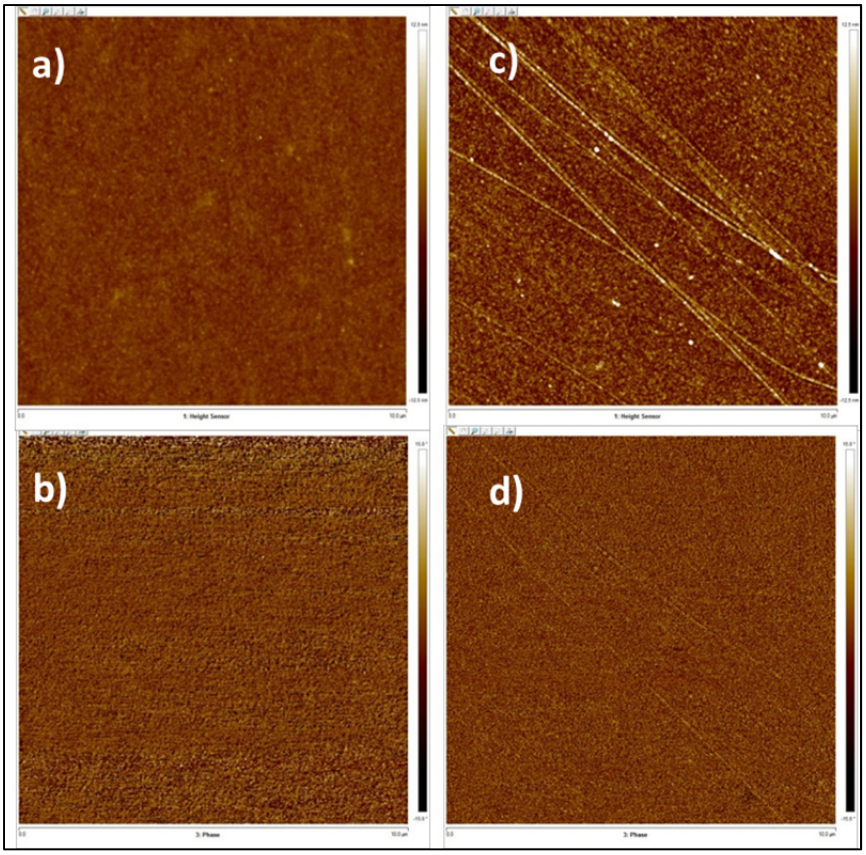

Figure 4.10 AFM topographic (a.c) and phase (b,d) images of LP (a,b) and LP+CS (c,d) (10µm x 10µm)

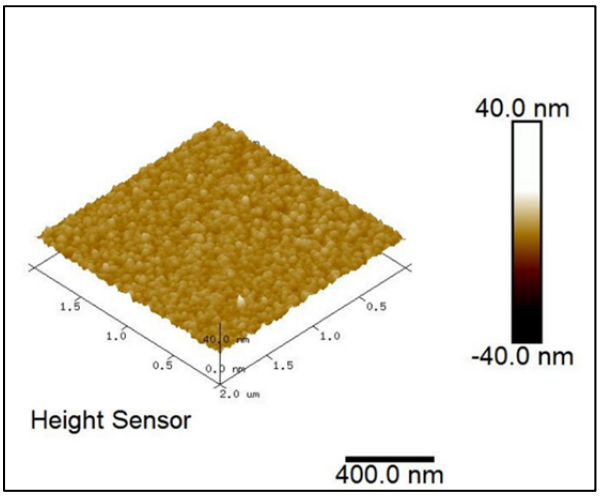

Figure 4.11 AFM height measurements 3D image for LP+CS sample (2µm x 2µm)

4.2.1.3 CS grafting potential by Toluidine blue

The quantification of CS grafted by EDC/NHS chemistry on LP and commercial amine plates (AP) was done by Toluidine blue O (TBO). Figure 4.12 shows the values obtained for LP+CS and AP+CS as well as LP, AP and PET controls (without CS), while Figure 4.13 confirms the homogeneity of the grafting on LP. As expected, PET, LP and AP present a negligent quantity of TBO desorbed, while LP+CS and AP+CS desorbed an average of 13.6±2 and 63±12 pmol/mm^2 of TBO respectively ($p<0.05$).

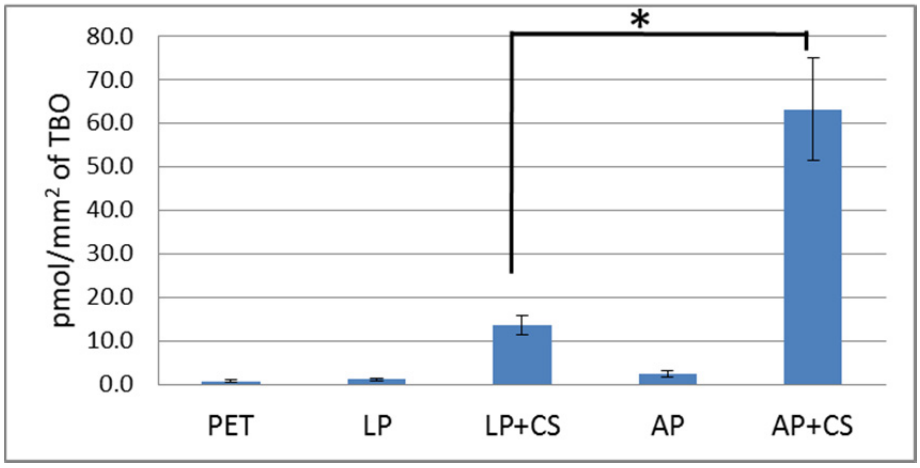

Figure 4.12 TBO surface densities on PET, LP, LP+CS, AP and AP+CS (N=4, n=4) (*$p<0.05$)

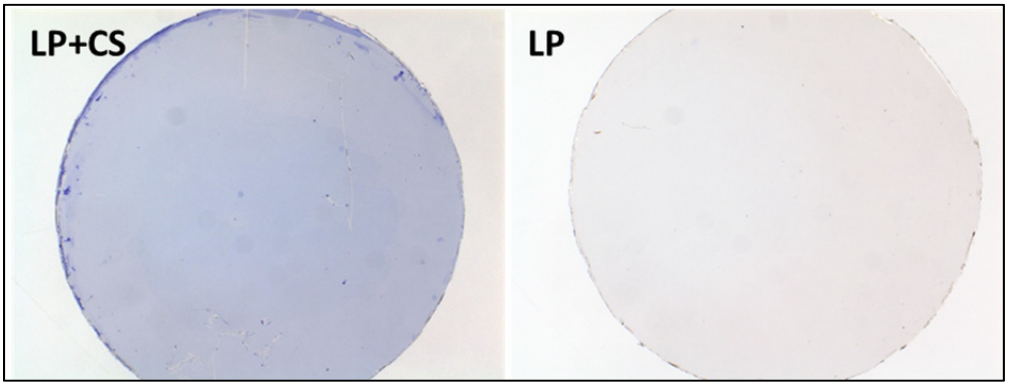

Figure 4.13 TBO bounded on LP and LP+CS before desorption of the dye

Since the TBO value was found to be much higher for AP+CS than for LP+CS, further experiments were performed to observe the effect of diluting the CS grafting solution on AP. As observed in Figure 4.14, the more the grafting solution was diluted, the less TBO desorbed after interacting with CS, which means less CS grafted. Generally the data follow a logarithmic tendency (R^2=0.9476, see Figure 4.14) with rapid increase at low concentrations, followed by a trend towards a plateau. However, for small concentrations the tendency could be considered as linear (until 0.01%; R^2=0.9941). From the linear regression of the first points we can deduce that in order to obtain the same value of TBO desorbed in LP+CS (13.6±2 pmol/mm^2), the concentration of CS during the grafting should be much lower than 1% (w/v) on AP (around 0.00514%).

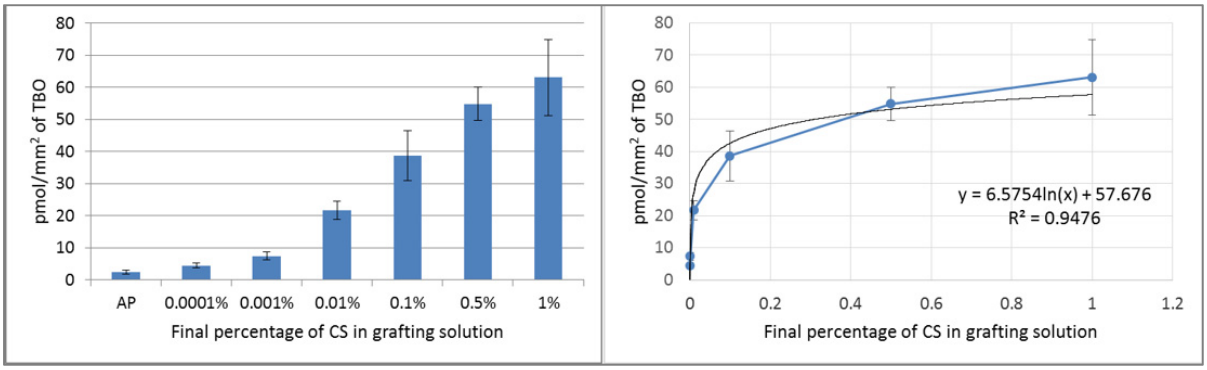

Figure 4.14 Grafting of CS at different concentrations on AP (N=4, n=4)

It is unclear why there is such a large difference in the CS grafting capacity between LP and AP, especially since AP fabrication method is unknown (commercial intellectual property). Since CS is grafted to the primary amines of LP and AP, amino group surface density was further investigated by Orange II method, as described in the next section.

4.2.1.4 Amino group density by Orange II

The amine rich surfaces (LP and AP) were analyzed by Orange II in order to quantify their amino groups and observe differences between the materials, which could explain the Toluidine blue results. The amino groups surface density is presented as pmol of Orange II

desorbed per mm^2. The higher the value, the more amino groups the surface has, since a higher quantity of Orange II interacted with the surface.

Figure 4.15 presents the values obtained for Orange II. As expected, PET has a negligible value since there are no amino groups present. However LP has an average value of 199±28 $pmol/mm^2$ and the commercial amine plates have a value of 226±55 $pmol/mm^2$. The means only differ in 27 $pmol/mm^2$ (AP is ≈14% higher than LP). Although their means are statistically different ($p<0.05$), the difference between them is small and both surfaces can be considered as amine-rich surfaces. Moreover, their comparison by Orange II might not be valid since recent work in the laboratory showed that Orange II is absorbed in LP coating, leading to data depending on the thickness of the amine-rich coating (here ≈100 nm thick) (Boespflug, 2015). The amine-rich coating thickness and the amino group distribution is unknown on AP, but it is likely that the amino groups on AP are highly available and concentrated in the top layer of the surface, which could explain the higher amount of grafted CS.

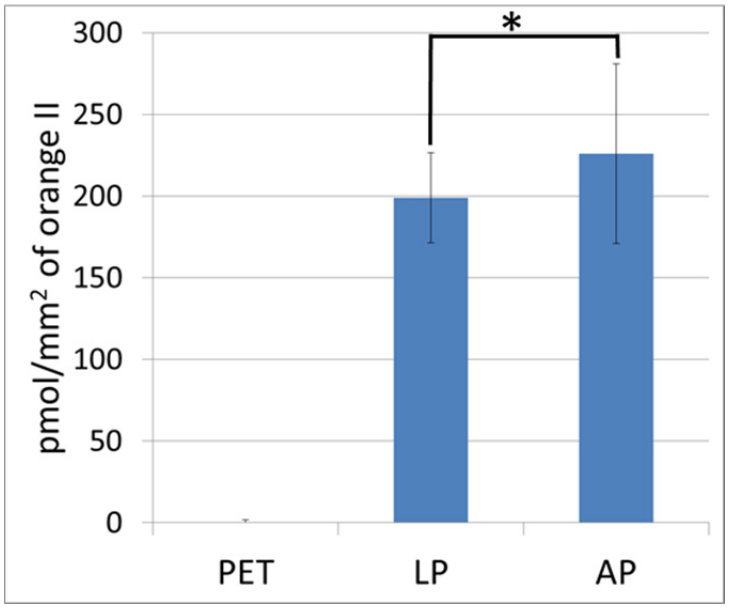

Figure 4.15 Orange II surface densities on LP and AP (N=4, n=4) (*$p<0.05$)

4.2.2 Adhesion and growth of hMSC on LP based bioactive coatings

Bioactive surfaces were tested for hMSC adhesion and growth, and compared to bare PET and conventional polystyrene culture plates (PCP) as controls. hMSC from two different lots (Lonza lot and Texas A&M Institute for Regenerative Medicine lot) were tested, since hMSC are known to present high variability depending on the donor (or source) (see section 1.2 in the literature data). Cells were first tested for adhesion and growth in complete medium (10% FBS). Then, cell survival in serum free media was evaluated. Results are presented as per lot of stem cells.

4.2.2.1 Adhesion

Adhesion Lonza lot

Results of adhesion at 24h of Lonza lot hMSC can be observed in Figure 4.16 and Figure 4.17. Two different densities were used at 24h: 10,000 cells per surface and 15,000 cells per surface. Slight differences were observed with the density change. LP, in both conditions, achieved the best adhesion, as proven by Tukey test ($p<0.05$). However at 10,000 cells (Figure 4.16) there is no significant difference between the adhesion on the polystyrene culture plate (PCP), PET or LP+CS, while at 15,000 cells the adhesion on LP+CS is significantly higher than on PCP or PET ($p<0.05$) (Figure 4.17).

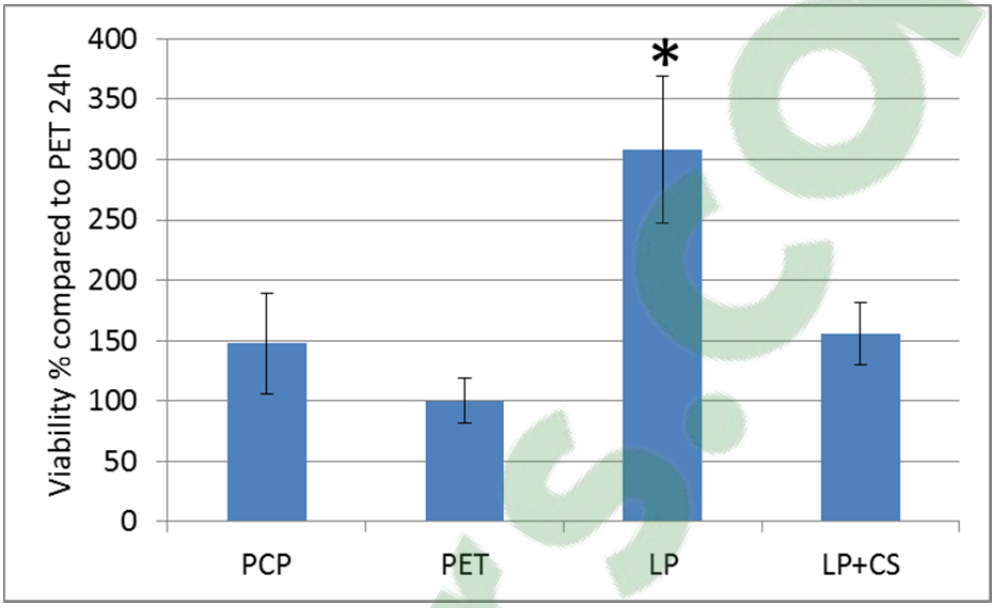

Figure 4.16 Adhesion of hMSC on LP based bioactive surfaces (10,000 cells/surface) (cells source = Lonza). Results are expressed as percentage of alamar blue fluorescence signal compared to the signal of PET after 24h (N=2, n=4) (*p<0.05)

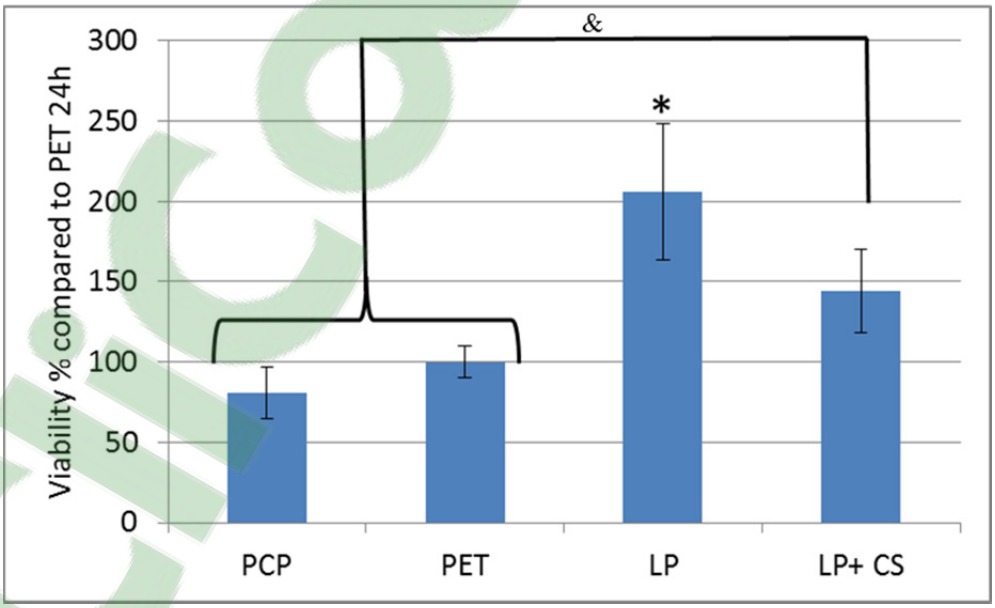

Figure 4.17 Adhesion of hMSC on LP based bioactive surfaces (15,000 cells/surface) (cells source = Lonza). Results are expressed as percentage of alamar blue fluorescence signal compared to the signal of PET after 24h (N=4, n=4) (* p<0.05 with all other surfaces; $^{\&}$ p<0.05 with PCP and PET)

Adhesion Texas lot

The results of adhesion at 24h with hMSC from Texas lot are presented in Figure 4.18. In this case, cell density (5,000 or 10,000 cells per surface) did not influence the results and they were compiled and presented in percentage compared to PET condition at 24h. As observed, results obtained are similar to Lonza lot at 15,000 cells/surface where LP and LP+CS have a significantly higher adhesion than PCP or PET according to Tukey test ($p<0.05$). Moreover the adhesion between LP and LP+CS is statistically the same, in contrast with Lonza lot where the highest adhesion was on LP.

Figure 4.19 illustrates the cells after 24h adhesion, stained by crystal violet. The images show the difference in cell density between the surfaces. As observed, LP and LP+CS show a higher number of cells compared to PET and this is supported also by the viability results (Figure 4.18), meaning the bioactive surfaces enhanced the adhesion.

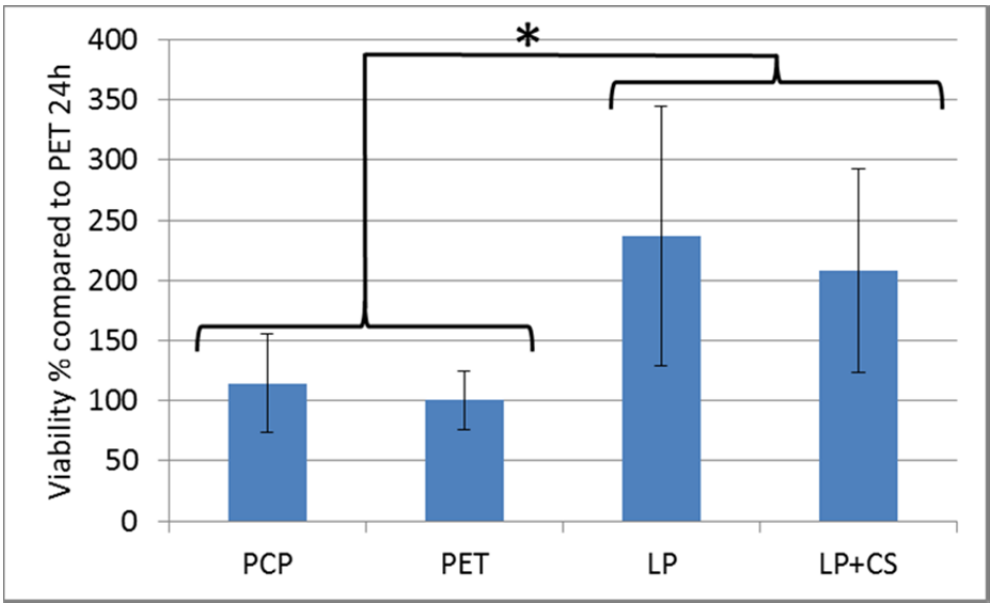

Figure 4.18 Adhesion of hMSC on LP based bioactive surfaces (cells source = Texas A&M Institute for Regenerative Medicine). Results are expressed as percentage of alamar blue fluorescence signal compared to the signal of PET after 24h (N=8, n=4) (*$p<0.05$)

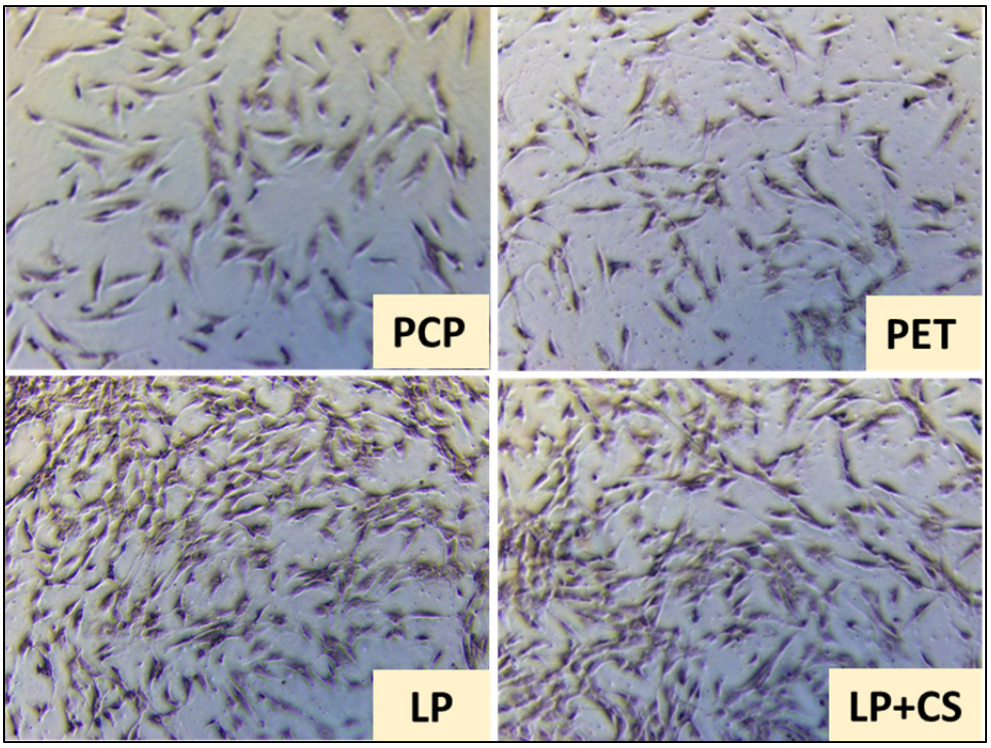

Figure 4.19 Representative images of hMSC adhesion (cells source = Texas A&M Institute for Regenerative Medicine) at 24h in PCP, PET, LP and LP+CS

4.2.2.2 Growth

Growth Lonza lot

Lonza cells at density of 10,000 cells per surface were left to grow in complete medium and viability by alamar blue was evaluated after 4d and 6d. Results in Figure 4.20 show that LP was the surface with the highest viability of cells at 4d and 6d, which is logical considering it was the surface with the highest adhesion. LP+CS exhibit a higher viability than PET or PCP at 6 days of growth despite that their adhesion at this density was statistically the same. The previous can be represented also by a growth ratio chart (Figure 4.21) where the growth at different time points is compared to the adhesion per surface type. In Figure 4.21 we can observe that the highest growth ratio in relation to its own adhesion is found on LP+CS ($p<0.05$). However this conclusion might be valid only when comparing to PCP or PET since at 6 days LP surface was already over confluent and cells did not have place left to grow.

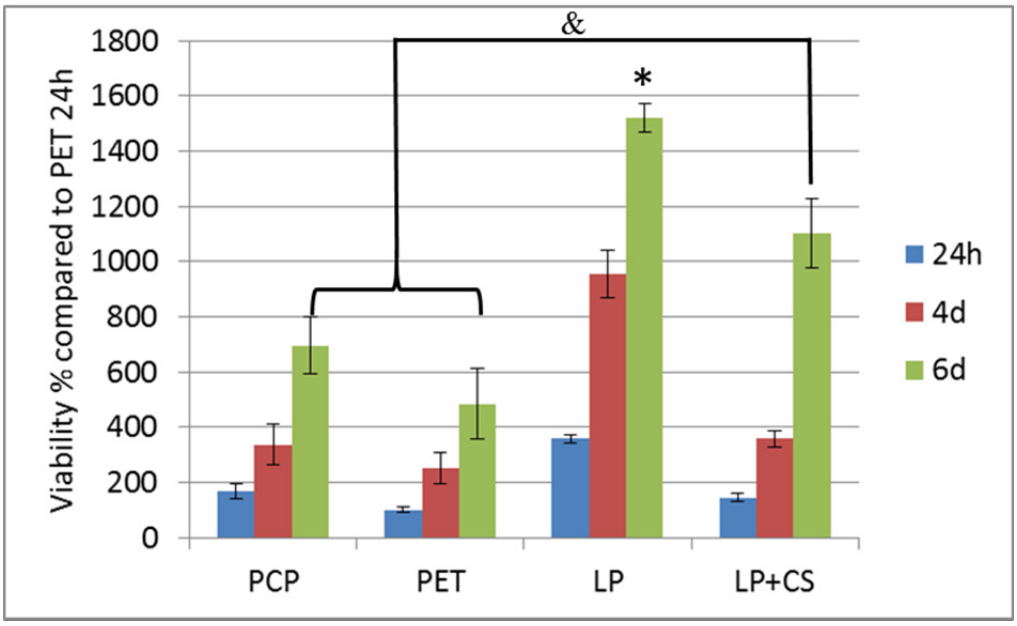

Figure 4.20 Growth of hMSC on LP based bioactive surfaces (10,000 cells/surface) (cells source = Lonza). Results are expressed as percentage of alamar blue fluorescence signal compared to the signal of PET after 24h (N=1, n=4, representative of 2 independent experiments) (* $p<0.05$ with all other surfaces at the same time point; $^{\&}$ $p<0.05$ with PCP and PET)

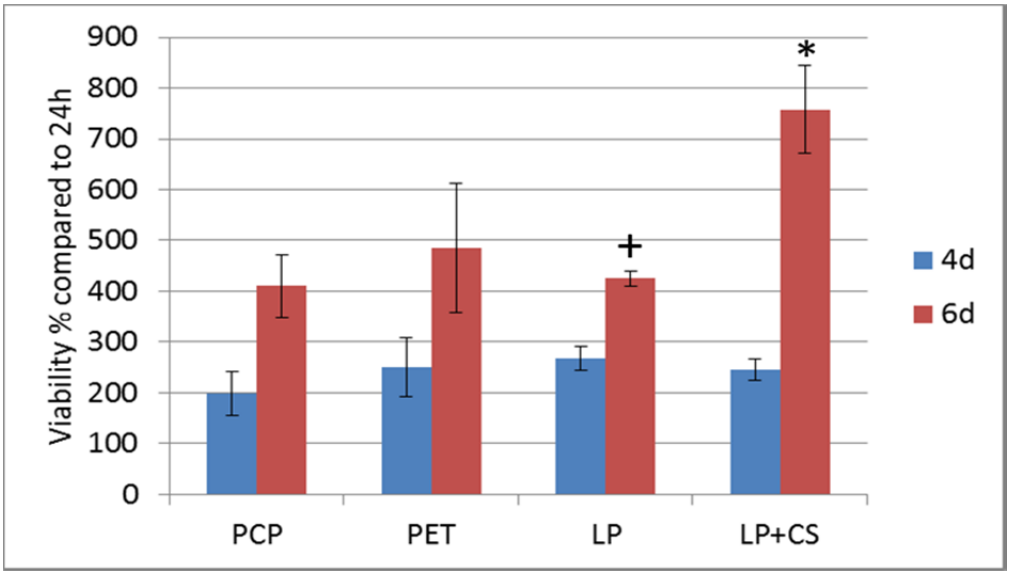

Figure 4.21 Growth ratio per surface type of hMSC on LP based bioactive surfaces (10,000 cells/surface) (cells source = Lonza). Results are expressed as percentage of alamar blue fluorescence signal compared to the initial signal (at 24h) on each surface (N=1, n=4, representative of 2 independent experiments) (* $p<0.05$; + confluency reached)

Growth Texas lot

In the case of the Texas lot, Figure 4.22 shows the growth until 4 days only, since at this time point cells were already over confluent on LP and LP+CS. Once again, cell metabolic activity (indicative of higher cell number) was statistically increased on LP and LP+CS at 4d compared with PCP and PET, as proven by ANOVA with Tukey analysis ($p<0.05$). There was no statistical difference between LP and LP+CS or between PCP and PET.

Figure 4.23 confirms higher cell density (and cell confluency) on LP and LP+CS. All together this shows that the bioactive surfaces enhance MSC growth.

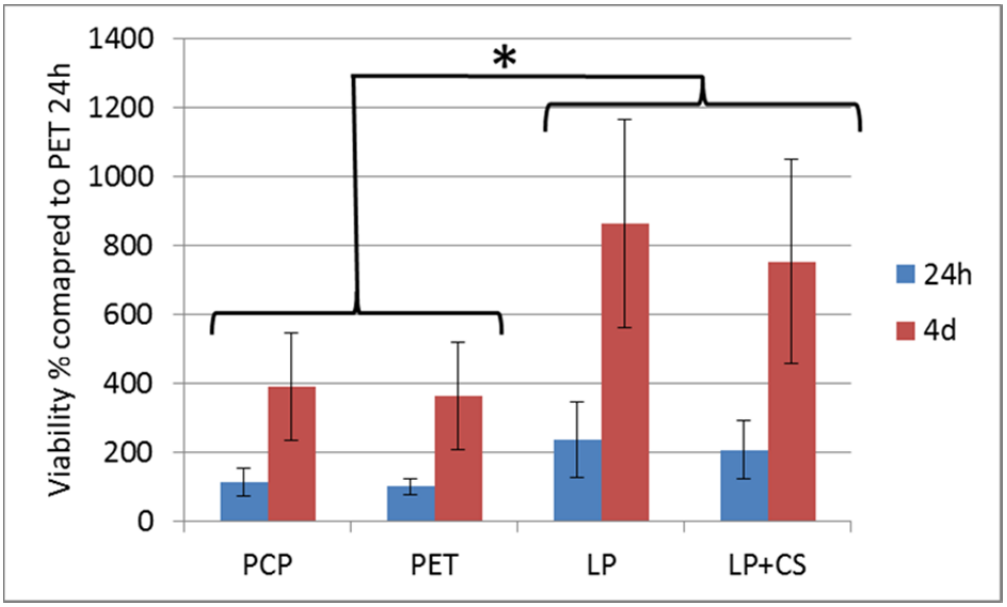

Figure 4.22 Growth of hMSC on LP based bioactive surfaces (cells source = Texas A&M Institute for Regenerative Medicine). Results are expressed as percentage of alamar blue fluorescence signal compared to the signal of PET after 24h (N=8, n=4) (*$p<0.05$)

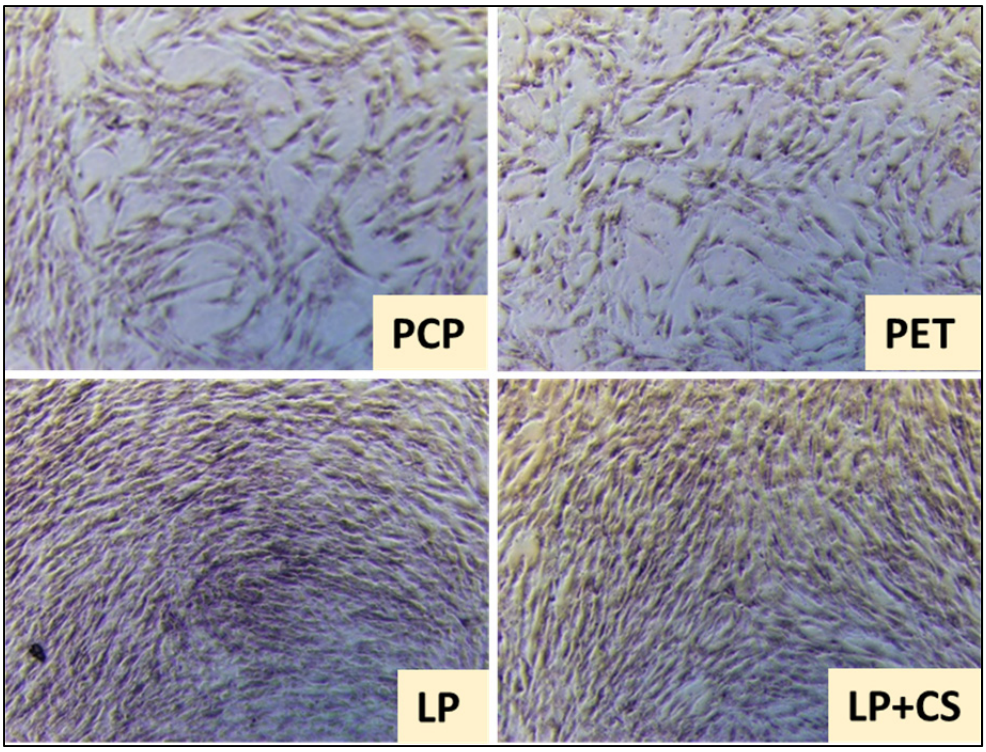

Figure 4.23 Representative images of hMSC growth (cells source = Texas A&M Institute for Regenerative Medicine) at 4d in PCP, PET, LP and LP+CS

4.2.3 Survival of hMSC on LP based bioactive coatings

Cells from Lonza lot (15000 cells per well) were left to adhere in complete medium for 24h (adhesion) and then exposed to serum free conditions for 3 or 7 days. As observed in Figure 4.24 cells viability decreases on each surface after 3 days in serum free medium and even more after 7 days.

After 7 days, the viability is the lowest on PCP and PET followed by LP+CS, cell number on LP being significantly higher than the 3 other surfaces ($p<0.05$). This may be explained by the higher initial number of cells. Indeed, it is known that the more cells adhered before the exposure to serum free medium, the more time they may resist to serum free conditions due to cell-cell interactions (Yasui et al., 2000). The number of cells remaining in the other

conditions was negligible and the morphology of cells on LP at 7 days can be observed in Figure 4.25.

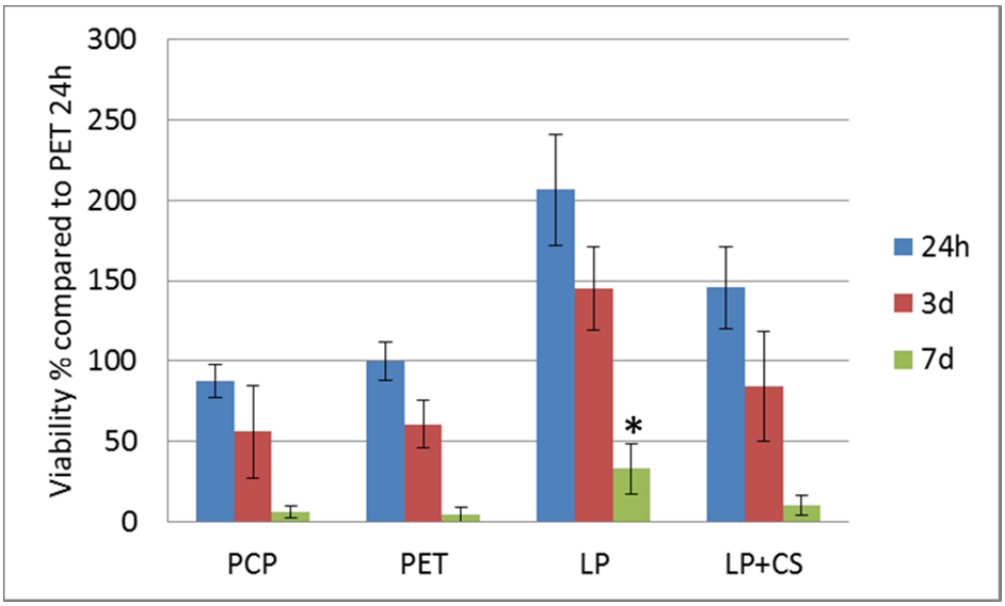

Figure 4.24 Survival of hMSC (cell source = Lonza lot) after 3d or 7d in serum free medium. Results are expressed as percentage of alamar blue fluorescence signal compared to the signal of PET after 24h in complete medium (N=3,n=4) (*p<0.05)

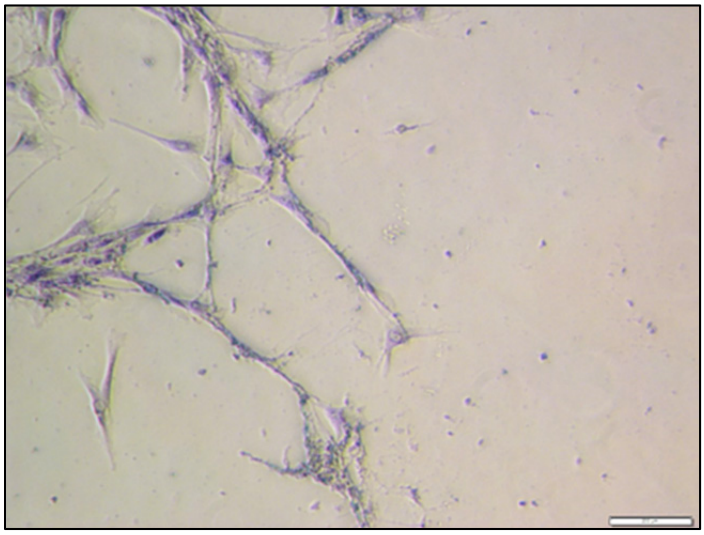

Figure 4.25 Representative image of hMSC (cell source = Lonza) remaining on LP after 7 days in serum free medium

4.2.4 Adhesion and growth of hMSC on amine plate based bioactive coatings

In order to explore the influence of different amine-rich surfaces in the CS grafting and its effect on MSC, commercial amine plates (AP) with CS were also tested.

4.2.4.1 Adhesion and growth with different CS grafted densities

Unexpectedly, hMSC behavior on AP+CS surfaces in complete medium (10% FBS) was quite different than on LP+CS surfaces, when using a concentration of 1% (w/v) of CS for grafting CS. The cells did not adhere and they had a round morphology, indicating that the surface properties prevented cell adhesion (Figure 4.26). This effect was immediately related with the results obtained with TBO (4.2.1.3) where it can be observed that AP can graft almost five fold more CS than LP when using the same grafting solution.

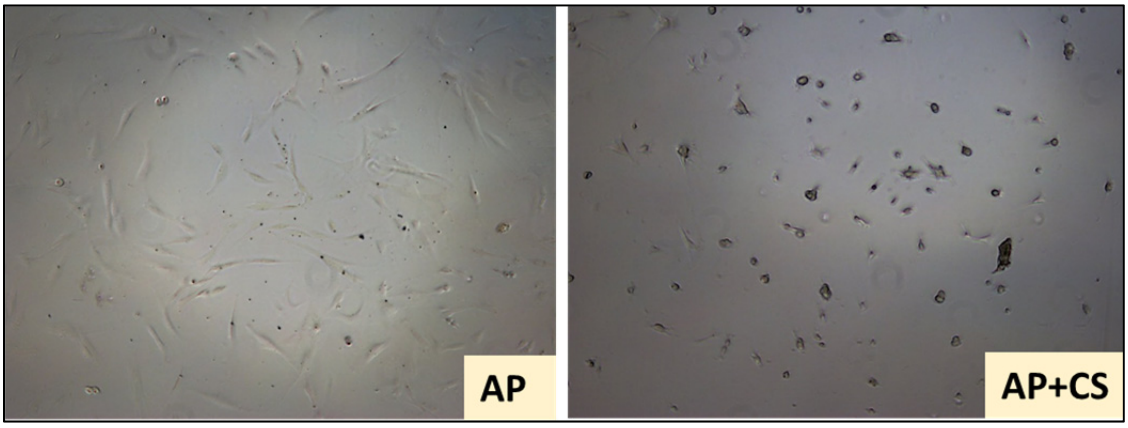

Figure 4.26 Morphology of hMSC (cell source = Stem cell technologies lot) when seeded on AP and AP+CS prepared using a concentration of 1% (w/v) of CS

To confirm that this negative effect was due to the large amount of CS grafted on the surface, we tested the effect of decreasing the concentration of CS during grafting on cell adhesion. Figure 4.27 shows the results obtained by seeding hMSC on surfaces prepared at different CS concentrations. The brace on the image show the surfaces where cells adhesion and growth was decreased compared to bare AP controls. From 1%(w/v) of CS until 0.1% of CS, cell adhesion was prevented (as confirmed by the time point at 24h) and only a few cells left were

able to grow in the following days (4d and 7d). At 0.01% of CS in the grafting solution, cells presented an intermediary behavior.

In contrast, excellent adhesion and growth was observed on AP coating with very low concentrations of CS (0.001% and 0.0001%), with no statistical difference compared with polystyrene culture plate (PCP), but also no further benefit compared to bare AP.

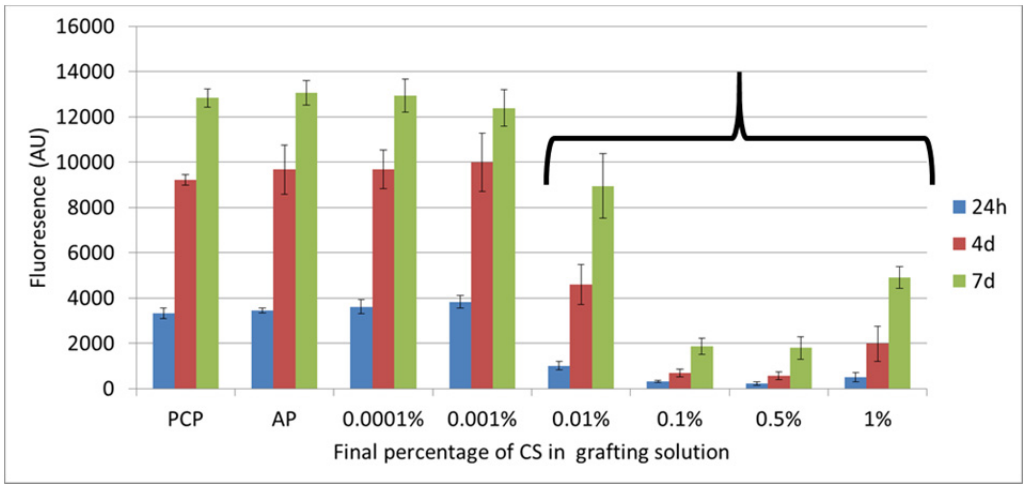

Figure 4.27 Adhesion and growth of hMSC (cell source = Stem cell technologies lot) on amine plate (AP) based bioactive coatings prepared using different percentages of CS in the grafting solution. Bare AP and PCP are used as controls. Results are presented as alamar blue fluorescence signal (N=1, n=4, representative of 2 independent experiments)

4.2.4.2 Antifouling effect of CS analyzed by protein adsorption

In order to investigate if grafted CS leads to antifouling effect on cells, protein adsorption properties of these various surfaces were tested by using bovine albumin labeled with Texas Red fluorescent dye, as previously described in the materials and methods chapter. Figure 4.28 shows the results, where lower fluorescence means that prevention of protein adsorption was more efficient (indicating antifouling properties).

As indicated by the thick brace in Figure 4.28, it is clear that the concentrations of CS that prevented cell adhesion (Figure 4.27) are the same ones that prevented protein adsorption.

The lowest concentrations of CS (0.001% and 0.0001%) also prevented protein adsorption since they are significantly different from AP ($p<0.05$), however the difference is small. We can conclude that there is a clear link between the amount of CS on the surface, the antifouling properties and cell anti-adhesive properties of the surface.

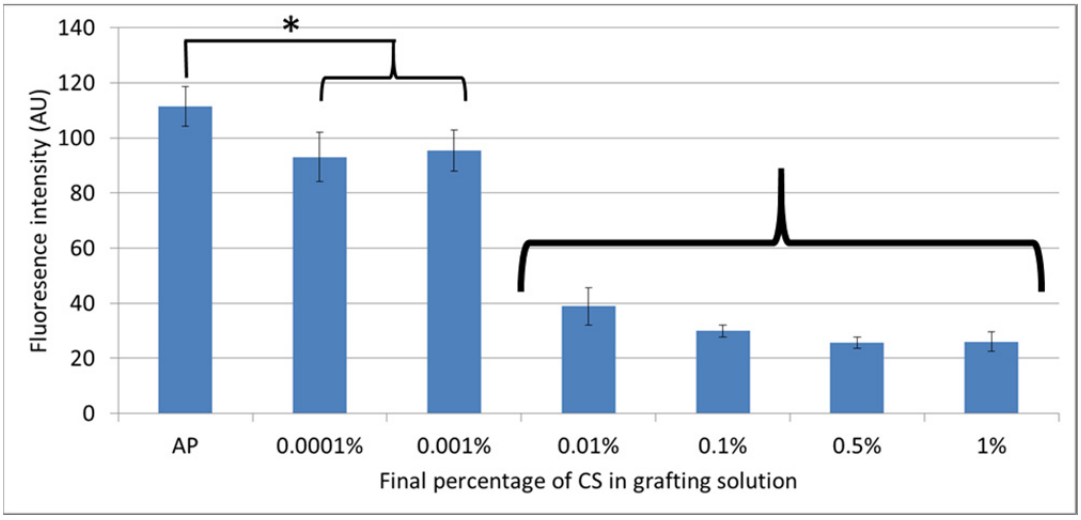

Figure 4.28 Protein adsorption on amine plate based bioactive coatings prepared using different percentages of CS in the grafting solution. Results are presented as fluorescence intensity units (N=1, n=4, representative of 2 independent experiments) (*$p<0.05$)

4.3 Effect of CS in chitosan hydrogels (3D scaffolds)

Chitosan hydrogels with and without CS were compared for their mechanical properties (assessed by rheology) and their ability to maintain viability of encapsulated MSC over 1 week. A concentration of 1% (w/v) CS in the hydrogel was first tested since previous work from LBeV indicated that this concentration strongly enhances L929 mouse fibroblasts viability and increases the storage modulus (G'), indicative of high rheological properties (Alinejad Y., 2016 unpublished). Figure 4.29 suggests that adding CS increases the rheological properties of the hydrogel. However these results are not reliable since the chitosan-CS gel precipitated upon formation and expulsed water, resulting in a non-cohesive hydrogel as observed in Figure 4.30. Rheological results were similar when hydrogels were prepared with culture media for cell encapsulation (data not shown).

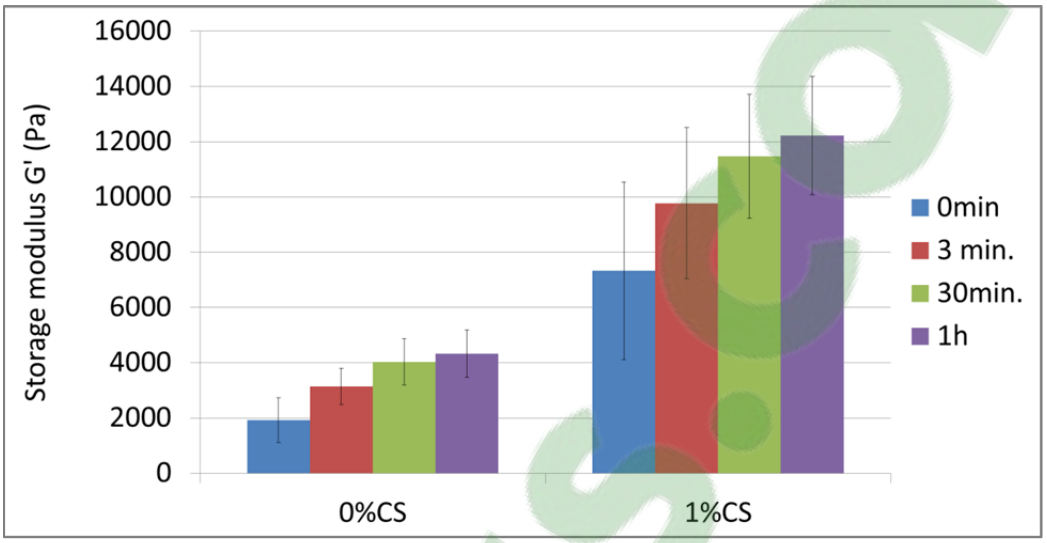

Figure 4.29 Evolution of the storage modulus, G', at different time points at 37°C for chitosan-based hydrogels with 1% or 0% of CS (N=1, n=4)

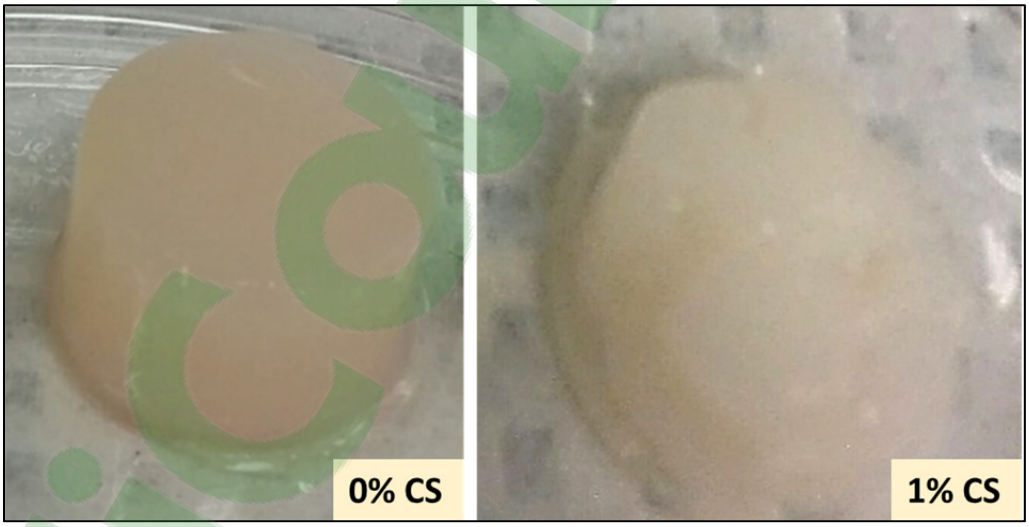

Figure 4.30 Photograph of chitosan-based hydrogels with 1% or 0% CS after 1h of incubation at 37°C

When cells were encapsulated in both hydrogels using alpha MEM medium with 10% FBS, their viability rapidly decreased with time, as observed in Figure 4.31. Therefore, NutriStem XF medium (Biological industry, Israel) which is more specialized for MSC, was used for further experiments.

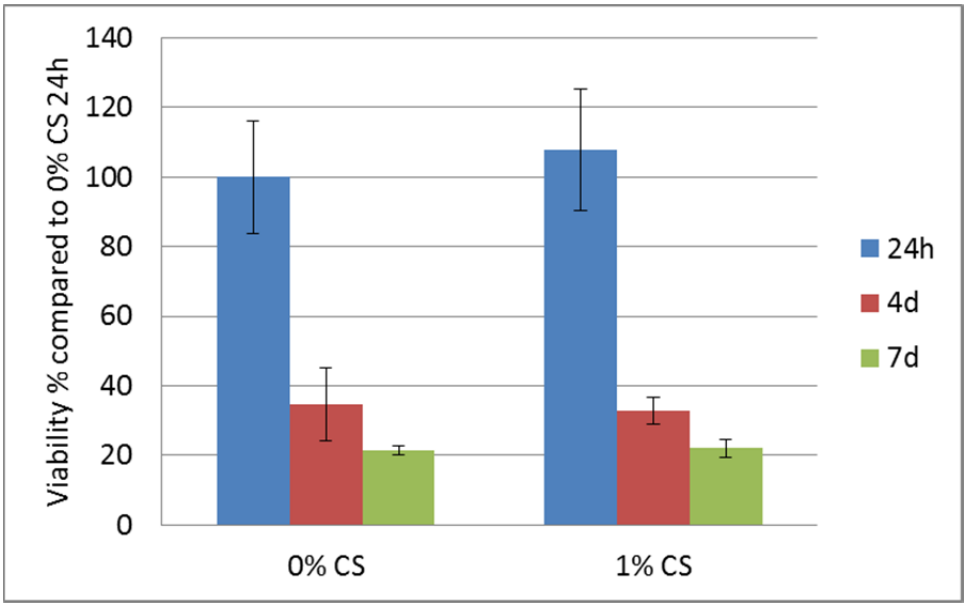

Figure 4.31 Viability of hMSC entrapped in chitosan hydrogels with 1% or 0% CS after 24h, 4 and 7 days in alpha MEM medium (cells source = Texas A&M Institute for Regenerative Medicine). Results are expressed as percentage of alamar blue fluorescence signal compared to signal at 24h in hydrogels with 0% CS (N=1, n=4)

When using NutriStem XF medium, the initial fluorescence signal (at 24h) was similar to the one obtained with alpha MEM media, without difference between hydrogel with or without CS. Cell viability was maintained in hydrogels without CS (Figure 4.32), since there was no significant difference between results at each time point. However in hydrogels containing 1% of CS, cell viability strongly decreased after 4 and 7 days.

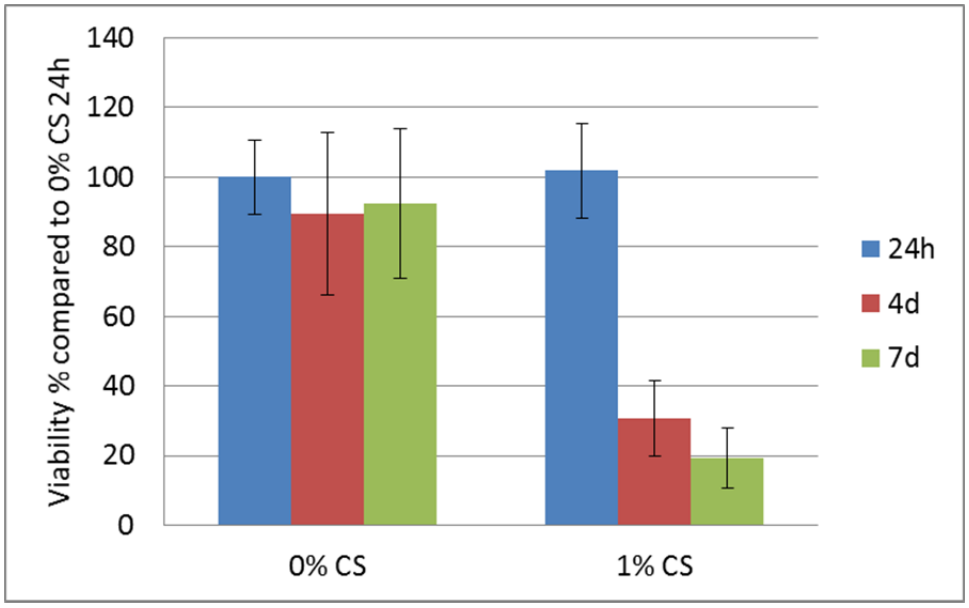

Figure 4.32 Viability of hMSC entrapped in chitosan hydrogels with 1% or 0% CS after 24h, 4 and 7 days in NutriStem XF medium (cells source = Texas A&M Institute for Regenerative Medicine). Results are expressed as percentage of alamar blue fluorescence signal compared to signal at 24h in hydrogels with 0% CS (N=3, n=3)

Since the concentration of CS at 1% (w/v) gave disappointing results, both in terms of gel structure and cell survival, another test was performed with hydrogel containing a much lower CS concentration. Based on literature data on the effect of CS in solution, (Laplante et al., 2005; Lerouge et al., 2007; Raymond et al., 2004) a final concentration of 500µg/ml (0.05% w/v) of CS in the hydrogel was chosen.

At this CS concentration, there is no significant difference in rheological properties between the hydrogels with or without CS (Figure 4.33) and the CS-hydrogel was cohesive and maintained the water within its structure (Figure 4.34). Encapsulated cells maintained viability until 7 days, as shown by similar alamar blue signal at each time point (Figure 4.35). However no benefit could be found when comparing with hydrogel without CS.

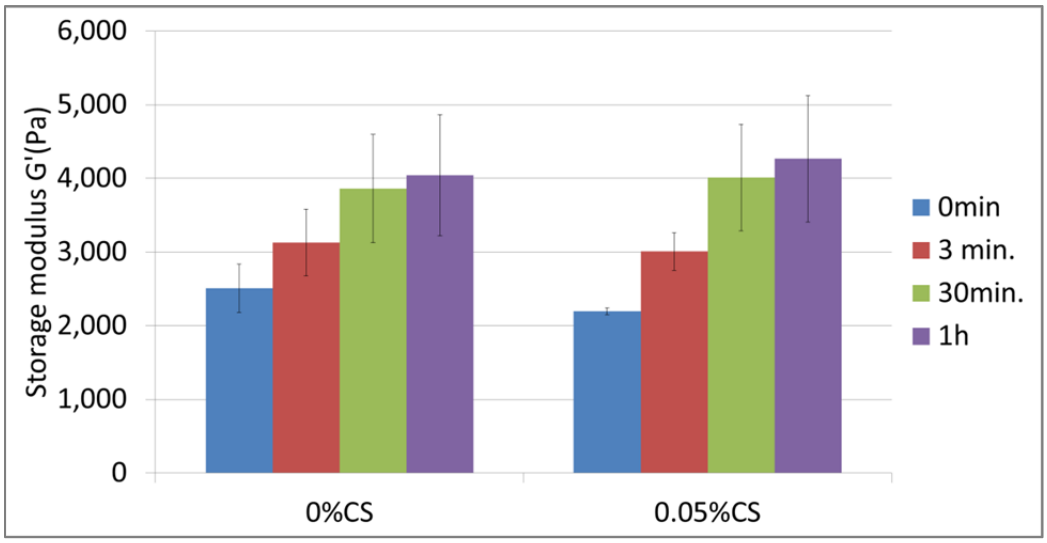

Figure 4.33 Evolution of the storage modulus, G', at different time points at 37°C for chitosan-based hydrogels with 0.05% or 0% of CS (N=1, n=3)

Figure 4.34 Photograph of chitosan-based hydrogel with 0.05% CS after 1h of incubation at 37°C

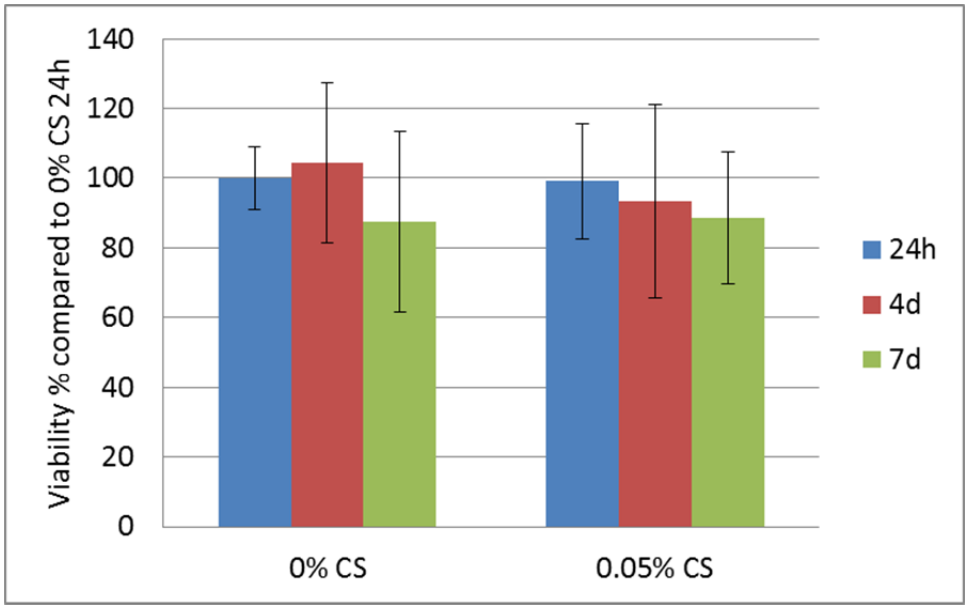

Figure 4.35 Viability of hMSC entrapped in chitosan hydrogels with 0.05% or 0% CS after 24h, 4 and 7 days in NutriStem XF medium (cells source = Texas A&M Institute for Regenerative Medicine). Results are expressed as percentage of alamar blue fluorescence signal compared to signal at 24h in hydrogels with 0% CS (N=2, n=3)

CHAPTER 5

GENERAL DISCUSSION, LIMITS AND PERSPECTIVES

The general objective of this project was to study the potential of extracellular matrix components such as chondroitin sulfate and growth factors to enhance the bioactivity of biomaterials such as implantable devices and 3D scaffolds. More particularly we investigated whether these molecules facilitated the adhesion, growth and survival of hMSC, which play a major role in tissue repair and tissue engineering applications. The project was divided into 3 specific objectives 1) Study the effect of growth factors and CS in solution on hMSC growth and survival, 2) Demonstrate the capacity of bioactive surfaces with immobilized CS to enhance adhesion growth and survival of hMSC and 3) Study the capacity of chitosan based hydrogels (3D scaffolds) with CS to enhance hMSC viability. In the following text, for each specific objective, main results will be briefly summarized, then further detailed and discussed.

For the first specific objective, EGF, VEGF and FGF as well as CS were tested in solution in order to study their effect on hMSC. None of the growth factors were found to exhibit an effect in the conditions tested. CS in serum containing media did not exhibit an effect. However, in serum free medium CS caused an unexpected decrease in cell viability by inducing cell detachment from the culture plate. The effect has been proven to be dose dependent and not exclusive for hMSC since it was also observed on rat MSC and VSMC.

Effect of GF in solution

Testing GF in solution aimed to select one to be grafted on biomaterials surfaces to enhance MSC survival and growth. EGF and VEGF were chosen for their effect reported in literature and because of the availability of oriented immobilization methods thanks to our collaborator (De Cresenzo, Ecole Polytechnique). The absence of effect was surprising since literature data suggest that GF can influence MSC survival and growth (Rodrigues et al., 2013; Rodrigues, Griffith et Wells, 2010; Tamama et al., 2006).

Thus, EGF is a mitogen for various types of cells. Human MSC express EGFR/ErbB-1, and a few studies showed a mitogenic effect on MSC (Tamama et al., 2006) and an anti-apoptotic effect (Soulez et al., 2010).

Previous studies from the lab also showed pro-survival effect of EGF at 10 ng/ml on VSMC in serum free medium (Lequoy et al., 2014). However, here, there was no significant effect when compared to media without GF, even when increasing the concentration up to 100ng/ml. EGF in rMSC did not confer a pro-survival effect either, as observed in the annex results. This discrepancy can be explained by different factors:

In the literature data, most of the reported effects of EGF on hMSC have been analyzed after short time points of exposure to the GF and the results were not presented as cell viability as in this project. For example, EGF in solution has been shown to increase MSC cell proliferation in media with 2% FBS only for a period of 96h and with a very low initial number of cells (Tamama et al., 2006). Moreover the anti-apoptotic effect of EGF in solution in SF medium has been observed through inhibition of apoptotic cascades after 8h by immunoblot analysis (Soulez et al., 2010). Therefore it is possible that, at the time points used in this project, EGF cannot improve cells viability in serum free medium nor enhance proliferation in serum containing conditions. The exact testing conditions, such as the initial cell density, method for initial cell adhesion and type of culture media may also influence the results. Cell source is not a significant factor since here we tested MSC from several sources.

In the case of VEGF, it has been reported that concentrations up to 10ng/ml may reduce cellular stress, increase pro-survival factor expression and cell proliferation (Pons et al., 2008). However the time points used in this study are for less than 24h and they used long-term cultured MSCs. On the other hand, some studies suggest that MSCs do not express the VEGF receptor and that it stimulates MSC by activation and downstream signalling of other growth factors (Ball, Shuttleworth et Kielty, 2007; Rodrigues, Griffith et Wells, 2010). The previous findings could explain why, in our study, VEGF did not exhibited a significant effect on young hMSC at time points such as 4 days and 7 days.

Finally basic FGF (also called FGF-2 or bFGF) was previously reported to increase growth rate and life span of hMSC in monolayer cultures when used at a concentration of 1ng/ml in complete media, especially when cells were seeded at low density (Tsutsumi et al., 2001). However when we tested this concentration in serum free or 2% FBS, there was no survival effect observed. It is probable that the concentration tested was too low, or that the type of FGF was not the best for enhancing proliferation or survival, since other reports use FGF-4 at concentrations such as 25ng/ml in order to reduce hMSC duplication time (Farre et al., 2007). In addition FGF-4 has also been reported for other effects on hMSC such as enrichment of mesenchymal cell progenitors and expansion of the life span (Bianchi et al., 2003; Yanada et al., 2006). Further study of GF effect on hMSC is required in order to find a significant effect in proliferation or survival of cells. One possibility is the previously mentioned FGF-4 at different concentrations up to 25 ng/ml. Other kind of growth factors have also reported some effects on MSC, such as PDGF, which was shown to increase proliferation and survival (Chase et al., 2010; Krausgrill et al., 2009). TGF β could have also been used for increasing hMSC proliferation and additionally chondrogenic differentiation might be induced also. This could be useful for particular tissue engineering applications (e.g. cartilage regeneration) (Rodrigues, Griffith et Wells, 2010).

Since no significant effect in solution was observed with any of the GF studied, we hypothesized that there would probably not be more effect when immobilized on biomaterial's surface and chose to focus the rest of the project on CS effect only. Yet, of course it is still possible that a grafted GF enhances more drastically cell behavior than soluble GF due to sustained effect during longer period of time at the site of interest, this could be the subject of other further work.

Effect of CS in solution

For evaluating the effect of CS in solution on hMSC, cells were exposed to 250 µg/ml of CS in culture media (after a period of 24h adhesion in complete media: 10% FBS), a concentration which has been used for testing CS effect on VSMC resistance to apoptosis (Lerouge et al., 2007). While CS addition to complete media did not influence cells, hMSC

exposed to 250 µg/ml of CS in serum free conditions showed a significant decrease in viability when compared to SF media without CS. Cells which were already adhered to the culture plate (during the first 24h in complete media) started to detach upon exposure to SF+CS by exhibiting a round morphology and a decrease in viability. To further investigate this effect, dose response experiments of CS in solution in SF at different concentrations were performed. As observed in the results, the more CS in the SF media, the faster the cells started to detach and as time of exposure continues, cell detachment begins at lower CS concentrations. This behavior was not exclusive to hMSC, since the same detachment effect was observed with VSMC.

To the best of our knowledge, this is the first time such a cell detachment effect is described with CS. Previous work at LBeV showed that grafting CS on biomaterials surface permitted good endothelial and VSMC adhesion and growth (Thalla et al., 2014). It therefore appears that the effect of CS when in SF solution is very different from that when immobilized. Other previous studies had shown anti-apoptotic effect of CS in SF media on VSMC, at similar concentrations that the ones used in this project (Charbonneau et al., 2007; Raymond et al., 2004), but results were expressed as percentage of apoptotic cells and not as total viability, additionally they were performed at very early time points (less than 24h of exposure to CS in SF). This could explain why they didn't describe a cell detachment effect.

A few studies from the literature can help explain these results. Thus Aguiar *et al.* 2005 described an impaired cell attachment effect in culture plates pre-coated with fibronectin and other ECM adhesive proteins, when sulfated GAGs (CS or heparin) are added in solution. The study suggests that cell adhesion is affected due to GAG chains competition for fibronectin and other adhesive protein binding sites (Aguiar et al., 2005). Sulfated GAGs are involved in the mechanisms of cell adhesion to adhesive ECM proteins due to the presence of proteoglycan binding sites in the adhesive proteins. Families of transmembrane proteoglycans such as Syndecan family, can act as co-receptors to modulate integrin-mediated cell-matrix adhesion (Woods et Couchman, 1998). Together with integrins they form a dual receptor system for cell-matrix adhesion. Particularly CS proteoglycans have

been implicated in cell attachment via interactions with ECM proteins such as fibronectin and integrins. It has been described that adhesion to the Hep III domain of fibronectin involves the cooperation of activated α4β1 integrin and CS proteoglycans (Moyano et al., 1999).

Similarly, a peptide sequence found in the cell attachment domain of fibronectin, called RGD (for the tripeptide L-arginyl-glycyl-L-aspartic acid; Arg-Gly-Asp) which is well known to promote cell adhesion when immobilized on biomaterials surface, has proven to detach cells from their substratum when added in solution into the culture media (Hayman, Pierschbacher et Ruoslahti, 1985). This, suggest that when in solution, the RGD peptides compete for the attachment receptors at the cells surface against the substratum-bound molecules.

In this master project, adhesion was not carried out in presence of CS since cells were previously adhered during 24h in complete media. However after exposure to SF+CS, cells might lose the interaction with the adhesive proteins left (which were initially absorbed during the adhesion period) due to CS competition for their binding sites. Another possibility is that CS molecules suspended in the medium interact with the attachment receptors of the adhered cells and induce their detachment, consequently losing affinity to the substratum. In the future, it could be worth to explore the mechanisms that CS in solution in SF induce on adhered hMSC by techniques such as RT-PCR, where expression of integrins and other cell-adhesion mediators could be analyzed.

In serum-containing media, no positive or negative effect (cell detachment) was observed, probably because serum contains adhesive proteins which interact with the CS and thus neutralize its effect. For all these reasons, cell detachment in the presence of CS in solution doesn't mean that when grafted on biomaterials surface, the biomolecule won't have a positive effect on cell adhesion. Therefore, the effect of immobilized CS was studied.

Effect of immobilized CS on hMSC

For the second specific objective, CS was immobilized by covalent bonding on amine-rich substrates (plasma polymerized LP coating or commercial AP plates (unknown process)) and the physicochemical properties of the bioactive surfaces were studied. The biological response of the bioactive surfaces was analyzed by adhesion, growth and survival experiments with hMSC. Physicochemical characterization results indicated an increase in wettability when CS is grafted on LP as assessed by contact angle, and changes in topography as shown by AFM. Previous studies already demonstrated that CS was grafted, based on the presence of sulfur by XPS or sulfur containing ions by Tof-SIMS (Charbonneau et al., 2011; Charbonneau et al., 2012). In the present study, quantification of CS was performed using Toluidine Blue O, which showed a big difference in CS grafting potential, since AP grafted almost 5 times more CS than LP. Cell culture experiments resulted in improved cell adhesion and growth on LP based bioactive surfaces, whereas cell adhesion was prevented on amine plate based bioactive coatings in complete media (10% FBS). In serum free conditions, no pro-survival advantage was observed on LP based bioactive surfaces.

How can the difference between the two surfaces be explained and why do they impact cell behavior so much?

In this study, LP is the NH_2-rich surface targeted for clinical transfer but commercial amine plates were also used for comparison and simplicity purposes (AP is much easier to use and already sterile). Since cell behavior was found to be different between the two grafted surfaces, quantification of grafted CS (by TBO) and NH_2 (by Orange II) was studied. The difference in CS grafting capacity between AP and LP could be explained due to the distribution of amino groups (which is unknown on AP due to commercial intellectual property), since CS can only be grafted to available amino groups on the top of the surface. Orange II results between AP and LP were not so different. However this technique is probably not well adapted to such a comparison, since it has been recently reported that Orange II measurement varies as a function of the thickness of the LP amine-rich coating (Boespflug, 2015). The thicker the coating, the higher amount of Orange II quantified,

because it considers not only the groups available on the upper layer but also in depth (the small molecule can diffuse into the coating, unlike CS macromolecule). In contrast, in AP coating (which thickness is unknown), amino groups could be concentrated at the top, so that a higher amount is available for CS grafting. We can't confirm this, since the fabrication method and thickness of AP is unknown, but it is the most likely explanation for the discrepancies in CS-grafting potential, while we know that amino groups in LP are also found inside the thickness of the polymerized coating (100 nm thick). Although not easy to perform on commercial amine plates, angle resolved XPS would be a better technique to quantify amino groups in the top surface layer, where CS can be grafted.

It is important to note that uncovalently bounded CS was removed prior to Toluidine blue measurements (by a series of rinses in the ultrasonic bath as indicated in the methodology). Therefore it is likely that the amount of CS grafted on AP saturated the surface and instead of enhancing cell adhesion it prevented this. This hypothesis was further verified by studying the protein adsorption and cell adhesion properties of AP+CS with decreasing amounts of CS grafted (by diluting the grafting solution). TBO assay was used to confirm the gradient of CS grafted. Results indicated that protein adhesion was prevented on AP+CS for most of CS concentrations, except for the lower ones. Previous studies from the laboratory suggested that CS promotes selective protein adsorption (Thalla et al., 2014). Yet this seems to be only true when CS amount on the surfaces is limited, as it is in the case when grafting CS on LP but not on AP surfaces. If protein adsorption is prevented on the surface, cells don't have a protein layer to interact with, thus preventing its adhesion too. This was confirmed with the cell assays on AP+CS were the same concentrations that prevented protein adsorption affected cell adhesion. In the future, testing LP and AP with the same amount of CS grafted by diluting the grafting solution for AP (≈0.005% according to TBO results), could be interesting for comparing cell behavior between both substrates. Since a big range of CS concentrations still render the surface antifouling for cells and proteins, this could also indicate that the arrangement of the grafted CS and the stereochemistry of the grafting on this material is not convenient for enhancing bioactivity. Further testing could be done to study CS conformation and fibronectin adsorption as a function of the underlying substrate.

Whatever the explanation, LP+CS appears as a promising bioactive coating for hMSC

Cell behavior showed some differences among the two hMSC lots tested (Lonza lot and Texas A&M Institute for Regenerative Medicine lot). In terms of adhesion Lonza lot demonstrated a high affinity for LP material, while in the case of Texas lot cells were equally attracted by LP and LP+CS. This could be due to donor variability since primary stem cell lines such as hMSC are susceptible to present changes in behavior depending on the donor, as mentioned in the literature review (Siddappa et al., 2007). Despite variation between cell lots, both presented an increased adhesion on the bioactive coatings compared to tissue culture plates or bare PET films. Therefore this technique could be used to recover implantable devices for enhancing cell colonization. In terms of cell growth, bioactive coatings also presented an increase in viability after 4 and 7 days in culture compared to PET and PCP. Moreover, with Lonza lot, LP+CS also present a higher growth ratio when compared to PCP and PET at 7 days (conclusion not valid when comparing to LP, since it reached confluency sooner which could have limited cell growth). In the case of Texas cells, confluency arrived so rapidly in the bioactive surfaces that by 4 days, LP and LP+CS had no more space for cells to grow, evidencing the potential in enhancing cell growth in these bioactive coatings.

In regards to pro-survival effect in SF, results were not promising since none of the surfaces prevented cell death. The term “survival” is used here since we do not expect cell growth in SF conditions. After 7 days cell viability decreased in all surfaces, and LP presented the highest number of remaining cells, while all other surfaces presented a negligible amount of cells. This could be explained due to the high initial cell adhesion on LP, since it has been reported that cell-cell interactions help resist SF conditions (Yasui et al., 2000). Pro-survival advantages at time points such as more than 24h have only been observed in our lab (with other cell lines such as VSMC) when adding growth factors or grafting them to LP+CS coatings (Lequoy et al., 2014). Since a growth factor which could exhibit a pro-survival effect on hMSC was not identified in this setting, it is not surprising that CS by itself could not enhance cell survival after prolonged exposure to SF.

The use of CS in the coating rather than just LP is convenient because despite LP excellent cell adhesion, its positive charge could also promote platelet adhesion and activation contributing to surface-induced thrombosis, as proven by blood perfusion assays done on LP (Thalla et al., 2014). In contrast, Thalla *et al.,* 2014 have previously shown that CS coating prevent platelet adhesion and activation while favoring a stable endothelial lining by promoting endothelial cells adhesion and growth. Therefore immobilized CS presents the advantage of preventing thrombus formation while favoring hMSC adhesion and growth.

Effect of CS in chitosan hydrogels

For the third specific objective, CS was incorporated to chitosan based hydrogels previously developed at LBeV. The best gelling agent formulation for cells viability was determined from previous experiments done with fibroblasts (Ceccaldi et al., submitted 2015) and CS was incorporated to the hydrogel by dissolving it in the gelling agent. These experiments were performed since preliminary work at LBeV indicated that CS could strongly enhance fibroblast viability when added at a concentration of 1% (w/v) (Alinejad Y., 2016 unpublished). Yet, in the present work it was not found to be the case for hMSC: while the initial number of viable cells was similar at 24h in both hydrogels (0 and 1% CS), it strongly decreased at day 4 and 7 in the presence of CS when using NutriStem XF medium. In alpha MEM medium both hydrogels exhibited a decrease in viability after 4 and 7 days. Interestingly, while NutriStem XF media (which is more specialized for MSC) enhanced cells viability in hydrogels without CS, no benefit was observed in hydrogels with CS. Therefore, a possible explanation could be that CS interacts with the adhesive proteins and growth factors in the specialized media impairing its availability for cells. Moreover we observed that CS at this concentration caused the hydrogel to precipitate and expulse water which resulted in a "shrunk" hydrogel in culture when compared to hydrogels without CS. It is possible that since CS has a negative charge and chitosan a positive one, electrostatic interactions take place and impair the normal gelation and retention of water inside the hydrogel. Therefore, the lack of cell survival after 4 and 7 days could also be related to a lack of nutrient diffusion caused by the hydrogel morphology, since at 24h cells are as viable as in the hydrogel without CS. It is possible that the "shrunk" hydrogel is too compact and its

porosity is not adequate for the medium and its nutrients to diffuse properly into the hydrogel. As detailed in the literature review section, it has been reported that lack of nutrients and oxygen diffusion inside 3D scaffolds results in impaired cell viability (Bergemann et al., 2015). Further work needs to be done to prove this hypothesis such as analyzing the porosity of the CS-hydrogel with techniques such as scanning electron microscopy, protein diffusion through the gel and exploring the swelling behavior of the hydrogel to observe if CS prevents water absorption.

We then tested a CS concentration which would not impair good gel formation and which corresponds to those previously shown to influence cell behaviour. Since in this project it was observed that concentrations such as 250 µg/ml influence MSC behavior (as in the case of hMSC with CS in solution in SF) and in the literature concentrations of CS in solution range up to 500µg/ml (Lerouge et al., 2007), a new final concentration of 500µg/ml of CS in the hydrogel was chosen. The new CS-hydrogel maintained cells viability for up to 7 days and didn't shrink after gelation. However no statistic difference in viability was observed between hydrogels with and without CS at all time points.

The presence of CS in the hydrogel could be beneficial for hMSC differentiation, as detailed later in this discussion. Further optimization of a CS percentage which could maintain or enhance viability without affecting the gelation and structure of the gel is needed. Additionally CS release assays need to be done in order to know if any CS is being released out of the gel to the aqueous media. The assay could be done by immerging hydrogels with different CS percentages into aqueous media at different time points and analyzing the released CS by colorimetric methods such as Dimethylmethylene Blue Assay (Farndale, Sayers et Barrett, 1982). Nevertheless if electrostatic interactions between chitosan and CS take place, as suspected in this project, it is probable that at least a part of CS is effectively retained inside the hydrogel.

Future perspectives

As a future perspective, CS in biomaterials with hMSC can present advantages not only in cell adhesion and growth through cell-surface interactions like in the case of the bioactive coatings from this project, but other aspects such as differentiation can be explored. As mentioned on the literature review, CS potential in differentiation on biomaterials, especially for osteogenic and chondrogenic differentiation, has been explored (Anjum et al., 2006; Sawatjui et al., 2015; Varghese et al., 2008). The surface modification techniques for implantable devices presented in this project could be profited for adherent cells differentiation such as osteogenic differentiation. In the case of 3D scaffolds such as the hydrogels developed in this project, which maintain hMSC viability, chondrogenic differentiation assays could be particularly interesting. Cells under chondrogenic differentiation tend to form aggregates and secrete ECM factors, which could be enhanced by the presence of CS (Varghese et al., 2008). However further optimization of the CS concentration for this particular application is needed. If differentiation can be enhanced either on the bioactive surfaces or in the hydrogels, its potential for tissue engineering and repair is very promising. Other possible pathway for the project is to continue to explore different growth factors as previously suggested in order to find one with a pro-survival effect on hMSC which could be interesting to further incorporate to biomaterials. Growth factors could be further immobilized to CS in the bioactive surfaces by the methods previously tested at LBeV, i.e. by covalent bonding (Charbonneau et al., 2012) or oriented tethering through coil-coil interactions (Lequoy et al., 2014). The growth factors could also be further incorporated to the hydrogels. However methods to retain them inside the hydrogel will have to be explored since in aqueous media, the growth factors could be released and their effect inside the hydrogel might be lost. Nevertheless, affinity of CS with GF, especially FGF (Milev et al., 1998) could help retain GF inside the gel, and could be a further advantage in using this biomolecule. Additionally GF could be used not only for enhancing proliferation or survival of MSC but also for triggering differentiation.

Study limitations

This project presented several limitations. Since the CS was not sterilized by the manufacturer, it was previously dissolved in aqueous media and filtered through a 0.20 μM sterile filter, however big quantities of the original liquid were lost after filtration and the final CS percentage might have changed. In this project CS "stock" filtrates were created and used for the experiments repetitions in order to reduce the variability and yield reproducible results. Therefore, one of the main aspects that needs to be optimized in this project is the sterilization of CS. Other options like sterilization by autoclave can be explored but its effect needs to be analyzed, since heat could damage CS structure impairing the bioactivity. Another limiting factor was the technique to assess viability within hydrogels, as previously described in the material and methods: the alamar blue solution with the hydrogel were homogenized, however the process itself is very variable since it is possible that big pieces of hydrogel remained undestroyed, and therefore alamar blue solution was not in contact with some cells entrapped inside the bigger hydrogel pieces. Additionally, pieces of hydrogels could have affected the fluorescence lecture. In this project cell viability was understood as cell metabolic activity, however it cannot be said with certainty if what is observed is loss/increase of viability or growth, since it is in terms of metabolic activity. Different options to assess cell viability such as live/dead, flow cytometry, BrdU assay, TUNEL and fluorescence microscopy (nuclei staining) could be used to complement the alamar blue results. Another limiting factor was that entrapping cells within hydrogels required a large number of cells, especially when optimization of hydrogels needs to be done and many different conditions need to be tested. Expansion of hMSC require specialized mediums and they can only be used at early passages. After 10 passages hMSC lose their differentiation potential or become senescent (stop growing) (Estrada et al., 2013; Hayflick et Moorhead, 1961; Zaim et al., 2012). This has strongly limited the number of conditions tested within the same test. Thus, by means of time and cost, only two CS concentration within hydrogels could be tested. Further CS optimization in relation to its bioactivity and hydrogel morphology needs to be done.

CONCLUSION

The objective of this project was to study the potential of extracellular matrix components such as chondroitin sulfate and growth factors to enhance the bioactivity of biomaterials such as implantable devices and 3D scaffolds. More particularly we investigated whether these molecules facilitated the adhesion, growth and survival of hMSC, which play a major role in tissue repair and tissue engineering applications

The GF studied didn't show a significant effect on hMSC, so the project was focused on CS only. The effect of CS on MSC was complex and relative to its concentration and immobilization methods. In serum free solution, CS detached cells from the culture plate, probably due to competition for protein and cells binding sites, while in serum containing medium cell viability was not affected, probably because proteins in the serum neutralized CS effect.

CS is a potential ECM biomolecule for enhancing bioactivity of implantable devices as proven by increased adhesion and growth on bioactive coatings based on LP. CS is particularly appealing for implants in contact with blood since CS surfaces also decrease platelet adhesion and activation. A pro-survival effect of CS on the bioactive coatings was not observed. However further investigation of growth factors for improving hMSC viability in SF could lead to an interesting molecule to further incorporate and enhance the survival of cells on the coating. In contrast to LP, grafting CS on commercial AP surface did not show beneficial effects, since the coatings were antifouling for cells and proteins, probably due to higher density of amino groups at the top surface. This shows the influence of CS concentration and maybe CS conformation on the protein and cell behavior, a compromise that needs to be found to avoid a deleterious anti-fouling effect.

In regards to CS incorporated into 3D scaffolds such as hydrogels, no conclusions could be drawn yet in regards to potential beneficial effect, but CS might play a role in enhancing hMSC differentiation. Further optimization of CS-hydrogels is needed in order to find an

adequate concentration of CS which does not impair its gelation and maintain or enhance hMSC viability or differentiation.

APPENDIX I

EGF AND CS EFFECT ON RAT MSC

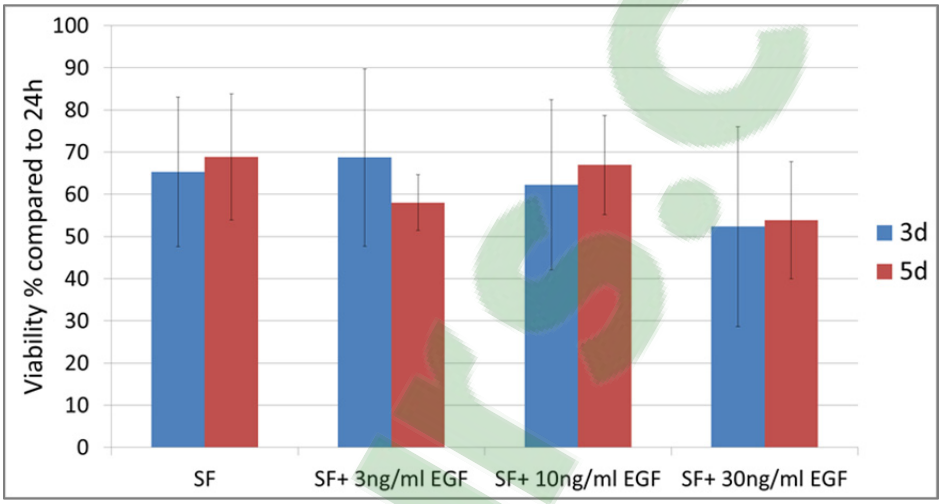

Figure-A I-1 Effect of EGF in solution on rMSC viability after 3 or 5 days in serum free (SF) medium. Results are expressed as percentage of alamar Blue fluorescence signal compared to signal after 24h adhesion in complete medium (N=2, n=4)

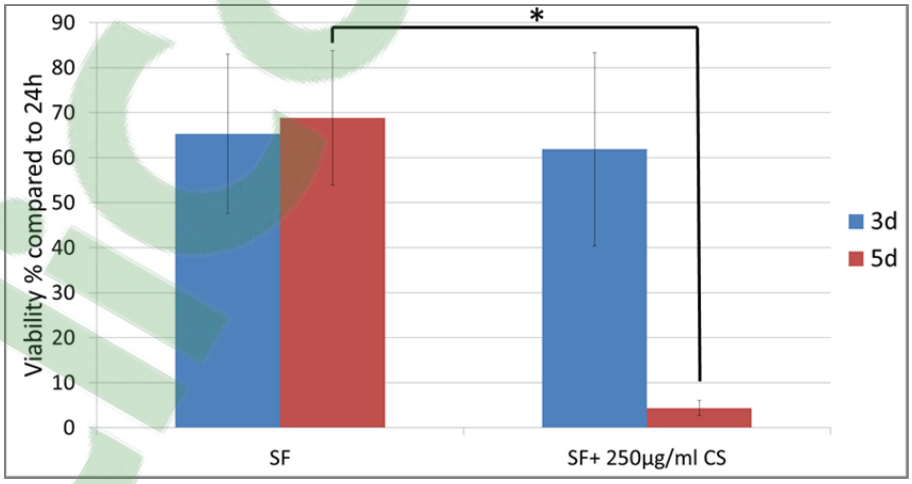

Figure-A I-2 Effect of CS in solution on rMSC viability after 3 or 5 days in serum free (SF) medium. Results are expressed as percentage of alamar Blue fluorescence signal compared to signal after 24h adhesion in complete medium (N=2, n=4) (*$p<0.05$)

LIST OF BIBLIOGRAPHIC REFERENCES

Abdi, Reza, Paolo Fiorina, Chaker N. Adra, Mark Atkinson et Mohamed H. Sayegh. 2008. « Immunomodulation by Mesenchymal Stem Cells : A Potential Therapeutic Strategy for Type 1 Diabetes ». *Diabetes,* vol. 57, n° 7, p. 1759-1767.

Aguiar, C. B., B. Lobao-Soares, M. Alvarez-Silva et A. G. Trentin. 2005. « Glycosaminoglycans modulate C6 glioma cell adhesion to extracellular matrix components and alter cell proliferation and cell migration ». *BMC Cell Biol,* vol. 6, p. 31.

Ailawadi, G., J. L. Eliason et G. R. Upchurch, Jr. 2003. « Current concepts in the pathogenesis of abdominal aortic aneurysm ». *J Vasc Surg,* vol. 38, n° 3, p. 584-8.

Anjum, Fraz, Philipp S. Lienemann, Stéphanie Metzger, Jeff Biernaskie, Michael S. Kallos et Martin Ehrbar. 2006. « Enzyme responsive GAG-based natural-synthetic hybrid hydrogel for tunable growth factor delivery and stem cell differentiation ». *Biomaterials*.

Assaad, E., M. Maire et S. Lerouge. 2015. « Injectable thermosensitive chitosan hydrogels with controlled gelation kinetics and enhanced mechanical resistance ». *Carbohydr Polym,* vol. 130, p. 87-96.

Azarnoush, K., A. Maurel, L. Sebbah, C. Carrion, A. Bissery, C. Mandet, J. Pouly, P. Bruneval, A. A. Hagege et P. Menasche. 2005. « Enhancement of the functional benefits of skeletal myoblast transplantation by means of coadministration of hypoxia-inducible factor 1alpha ». *J Thorac Cardiovasc Surg,* vol. 130, n° 1, p. 173-9.

Ball, S. G., C. A. Shuttleworth et C. M. Kielty. 2007. « Mesenchymal stem cells and neovascularization: role of platelet-derived growth factor receptors ». *J Cell Mol Med,* vol. 11, n° 5, p. 1012-30.

Bao, P., A. Kodra, M. Tomic-Canic, M. S. Golinko, H. P. Ehrlich et H. Brem. 2009. « The role of vascular endothelial growth factor in wound healing ». *J Surg Res,* vol. 153, n° 2, p. 347-58.

Basmanav, F. B., G. T. Kose et V. Hasirci. 2008. « Sequential growth factor delivery from complexed microspheres for bone tissue engineering ». *Biomaterials,* vol. 29, n° 31, p. 4195-204.

Benoit, D. S., et K. S. Anseth. 2005. « Heparin functionalized PEG gels that modulate protein adsorption for hMSC adhesion and differentiation ». *Acta Biomater,* vol. 1, n° 4, p. 461-70.

Benoit, D. S., M. P. Schwartz, A. R. Durney et K. S. Anseth. 2008. « Small functional groups for controlled differentiation of hydrogel-encapsulated human mesenchymal stem cells ». *Nat Mater,* vol. 7, n° 10, p. 816-23.

Benoit, D. S., M. C. Tripodi, J. O. Blanchette, S. J. Langer, L. A. Leinwand et K. S. Anseth. 2007. « Integrin-linked kinase production prevents anoikis in human mesenchymal stem cells ». *J Biomed Mater Res A,* vol. 81, n° 2, p. 259-68.

Bergemann, C., P. Elter, R. Lange, V. Weissmann, H. Hansmann, E. D. Klinkenberg et B. Nebe. 2015. « Cellular Nutrition in Complex Three-Dimensional Scaffolds: A Comparison between Experiments and Computer Simulations ». *Int J Biomater,* vol. 2015, p. 584362.

Bianchi, Giordano, Andrea Banfi, Maddalena Mastrogiacomo, Rosario Notaro, Lucio Luzzatto, Ranieri Cancedda et Rodolfo Quarto. 2003. « Ex vivo enrichment of mesenchymal cell progenitors by fibroblast growth factor 2 ». *Experimental Cell Research,* vol. 287, n° 1, p. 98-105.

Biophy Research. 2013. « Document technique Angle de Contact ». < http://www.biophyresearch.com/wp-content/uploads/2013/04/Document-technique-Angle-de-Contact-v01.pdf >. Consulted on December 21, 2015.

Boespflug, G. 2015. « Fabrication, caractérisation et application de surfaces organiques fonctionnalisées pour le génie tissulaire ». École Polytechnique de Montréal.

Bonewald, L. F., et S. L. Dallas. 1994. « Role of active and latent transforming growth factor beta in bone formation ». *J Cell Biochem,* vol. 55, n° 3, p. 350-7.

Bowen, W.R., et N. Hilal. 2009. *Atomic Force Microscopy in Process Engineering: An Introduction to AFM for Improved Processes and Products*. Elsevier Science.

Bracco, G., et B. Holst (3-34). 2013. *Surface Science Techniques*. Springer Berlin Heidelberg, 663 p.

Ceccaldi, C. , E. Assaad, E. Hui, L. Bonneton et S. Lerouge. submitted 2015. « Injectable Thermosensitive Scaffolds With Enhanced Mechanical Properties For Cell Therapy ». *Biomacromolecules*

Charbonneau, C., J. E. Gautrot, M. J. Hebert, X. X. Zhu et S. Lerouge. 2007. « Chondroitin-4-sulfate: a bioactive macromolecule to foster vascular healing around stent-grafts after endovascular aneurysm repair ». *Macromol Biosci,* vol. 7, n° 5, p. 746-52.

Charbonneau, C., B. Liberelle, M. J. Hebert, G. De Crescenzo et S. Lerouge. 2011. « Stimulation of cell growth and resistance to apoptosis in vascular smooth muscle cells

on a chondroitin sulfate/epidermal growth factor coating ». *Biomaterials,* vol. 32, n° 6, p. 1591-600.

Charbonneau, C., J. C. Ruiz, P. Lequoy, M. J. Hebert, G. De Crescenzo, M. R. Wertheimer et S. Lerouge. 2012. « Chondroitin sulfate and epidermal growth factor immobilization after plasma polymerization: a versatile anti-apoptotic coating to promote healing around stent grafts ». *Macromol Biosci,* vol. 12, n° 6, p. 812-21.

Chase, L. G., U. Lakshmipathy, L. A. Solchaga, M. S. Rao et M. C. Vemuri. 2010. « A novel serum-free medium for the expansion of human mesenchymal stem cells ». *Stem Cell Res Ther,* vol. 1, n° 1, p. 8.

Chastain, S. R., A. K. Kundu, S. Dhar, J. W. Calvert et A. J. Putnam. 2006. « Adhesion of mesenchymal stem cells to polymer scaffolds occurs via distinct ECM ligands and controls their osteogenic differentiation ». *J Biomed Mater Res A,* vol. 78, n° 1, p. 73-85.

Chu, P. K., J. Y. Chen, L. P. Wang et N. Huang. 2002. « Plasma-surface modification of biomaterials ». *Materials Science and Engineering: R: Reports,* vol. 36, n° 5–6, p. 143-206.

Chuah, Yon Jin, Yi Ting Koh, Kaiyang Lim, Nishanth V. Menon, Yingnan Wu et Yuejun Kang. 2015. « Simple surface engineering of polydimethylsiloxane with polydopamine for stabilized mesenchymal stem cell adhesion and multipotency ». *Scientific Reports,* vol. 5, p. 18162.

Chung, C., et J. A. Burdick. 2009. « Influence of three-dimensional hyaluronic acid microenvironments on mesenchymal stem cell chondrogenesis ». *Tissue Eng Part A,* vol. 15, n° 2, p. 243-54.

Cook Medical. 2016. « Zenith abdominal product portfolio ». < https://www.cookmedical.com/aortic-intervention/zenith-abdominal-product-portfolio/ >. Consulted on May 23, 2016.

Curran, J. M., R. Chen et J. A. Hunt. 2005. « Controlling the phenotype and function of mesenchymal stem cells in vitro by adhesion to silane-modified clean glass surfaces ». *Biomaterials,* vol. 26, n° 34, p. 7057-67.

Curran, J. M., R. Chen et J. A. Hunt. 2006. « The guidance of human mesenchymal stem cell differentiation in vitro by controlled modifications to the cell substrate ». *Biomaterials,* vol. 27, n° 27, p. 4783-93.

Curran, J. M., F. Pu, R. Chen et J. A. Hunt. 2011. « The use of dynamic surface chemistries to control msc isolation and function ». *Biomaterials,* vol. 32, n° 21, p. 4753-4760.

Danmark, S., A. Finne-Wistrand, A. C. Albertsson, M. Patarroyo et K. Mustafa. 2012. « Integrin-mediated adhesion of human mesenchymal stem cells to extracellular matrix proteins adsorbed to polymer surfaces ». *Biomed Mater,* vol. 7, n° 3, p. 035011.

Das, R., H. Jahr, G. J. van Osch et E. Farrell. 2010. « The role of hypoxia in bone marrow-derived mesenchymal stem cells: considerations for regenerative medicine approaches ». *Tissue Eng Part B Rev,* vol. 16, n° 2, p. 159-68.

Dee, Kay C., David A. Puleo et Rena Bizios. 2003. « Protein-Surface Interactions ». In *An Introduction To Tissue-Biomaterial Interactions*. p. 37-52. John Wiley & Sons, Inc. < http://dx.doi.org/10.1002/0471270598.ch3 >.

Deschepper, Mickael, Mathieu Manassero, Karim Oudina, Joseph Paquet, Laurent-Emmanuel Monfoulet, Morad Bensidhoum, Delphine Logeart-Avramoglou et Herve Petite. 2013. « Proangiogenic and Prosurvival Functions of Glucose in Human Mesenchymal Stem Cells upon Transplantation ». *STEM CELLS,* vol. 31, n° 3, p. 526-535.

Di Nicola, M., C. Carlo-Stella, M. Magni, M. Milanesi, P. D. Longoni, P. Matteucci, S. Grisanti et A. M. Gianni. 2002. « Human bone marrow stromal cells suppress T-lymphocyte proliferation induced by cellular or nonspecific mitogenic stimuli ». *Blood,* vol. 99, n° 10, p. 3838-43.

Discher, Dennis E., David J. Mooney et Peter W. Zandstra. 2009. « Growth factors, matrices, and forces combine and control stem cells ». *Science (New York, N.Y.),* vol. 324, n° 5935, p. 1673-1677.

Dominici, M., K. Le Blanc, I. Mueller, I. Slaper-Cortenbach, F. Marini, D. Krause, R. Deans, A. Keating, Dj Prockop et E. Horwitz. 2006. « Minimal criteria for defining multipotent mesenchymal stromal cells. The International Society for Cellular Therapy position statement ». *Cytotherapy,* vol. 8, n° 4, p. 315-7.

Dufrene, Y. F. 2002. « Atomic force microscopy, a powerful tool in microbiology ». *J Bacteriol,* vol. 184, n° 19, p. 5205-13.

Estrada, J. C., Y. Torres, A. Benguria, A. Dopazo, E. Roche, L. Carrera-Quintanar, R. A. Perez, J. A. Enriquez, R. Torres, J. C. Ramirez, E. Samper et A. Bernad. 2013. « Human mesenchymal stem cell-replicative senescence and oxidative stress are closely linked to aneuploidy ». *Cell Death Dis,* vol. 4, p. e691.

Farndale, R. W., C. A. Sayers et A. J. Barrett. 1982. « A direct spectrophotometric microassay for sulfated glycosaminoglycans in cartilage cultures ». *Connect Tissue Res,* vol. 9, n° 4, p. 247-8.

Farre, J., S. Roura, C. Prat-Vidal, C. Soler-Botija, A. Llach, C. E. Molina, L. Hove-Madsen, J. J. Cairo, F. Godia, R. Bragos, J. Cinca et A. Bayes-Genis. 2007. « FGF-4 increases in vitro expansion rate of human adult bone marrow-derived mesenchymal stem cells ». *Growth Factors,* vol. 25.

Franquesa, Marcella, Martin Johannes Hoogduijn, Oriol Bestard et Josep M Grinyó. 2012. « Immunomodulatory effect of Mesenchymal Stem Cells on B cells ». *Frontiers in Immunology,* vol. 3.

Friedenstein, A. J., Shapiro Piatetzky, II et K. V. Petrakova. 1966. « Osteogenesis in transplants of bone marrow cells ». *J Embryol Exp Morphol,* vol. 16, n° 3, p. 381-90.

Gauvin, Robert, Maxime Guillemette, Mehmet Dokmeci et Ali Khademhosseini. 2011. « Application of microtechnologies for the vascularization of engineered tissues ». *Vascular Cell,* vol. 3, n° 1, p. 1-7.

Ghouri, Maaz, et Zvonimir Krajcer. 2010. « Endoluminal Abdominal Aortic Aneurysm Repair: The Latest Advances in Prevention of Distal Endograft Migration and Type 1 Endoleak ». *Texas Heart Institute Journal,* vol. 37, n° 1, p. 19-24.

Gigout, A., J. C. Ruiz, M. R. Wertheimer, M. Jolicoeur et S. Lerouge. 2011. « Nitrogen-rich plasma-polymerized coatings on PET and PTFE surfaces improve endothelial cell attachment and resistance to shear flow ». *Macromol Biosci,* vol. 11, n° 8, p. 1110-9.

Gilbert, M. E., K. R. Kirker, S. D. Gray, P. D. Ward, J. G. Szakacs, G. D. Prestwich et R. R. Orlandi. 2004. « Chondroitin sulfate hydrogel and wound healing in rabbit maxillary sinus mucosa ». *Laryngoscope,* vol. 114, n° 8, p. 1406-9.

Grabarek, Z., et J. Gergely. 1990. « Zero-length crosslinking procedure with the use of active esters ». *Anal Biochem,* vol. 185, n° 1, p. 131-5.

Guo, L., N. Kawazoe, Y. Fan, Y. Ito, J. Tanaka, T. Tateishi, X. Zhang et G. Chen. 2008. « Chondrogenic differentiation of human mesenchymal stem cells on photoreactive polymer-modified surfaces ». *Biomaterials,* vol. 29, n° 1, p. 23-32.

Hamming, Lesley M, et Phillip B Messersmith. 2008. « Fouling resistant biomimetic poly (ethylene glycol) based grafted polymer coatings ». *Mater. Matters,* vol. 3, p. 52.

Handley, C. J., T. Samiric et M. Z. Ilic. 2006. « Structure, metabolism, and tissue roles of chondroitin sulfate proteoglycans ». *Adv Pharmacol,* vol. 53, p. 219-32.

Hass, R., C. Kasper, S. Bohm et R. Jacobs. 2011. « Different populations and sources of human mesenchymal stem cells (MSC): A comparison of adult and neonatal tissue-derived MSC ». *Cell Commun Signal,* vol. 9, p. 12.

Hayflick, L., et P. S. Moorhead. 1961. « The serial cultivation of human diploid cell strains ». *Exp Cell Res,* vol. 25, p. 585-621.

Hayman, E. G., M. D. Pierschbacher et E. Ruoslahti. 1985. « Detachment of cells from culture substrate by soluble fibronectin peptides ». *J Cell Biol,* vol. 100, n° 6, p. 1948-54.

Henderson, E. L., Y. J. Geng, G. K. Sukhova, A. D. Whittemore, J. Knox et P. Libby. 1999. « Death of smooth muscle cells and expression of mediators of apoptosis by T lymphocytes in human abdominal aortic aneurysms ». *Circulation,* vol. 99, n° 1, p. 96-104.

Hinek, A., J. Boyle et M. Rabinovitch. 1992. « Vascular smooth muscle cell detachment from elastin and migration through elastic laminae is promoted by chondroitin sulfate-induced "shedding" of the 67-kDa cell surface elastin binding protein ». *Exp Cell Res,* vol. 203, n° 2, p. 344-53.

Hoffman, Allan S., et Jeffrey A. Hubbell. 2013. « Chapter I.2.17 - Surface-Immobilized Biomolecules A2 - Lemons, Buddy D. RatnerAllan S. HoffmanFrederick J. SchoenJack E ». In *Biomaterials Science (Third Edition)*. p. 339-349. Academic Press. < http://www.sciencedirect.com/science/article/pii/B9780080877808000322 >.

Hoogduijn, Martin Johannes, et Frank J.M.F. Dor. 2011. « Mesenchymal stem cells in Transplantation and Tissue Regeneration ». *Frontiers in Immunology,* vol. 2.

Ishihara, M., K. Obara, T. Ishizuka, M. Fujita, M. Sato, K. Masuoka, Y. Saito, H. Yura, T. Matsui, H. Hattori, M. Kikuchi et A. Kurita. 2003. « Controlled release of fibroblast growth factors and heparin from photocrosslinked chitosan hydrogels and subsequent effect on in vivo vascularization ». *J Biomed Mater Res A,* vol. 64, n° 3, p. 551-9.

Jacob, M. P., C. Badier-Commander, V. Fontaine, Y. Benazzoug, L. Feldman et J. B. Michel. 2001. « Extracellular matrix remodeling in the vascular wall ». *Pathol Biol (Paris),* vol. 49, n° 4, p. 326-32.

Jebaramya, J, M Ilanchelian et S Prabahar. 2009. « Spectral studies of toluidine blue O in the presence of sodium dodecyl sulfate ». *sensors,* vol. 21, p. 22.

Kaiura, T. L., H. Itoh, S. M. Kubaska, 3rd, T. A. McCaffrey, B. Liu et K. C. Kent. 2000. « The effect of growth factors, cytokines, and extracellular matrix proteins on fibronectin production in human vascular smooth muscle cells ». *J Vasc Surg,* vol. 31, n° 3, p. 577-84.

Keskar, V., N. W. Marion, J. J. Mao et R. A. Gemeinhart. 2009. « In vitro evaluation of macroporous hydrogels to facilitate stem cell infiltration, growth, and mineralization ». *Tissue Eng Part A,* vol. 15, n° 7, p. 1695-707.

Kim, S. H., J. Turnbull et S. Guimond. 2011. « Extracellular matrix and cell signalling: the dynamic cooperation of integrin, proteoglycan and growth factor receptor ». *J Endocrinol,* vol. 209, n° 2, p. 139-51.

Kito, H., et T. Matsuda. 1996. « Biocompatible coatings for luminal and outer surfaces of small-caliber artificial grafts ». *J Biomed Mater Res,* vol. 30, n° 3, p. 321-30.

Kollmer, M., V. Keskar, T. G. Hauk, J. M. Collins, B. Russell et R. A. Gemeinhart. 2012. « Stem cell-derived extracellular matrix enables survival and multilineage differentiation within superporous hydrogels ». *Biomacromolecules,* vol. 13, n° 4, p. 963-73.

Krausgrill, B., M. Vantler, V. Burst, M. Raths, M. Halbach, K. Frank, S. Schynkowski, K. Schenk, J. Hescheler, S. Rosenkranz et J. Muller-Ehmsen. 2009. « Influence of cell treatment with PDGF-BB and reperfusion on cardiac persistence of mononuclear and mesenchymal bone marrow cells after transplantation into acute myocardial infarction in rats ». *Cell Transplant,* vol. 18, n° 8, p. 847-53.

Kuddannaya, S., Y. J. Chuah, M. H. Lee, N. V. Menon, Y. Kang et Y. Zhang. 2013. « Surface chemical modification of poly(dimethylsiloxane) for the enhanced adhesion and proliferation of mesenchymal stem cells ». *ACS Appl Mater Interfaces,* vol. 5, n° 19, p. 9777-84.

Laplante, P., M. A. Raymond, G. Gagnon, N. Vigneault, A. M. Sasseville, Y. Langelier, M. Bernard, Y. Raymond et M. J. Hebert. 2005. « Novel fibrogenic pathways are activated in response to endothelial apoptosis: implications in the pathophysiology of systemic sclerosis ». *J Immunol,* vol. 174, n° 9, p. 5740-9.

Lee, K. Y., et D. J. Mooney. 2001. « Hydrogels for tissue engineering ». *Chem Rev,* vol. 101, n° 7, p. 1869-79.

Lequoy, P., B. Liberelle, G. De Crescenzo et S. Lerouge. 2014. « Additive benefits of chondroitin sulfate and oriented tethered epidermal growth factor for vascular smooth muscle cell survival ». *Macromol Biosci,* vol. 14, n° 5, p. 720-30.

Lequoy, P., F. Murschel, B. Liberelle, S. Lerouge et G. De Crescenzo. 2016. « Controlled co-immobilization of EGF and VEGF to optimize vascular cell survival ». *Acta Biomater,* vol. 29, p. 239-247.

Lerouge, S., A. Major, P. L. Girault-Lauriault, M. A. Raymond, P. Laplante, G. Soulez, F. Mwale, M. R. Wertheimer et M. J. Hebert. 2007. « Nitrogen-rich coatings for promoting healing around stent-grafts after endovascular aneurysm repair ». *Biomaterials,* vol. 28, n° 6, p. 1209-17.

Li, Q., C. G. Williams, D. D. Sun, J. Wang, K. Leong et J. H. Elisseeff. 2004. « Photocrosslinkable polysaccharides based on chondroitin sulfate ». *J Biomed Mater Res A,* vol. 68, n° 1, p. 28-33.

Lieb, E., J. Tessmar, M. Hacker, C. Fischbach, D. Rose, T. Blunk, A. G. Mikos, A. Gopferich et M. B. Schulz. 2003. « Poly(D,L-lactic acid)-poly(ethylene glycol)-monomethyl ether diblock copolymers control adhesion and osteoblastic differentiation of marrow stromal cells ». *Tissue Eng,* vol. 9, n° 1, p. 71-84.

Liu, Y., T. He, H. Song et C. Gao. 2007. « Layer-by-layer assembly of biomacromolecules on poly(ethylene terephthalate) films and fiber fabrics to promote endothelial cell growth ». *J Biomed Mater Res A,* vol. 81, n° 3, p. 692-704.

Loh, Qiu Li, et Cleo Choong. 2013. « Three-Dimensional Scaffolds for Tissue Engineering Applications: Role of Porosity and Pore Size ». *Tissue Engineering. Part B, Reviews,* vol. 19, n° 6, p. 485-502.

Longobardi, L., L. O'Rear, S. Aakula, B. Johnstone, K. Shimer, A. Chytil, W. A. Horton, H. L. Moses et A. Spagnoli. 2006. « Effect of IGF-I in the chondrogenesis of bone marrow mesenchymal stem cells in the presence or absence of TGF-beta signaling ». *J Bone Miner Res,* vol. 21, n° 4, p. 626-36.

Lu, H., L. Guo, N. Kawazoe, T. Tateishi et G. Chen. 2009. « Effects of poly(L-lysine), poly(acrylic acid) and poly(ethylene glycol) on the adhesion, proliferation and chondrogenic differentiation of human mesenchymal stem cells ». *J Biomater Sci Polym Ed,* vol. 20, n° 5-6, p. 577-89.

Lysaght, M. J., A. Jaklenec et E. Deweerd. 2008. « Great expectations: private sector activity in tissue engineering, regenerative medicine, and stem cell therapeutics ». *Tissue Eng Part A,* vol. 14, n° 2, p. 305-15.

Malda, J., T. J. Klein et Z. Upton. 2007. « The roles of hypoxia in the in vitro engineering of tissues ». *Tissue Eng,* vol. 13, n° 9, p. 2153-62.

Masters, K. S. 2011. « Covalent growth factor immobilization strategies for tissue repair and regeneration ». *Macromol Biosci,* vol. 11, n° 9, p. 1149-63.

Merolli, A., et T.J. Joyce. 2009. *Biomaterials in Hand Surgery*. Springer.

Mi, F. L., S. S. Shyu, C. K. Peng, Y. B. Wu, H. W. Sung, P. S. Wang et C. C. Huang. 2006. « Fabrication of chondroitin sulfate-chitosan composite artificial extracellular matrix for stabilization of fibroblast growth factor ». *J Biomed Mater Res A,* vol. 76, n° 1, p. 1-15.

Milev, P., H. Monnerie, S. Popp, R. K. Margolis et R. U. Margolis. 1998. « The core protein of the chondroitin sulfate proteoglycan phosphacan is a high-affinity ligand of fibroblast growth factor-2 and potentiates its mitogenic activity ». *J Biol Chem,* vol. 273, n° 34, p. 21439-42.

Monette, A., C. Ceccaldi, E. Assaad, S. Lerouge et R. Lapointe. 2016. « Chitosan thermogels for local expansion and delivery of tumor-specific T lymphocytes towards enhanced cancer immunotherapies ». *Biomaterials,* vol. 75, p. 237-49.

Monfort, J., J. P. Pelletier, N. Garcia-Giralt et J. Martel-Pelletier. 2008. « Biochemical basis of the effect of chondroitin sulphate on osteoarthritis articular tissues ». *Ann Rheum Dis,* vol. 67, n° 6, p. 735-40.

Moyano, J. V., B. Carnemolla, J. P. Albar, A. Leprini, B. Gaggero, L. Zardi et A. Garcia-Pardo. 1999. « Cooperative role for activated alpha4 beta1 integrin and chondroitin sulfate proteoglycans in cell adhesion to the heparin III domain of fibronectin. Identification of a novel heparin and cell binding sequence in repeat III5 ». *J Biol Chem,* vol. 274, n° 1, p. 135-42.

Mwale, F., H. T. Wang, V. Nelea, L. Luo, J. Antoniou et M. R. Wertheimer. 2006. « The effect of glow discharge plasma surface modification of polymers on the osteogenic differentiation of committed human mesenchymal stem cells ». *Biomaterials,* vol. 27, n° 10, p. 2258-64.

Mwale, Fackson, Sonia Rampersad, Juan-Carlos Ruiz, Pierre-Luc Girard-Lauriault, Alain Petit, John Antoniou, Sophie Lerouge et Michael Wertheimer. 2011. « Amine-Rich Cell-Culture Surfaces for Research in Orthopedic Medicine ». vol. 1, n° 2, p. 115-133.

Nguyen, Alan, Vi Nguyen, Aaron W James et Michelle A Scott. 2015. « Craniomaxillofacial Sources of Mesenchymal Stem Cells: A Brief Review ». *International Journal of Orthopaedics,* vol. 2, n° 4, p. 333-340.

NIH. 2015. « Tissue Engineering and Regenerative Medicine ». < http://www.nibib.nih.gov/science-education/science-topics/tissue-engineering-and-regenerative-medicine#1156 >. Consulted on May 20, 2016.

Noel, Samantha, Benoit Liberelle, Lucie Robitaille et Gregory De Crescenzo. 2011. « Quantification of Primary Amine Groups Available for Subsequent Biofunctionalization of Polymer Surfaces ». *Bioconjugate Chemistry,* vol. 22, n° 8, p. 1690-1699.

Noth, U., L. Rackwitz, A. Heymer, M. Weber, B. Baumann, A. Steinert, N. Schutze, F. Jakob et J. Eulert. 2007. « Chondrogenic differentiation of human mesenchymal stem cells in collagen type I hydrogels ». *J Biomed Mater Res A,* vol. 83, n° 3, p. 626-35.

Nuttelman, C. R., M. C. Tripodi et K. S. Anseth. 2005. « Synthetic hydrogel niches that promote hMSC viability ». *Matrix Biol,* vol. 24, n° 3, p. 208-18.

O'Brien, Fergal J. 2011. « Biomaterials & scaffolds for tissue engineering ». *Materials Today,* vol. 14, n° 3, p. 88-95.

O'Brien, J., I. Wilson, T. Orton et F. Pognan. 2000. « Investigation of the Alamar Blue (resazurin) fluorescent dye for the assessment of mammalian cell cytotoxicity ». *Eur J Biochem,* vol. 267, n° 17, p. 5421-6.

Olsson, A. K., A. Dimberg, J. Kreuger et L. Claesson-Welsh. 2006. « VEGF receptor signalling - in control of vascular function ». *Nat Rev Mol Cell Biol,* vol. 7, n° 5, p. 359-71.

Park, H., J. S. Temenoff, Y. Tabata, A. I. Caplan, R. M. Raphael, J. A. Jansen et A. G. Mikos. 2009a. « Effect of dual growth factor delivery on chondrogenic differentiation of rabbit marrow mesenchymal stem cells encapsulated in injectable hydrogel composites ». *J Biomed Mater Res A,* vol. 88, n° 4, p. 889-97.

Park, K., K. J. Cho, J. J. Kim, I. H. Kim et D. K. Han. 2009b. « Functional PLGA scaffolds for chondrogenesis of bone-marrow-derived mesenchymal stem cells ». *Macromol Biosci,* vol. 9, n° 3, p. 221-9.

Parodi, J. C., J. C. Palmaz et H. D. Barone. 1991. « Transfemoral intraluminal graft implantation for abdominal aortic aneurysms ». *Ann Vasc Surg,* vol. 5, n° 6, p. 491-9.

Phinney, D. G., G. Kopen, W. Righter, S. Webster, N. Tremain et D. J. Prockop. 1999. « Donor variation in the growth properties and osteogenic potential of human marrow stromal cells ». *J Cell Biochem,* vol. 75, n° 3, p. 424-36.

Pittenger, M., P. Vanguri, D. Simonetti et R. Young. 2002. « Adult mesenchymal stem cells: potential for muscle and tendon regeneration and use in gene therapy ». *J Musculoskelet Neuronal Interact,* vol. 2, n° 4, p. 309-20.

Pons, J., Y. Huang, J. Arakawa-Hoyt, D. Washko, J. Takagawa, J. Ye, W. Grossman et H. Su. 2008. « VEGF improves survival of mesenchymal stem cells in infarcted hearts ». *Biochem Biophys Res Commun,* vol. 376, n° 2, p. 419-22.

Potier, E., E. Ferreira, A. Meunier, L. Sedel, D. Logeart-Avramoglou et H. Petite. 2007. « Prolonged hypoxia concomitant with serum deprivation induces massive human mesenchymal stem cell death ». *Tissue Eng,* vol. 13, n° 6, p. 1325-31.

Rammelt, S., T. Illert, S. Bierbaum, D. Scharnweber, H. Zwipp et W. Schneiders. 2006. « Coating of titanium implants with collagen, RGD peptide and chondroitin sulfate ». *Biomaterials,* vol. 27, n° 32, p. 5561-71.

Rampersad, S., J. C. Ruiz, A. Petit, S. Lerouge, J. Antoniou, M. R. Wertheimer et F. Mwale. 2011. « Stem cells, nitrogen-rich plasma-polymerized culture surfaces, and type X collagen suppression ». *Tissue Eng Part A,* vol. 17, n° 19-20, p. 2551-60.

Ratner, Buddy D., et Allan S. Hoffman. 2013. « Chapter I.2.12 - Physicochemical Surface Modification of Materials Used in Medicine A2 - Lemons, Buddy D. RatnerAllan S. HoffmanFrederick J. SchoenJack E ». In *Biomaterials Science (Third Edition)*. p. 259-276. Academic Press. < http://www.sciencedirect.com/science/article/pii/B9780080877808000279 >.

Raymond, M. A., A. Desormeaux, P. Laplante, N. Vigneault, J. G. Filep, K. Landry, A. V. Pshezhetsky et M. J. Hebert. 2004. « Apoptosis of endothelial cells triggers a caspase-dependent anti-apoptotic paracrine loop active on VSMC ». *Faseb j,* vol. 18, n° 6, p. 705-7.

Robey, T. E., M. K. Saiget, H. Reinecke et C. E. Murry. 2008. « Systems approaches to preventing transplanted cell death in cardiac repair ». *J Mol Cell Cardiol,* vol. 45, n° 4, p. 567-81.

Rodrigues, M., H. Blair, L. Stockdale, L. Griffith et A. Wells. 2013. « Surface tethered epidermal growth factor protects proliferating and differentiating multipotential stromal cells from FasL-induced apoptosis ». *Stem Cells,* vol. 31, n° 1, p. 104-16.

Rodrigues, M., L. G. Griffith et A. Wells. 2010. « Growth factor regulation of proliferation and survival of multipotential stromal cells ». *Stem Cell Res Ther,* vol. 1, n° 4, p. 32.

Rodrigues, Sofia N., Inês C. Gonçalves, M. C. L. Martins, Mário A. Barbosa et Buddy D. Ratner. 2006. « Fibrinogen adsorption, platelet adhesion and activation on mixed hydroxyl-/methyl-terminated self-assembled monolayers ». *Biomaterials,* vol. 27, n° 31, p. 5357-5367.

Roy, K. 2010. *Biomaterials as Stem Cell Niche*. Springer Berlin Heidelberg.

Ruiz, Juan-Carlos, Amélie St-Georges-Robillard, Charles Thérésy, Sophie Lerouge et Michael R. Wertheimer. 2010. « Fabrication and Characterisation of Amine-Rich Organic Thin Films: Focus on Stability ». *Plasma Processes and Polymers,* vol. 7, n° 9-10, p. 737-753.

Salinas, C. N., et K. S. Anseth. 2009. « Decorin moieties tethered into PEG networks induce chondrogenesis of human mesenchymal stem cells ». *J Biomed Mater Res A,* vol. 90, n° 2, p. 456-64.

Sarra-Bournet, Christian, Stephane Turgeon, Diego Mantovani et Gaetan Laroche. 2006. « Comparison of Atmospheric-Pressure Plasma versus Low-Pressure RF Plasma for Surface Functionalization of PTFE for Biomedical Applications ». *Plasma Processes and Polymers,* vol. 3, n° 6-7, p. 506-515.

Sawatjui, N., T. Damrongrungruang, W. Leeanansaksiri, P. Jearanaikoon, S. Hongeng et T. Limpaiboon. 2015. « Silk fibroin/gelatin-chondroitin sulfate-hyaluronic acid effectively enhances in vitro chondrogenesis of bone marrow mesenchymal stem cells ». *Mater Sci Eng C Mater Biol Appl,* vol. 52, p. 90-6.

Schmidt, David Richard, Heather Waldeck et Weiyuan John Kao. 2009. « Protein Adsorption to Biomaterials ». In *Biological Interactions on Materials Surfaces: Understanding and Controlling Protein, Cell, and Tissue Responses*, sous la dir. de Puleo, A. David, et Rena Bizios. Schmidt2009. p. 1-18. New York, NY: Springer US. < http://dx.doi.org/10.1007/978-0-387-98161-1_1 >.

Schoen, Frederick J., et Richard N. Mitchell. 2013. « Chapter II.1.5 - Tissues, the Extracellular Matrix, and Cell–Biomaterial Interactions A2 - Lemons, Buddy D. RatnerAllan S. HoffmanFrederick J. SchoenJack E ». In *Biomaterials Science (Third Edition)*. p. 452-474. Academic Press. < http://www.sciencedirect.com/science/article/pii/B9780080877808000395 >.

Schuleri, K. H., A. J. Boyle et J. M. Hare. 2007. « Mesenchymal stem cells for cardiac regenerative therapy ». *Handb Exp Pharmacol*, n° 180, p. 195-218.

Siddappa, R., R. Licht, C. van Blitterswijk et J. de Boer. 2007. « Donor variation and loss of multipotency during in vitro expansion of human mesenchymal stem cells for bone tissue engineering ». *J Orthop Res,* vol. 25, n° 8, p. 1029-41.

Silva, E. A., et D. J. Mooney. 2007. « Spatiotemporal control of vascular endothelial growth factor delivery from injectable hydrogels enhances angiogenesis ». *J Thromb Haemost,* vol. 5, n° 3, p. 590-8.

Siow, Kim Shyong, Leanne Britcher, Sunil Kumar et Hans J. Griesser. 2006. « Plasma Methods for the Generation of Chemically Reactive Surfaces for Biomolecule Immobilization and Cell Colonization - A Review ». *Plasma Processes and Polymers,* vol. 3, n° 6-7, p. 392-418.

Soulez, M., I. Sirois, N. Brassard, M. A. Raymond, F. Nicodeme, N. Noiseux, Y. Durocher, A. V. Pshezhetsky et M. J. Hebert. 2010. « Epidermal growth factor and perlecan fragments produced by apoptotic endothelial cells co-ordinately activate ERK1/2-dependent antiapoptotic pathways in mesenchymal stem cells ». *Stem Cells,* vol. 28, n° 4, p. 810-20.

Sridharan, Gokul, et Akhil A. Shankar. 2012. « Toluidine blue: A review of its chemistry and clinical utility ». *Journal of Oral and Maxillofacial Pathology : JOMFP,* vol. 16, n° 2, p. 251-255.

Stefani, Massimo. 2008. « Protein Folding and Misfolding on Surfaces ». *International Journal of Molecular Sciences,* vol. 9, n° 12, p. 2515-2542.

Tamama, K., V. H. Fan, L. G. Griffith, H. C. Blair et A. Wells. 2006. « Epidermal growth factor as a candidate for ex vivo expansion of bone marrow-derived mesenchymal stem cells ». *Stem Cells,* vol. 24, n° 3, p. 686-95.

Temenoff, J.S., et A.G. Mikos. 2008. *Biomaterials: The Intersection of Biology and Materials Science*. Pearson/Prentice Hall.

Thalla, P. K., H. Fadlallah, B. Liberelle, P. Lequoy, G. De Crescenzo, Y. Merhi et S. Lerouge. 2014. « Chondroitin sulfate coatings display low platelet but high endothelial cell adhesive properties favorable for vascular implants ». *Biomacromolecules,* vol. 15, n° 7, p. 2512-20.

Thermo Fisher Scientific. 2015. « Alamar blue cell viability Reagent ». < https://www.thermofisher.com/order/catalog/product/DAL1025 >. Consulted on January 14, 2016.

Tiraferri, Alberto, et Menachem Elimelech. 2012. « Direct quantification of negatively charged functional groups on membrane surfaces ». *Journal of Membrane Science,* vol. 389, p. 499-508.

Truica-Marasescu, Florina, et Michael R. Wertheimer. 2008. « Nitrogen-Rich Plasma-Polymer Films for Biomedical Applications ». *Plasma Processes and Polymers,* vol. 5, n° 1, p. 44-57.

Tsutsumi, S., A. Shimazu, K. Miyazaki, H. Pan, C. Koike, E. Yoshida, K. Takagishi et Y. Kato. 2001. « Retention of multilineage differentiation potential of mesenchymal cells during proliferation in response to FGF ». *Biochem Biophys Res Commun,* vol. 288, n° 2, p. 413-9.

Uebersax, L., H. P. Merkle et L. Meinel. 2008. « Insulin-like growth factor I releasing silk fibroin scaffolds induce chondrogenic differentiation of human mesenchymal stem cells ». *J Control Release,* vol. 127, n° 1, p. 12-21.

Uygun, B. E., S. E. Stojsih et H. W. Matthew. 2009. « Effects of immobilized glycosaminoglycans on the proliferation and differentiation of mesenchymal stem cells ». *Tissue Eng Part A,* vol. 15, n° 11, p. 3499-512.

van Susante, J. L. C., J. Pieper, P. Buma, T. H. van Kuppevelt, H. van Beuningen, P. M. van Der Kraan, J. H. Veerkamp, W. B. van den Berg et R. P. H. Veth. 2001. « Linkage of chondroitin-sulfate to type I collagen scaffolds stimulates the bioactivity of seeded chondrocytes in vitro ». *Biomaterials,* vol. 22, n° 17, p. 2359-69.

Varghese, S., N. S. Hwang, A. C. Canver, P. Theprungsirikul, D. W. Lin et J. Elisseeff. 2008. « Chondroitin sulfate based niches for chondrogenic differentiation of mesenchymal stem cells ». *Matrix Biol,* vol. 27, n° 1, p. 12-21.

Variola, F. 2015. « Atomic force microscopy in biomaterials surface science ». *Phys Chem Chem Phys,* vol. 17, n° 5, p. 2950-9.

Vats, A., N. S. Tolley, J. M. Polak et J. E. Gough. 2003. « Scaffolds and biomaterials for tissue engineering: a review of clinical applications ». *Clin Otolaryngol Allied Sci,* vol. 28, n° 3, p. 165-72.

Veevers-Lowe, Jennifer, Stephen G. Ball, Adrian Shuttleworth et Cay M. Kielty. 2011. « Mesenchymal stem cell migration is regulated by fibronectin through α5β1-integrin-mediated activation of PDGFR-β and potentiation of growth factor signals ». *Journal of Cell Science,* vol. 124, n° 8, p. 1288-1300.

Volkmer, E., I. Drosse, S. Otto, A. Stangelmayer, M. Stengele, B. C. Kallukalam, W. Mutschler et M. Schieker. 2008. « Hypoxia in static and dynamic 3D culture systems for tissue engineering of bone ». *Tissue Eng Part A,* vol. 14, n° 8, p. 1331-40.

Volpi, N. 2007. « Analytical aspects of pharmaceutical grade chondroitin sulfates ». *J Pharm Sci,* vol. 96, n° 12, p. 3168-80.

Von Recum, A.F. 1998. *Handbook Of Biomaterials Evaluation: Scientific, Technical And Clinical Testing Of Implant Materials, Second Edition*. Taylor & Francis.

Vroman, Leo, Ann L. Adams, Madeleine Klings, Gena C. Fischer, Priscilla C. Munoz et Regina P. Solensky. 1977. « REACTIONS OF FORMED ELEMENTS OF BLOOD WITH PLASMA PROTEINS AT INTERFACES* ». *Annals of the New York Academy of Sciences,* vol. 283, n° 1, p. 65-76.

Wang, X., E. Wenk, X. Zhang, L. Meinel, G. Vunjak-Novakovic et D. L. Kaplan. 2009. « Growth factor gradients via microsphere delivery in biopolymer scaffolds for osteochondral tissue engineering ». *J Control Release,* vol. 134, n° 2, p. 81-90.

Wei, Sun, Zhao Na, Xu Xiao et Jiao Kui. 2007. « Linear Sweep Polarographic Determination of Chondroitin Sulfate using Toluidine Blue as Electrochemical Probe ». *Chinese Journal of Analytical Chemistry,* vol. 35, n° 11, p. 1548-1552.

Woods, A., et J. R. Couchman. 1998. « Syndecans: synergistic activators of cell adhesion ». *Trends Cell Biol,* vol. 8, n° 5, p. 189-92.

Yanada, S., M. Ochi, K. Kojima, P. Sharman, Y. Yasunaga et E. Hiyama. 2006. « Possibility of selection of chondrogenic progenitor cells by telomere length in FGF-2-expanded mesenchymal stromal cells ». *Cell Prolif,* vol. 39, n° 6, p. 575-84.

Yasui, K., K. Kada, M. Hojo, J. K. Lee, K. Kamiya, J. Toyama, T. Opthof et I. Kodama. 2000. « Cell-to-cell interaction prevents cell death in cultured neonatal rat ventricular myocytes ». *Cardiovasc Res,* vol. 48, n° 1, p. 68-76.

Yew, T. L., M. C. Chang, Y. T. Hsu, F. Y. He, W. H. Weng, C. C. Tsai, F. Y. Chiu et S. C. Hung. 2013. « Efficient expansion of mesenchymal stem cells from mouse bone marrow under hypoxic conditions ». *J Tissue Eng Regen Med,* vol. 7, n° 12, p. 984-93.

Ying, W. Z., H. G. Zhang et P. W. Sanders. 2007. « EGF receptor activity modulates apoptosis induced by inhibition of the proteasome of vascular smooth muscle cells ». *J Am Soc Nephrol,* vol. 18, n° 1, p. 131-42.

Yorio, T., A. Clark et M.B. Wax. 2011. *Ocular Therapeutics: Eye on New Discoveries*. Elsevier Science.

Zaim, M., S. Karaman, G. Cetin et S. Isik. 2012. « Donor age and long-term culture affect differentiation and proliferation of human bone marrow mesenchymal stem cells ». *Ann Hematol,* vol. 91, n° 8, p. 1175-86.

Zhang, M., D. Methot, V. Poppa, Y. Fujio, K. Walsh et C. E. Murry. 2001. « Cardiomyocyte grafting for cardiac repair: graft cell death and anti-death strategies ». *J Mol Cell Cardiol,* vol. 33, n° 5, p. 907-21.

Zou, X. H., Y. Z. Jiang, G. R. Zhang, H. M. Jin, T. M. Nguyen et H. W. Ouyang. 2009. « Specific interactions between human fibroblasts and particular chondroitin sulfate molecules for wound healing ». *Acta Biomater,* vol. 5, n° 5, p. 1588-95.